



SkinLumina: Inclusive Multispectral Skin Analysis Device

Tatiana Cutrone – PSE
Ryan Rodriguez – PSE
Tiffany Thani – CPE
Abdullah Al-Gharabally – EE

Group 3

Advisors: Dr. Wei, Dr. Kar, Dr. Delfyett, Dr. Dogariu, Dr.
Eikenberry, Dr. Suboh, Dr. Phelps
Reviewers: Mike Armstrong, William Moore

Table of Contents

Chapter 1 Executive Summary.....	1
Chapter 2 Problem Description.....	1
2.1 Project Background and Motivation	1
2.2 Ethical and Social Considerations	2
2.2.1 Background on Optical Properties of Human Skin.....	2
2.2.2 Explanation of the Multispectral and Hyperspectral Imaging Applications.....	5
2.2.3 Consideration of Health Disparities in Dermatological Diagnostics	7
2.2.4 Photobiological Safety of LEDs	8
2.3 Goals and Objectives	9
2.3.1 <i>Optical System Architecture of SkinLumina</i>	11
2.3.2 <i>Core Functions</i>	13
2.3.3 <i>Existing/Related Works</i>	14
2.3.4 <i>Engineering Specifications</i>	15
2.3.5 <i>Hardware Block Diagram</i>	17
2.3.6 <i>Software Block Diagram</i>	18
2.3.7 <i>House of Quality</i>	19
Chapter 3 – Research and Investigation.....	20
3.1 Imaging Technology	21
3.1.1 Illumination Source.....	22
3.1.2 Filter Integration	24
3.2 Additional Supplemental Technologies	25
3.2.1 Use of Lambertian Reflectors in Diffuse Illumination Systems.....	26
3.3 Comparative Analysis of Imaging Methods and Design Strategies	27
3.4 Part Selection	28
3.4.1 Camera Selection	29
3.4.2 Filters	30
3.4.3 LED Specifications and Background.....	31
3.4.4 Lens Selection and System Design	37
3.4.5 Lambertian Reflectors.....	40
3.4.6 Polarizers.....	41

3.4.7 Aperture	42
3.4.8 Microcontroller Platform Selection	43
3.4.9 Single Board Computer Selection.....	45
3.5 Power Regulation and Safety.....	47
3.5.1 LED Driver Circuit Design for Multispectral Synchronization.....	51
3.5.2 Comparative Analysis of Chosen Hardware vs Alternatives.....	53
3.6.1 LED and Filter Wheel Timing Control Strategies	55
3.6.2 Data Throughput and Ease of Integration with App/Desktop Tools	57
3.6.3 LED & Filter Wheel Control Software Stack and Synchronization Logic.....	58
3.7 Software Technologies.....	59
3.7.1 Image Capture Libraries Comparison.....	60
3.7.2 Server-Side & Backend Framework Comparison.....	63
3.7.3 Image Classification Method Comparison.....	65
3.7.4 UI/UX Framework	66
Chapter 4 – Standards and Design Constraints.....	67
4.1 General Engineering Design Constraints.....	68
4.2 Design Constraint Comparison	70
4.3 Electrical and Biomedical Safety Standards	71
4.4 Power, Size, and Cost Constraints for Portability.....	74
4.5 Regulatory and Ethical Framework for Medical Devices.....	76
4.6 UCF Research Compliance and IRB Oversight.....	80
Chapter 5 Comparison of ChatGPT with Other Similar Platforms.....	82
5.1 Introduction.....	82
5.2 Advantages and Limitations	82
5.2.1 ChatGPT Case Study I.....	83
5.2.2 Advantages of AI	84
5.3 Application of ChatGPT, Copilot, GROK, SciSpace, and Claude	85
5.3.1 ChatGPT, Grok, SciSpace Case Study II.....	85
5.4 Technical Writing and Research.....	86
Chapter 6 Hardware Design	87
6.1 LED Clusters, Filter Wheels, Polarizers, and Lenses	87

6.1.1 Optical System Architecture	90
6.2 Microcontroller and Power Circuit Design.....	90
6.2.1 Sensor Integration and PCB layout.....	91
Chapter 7 Software Design	94
7.1 Image Capture and Control	95
7.1.1 Adaptive Capture Routine.....	97
7.2 Bluetooth/USB Transmission	100
7.2.1 UART Communication Protocol	101
7.3 LED and Filter Synchronizations.....	102
7.4 Data Processing.....	104
7.4.1 Tone Detection.....	104
<i>Fig 7. Fitzpatrick Skin Tone Classification Chart</i>	105
7.4.2 Data Classification.....	105
7.4.3 Software Architecture Diagram for Adaptive Capture Pipeline	110
7.4.4 Data Processing and Classification Full Pipeline	112
7.5 User interface	114
7.5.2 UI Image Fetching Workflow.....	115
7.5.3 Final User Interface.....	115
7.6 Security Considerations	118
7.7 Future Works	120
7.7.1 Personalized Skin Care Monitoring and Tracking.....	120
Chapter 8 System Fabrication/Prototype Construction.....	122
8.1 PCB Design.....	122
8.2 Housing of SkinLumina.....	123
8.2.1 LED Configurations.....	124
8.3 Battery and Raspberry Pi Design.....	125
8.3.1 Cable and Wire Management.....	125
Chapter 9 System Testing and Evaluation	127
9.1 Hardware and Software Testing.....	127
Power Regulation and Buck Converter Testing.....	127
Software Workflow and Synchronization Testing.....	129

Hexadecimal Color Detection Testing	129
9.2 Performance Evaluation.....	130
Spatial Resolution Testing	130
Thermal Management and Power Stability	132
9.3 Optoelectronic Feasibility Study and Testing.....	132
LED Illumination Profile Testing	132
Penetration Depth and Skin Phantom Testing	134
Polarization and Filter Wheel Isolation Testing	136
9.4 Overall System Integration	136
9.5 Project Testing and Integration Conclusion.....	137
9.6 After Senior Design Plan	138
Chapter 10 – Administrative Content.....	138
10.1 Budget	139
Budget Retroactive May 29th	139
10.2 Bill Of Materials	139
10.3 Work Distribution	141
10.4 Project Milestones.....	142
Project Milestones SD 1 and SD 2.....	143
Chapter 11 Conclusion	144
Appendices.....	vi
Appendix A – Copyright Permissions	vi
Appendix B – LLMs and other AI Chat Log/Resources	vi
Appendix C – References	vii

Chapter 1 Executive Summary

SkinLumina is a portable, multispectral imaging system designed to support inclusive dermatological diagnostics by adapting to a wide range of skin tones. Unlike traditional imaging devices, which often struggle with accuracy on darker complexions due to calibration biases, SkinLumina dynamically adjusts its lighting conditions and scanning parameters to accommodate the user's skin tone. By utilizing a combination of visible and near-infrared (NIR) wavelengths, paired with cross-polarization and optical filtering, the system aims to capture both surface and subsurface skin features with enhanced clarity. This functionality is critical for early detection of abnormalities such as melanoma, scars, or other irregularities that may otherwise go unnoticed in patients with high melanin concentrations.

The system combines visible and near-infrared (NIR) LED arrays, a motorized filter wheel, achromatic optics, and cross-polarization techniques to collect high-resolution images of both surface and subsurface skin features. This hardware is complemented by embedded firmware and software routines that control image acquisition, LED/filter synchronization, and dynamic brightness calibration based on real-time feedback. The electrical subsystems rely on a low-voltage, efficient power regulation architecture, while the optical path has been engineered for maximum efficiency and fidelity.

This final report provides a detailed overview of the technical and design decisions made throughout the course of the project. It includes extensive part selection and research, integration with UCF's research compliance procedures (including IRB standards) as well as other federal regulations and standards, and testing protocols tailored for both optical feasibility, safety and system performance. It also outlines the engineering constraints that guided the development of the SkinLumina device.

Overall, SkinLumina aims to create an inclusive multispectral imaging approach that can be applied in real dermatological settings to aid clinicians in providing patients with real-time personalized feedback across a broad range of skin tones.

Chapter 2 Problem Description

2.1 Project Background and Motivation

This chapter outlines the basis for our project including our goals and objectives, core functionalities as well as engineering requirements and technical specifications that will help guide the development of the SkinLumina project. These requirements and specifications serve as the foundational material that we are using to evaluate and select our components, system integration, and functionality as well as ensure that our final prototype device is up to the standards we have set for ourselves and the guidelines for our senior design classes at the University of Central Florida.

2.2 Ethical and Social Considerations

SkinLumina is a portable, multispectral imaging system designed to support inclusive dermatological diagnostics by adapting to a wide range of skin tones. Unlike traditional imaging devices, which often struggle with accuracy on darker complexions due to calibration biases, SkinLumina dynamically adjusts its lighting conditions and scanning parameters to accommodate the user's skin tone. By utilizing a combination of visible and near-infrared (NIR) wavelengths, paired with cross-polarization and optical filtering, the system aims to capture both surface and subsurface skin features with enhanced clarity. This functionality is critical for early detection of abnormalities such as melanoma, scars, or other irregularities that may otherwise go unnoticed in patients with high melanin concentrations.

The remainder of this paper outlines the engineering foundation and implementation strategy for the system. It begins by defining the core motivation and background research, then details our primary objectives and goals for the device. Sections on optical and electrical hardware explain the layout and selection of key components including LED clusters, CMOS imaging, and the filter wheel mechanism. The software section covers control logic, image capture, and user interaction features. Later sections address engineering requirements, system diagrams, budget constraints, and administrative planning, culminating in a unified vision for how SkinLumina will provide a more equitable and effective tool for dermatological assessment.

Dermatological imaging tools have played a key role in the early detection and diagnosis of skin conditions and potential life-threatening diseases like melanoma. However, even with recent technological advancements, there remains a significant gap in the effectiveness and namely inclusivity of these tools, for individuals with darker skin complexions. Many of these existing imaging systems are calibrated using standard reference skin tones, often lighter skin pigments. This creates a recurring bias that often leads to reduced diagnostic accuracy for patients with darker skin tones, or higher melanin concentrations. This can lead to prolonged diagnosis, misidentification of skin abnormalities, and health discrepancies in dermatological care.

This project is mainly motivated by trying to highlight the need for inclusiveness, as well as the need for an adaptable and emergent solution. We plan to leverage a multi-wavelength imaging approach, using both visible and near-infrared light, to design a portable, handheld, imaging system that adjusts to the user's unique skin properties. This system will help clinicians in making more accurate assessments across a broader range of skin tones, which will enhance diagnostic confidence and make a change in skin imaging and healthcare diagnostics.

2.2.1 Background on Optical Properties of Human Skin

The interaction of light with skin varies significantly depending on many factors such as melanin density, blood concentration, and specific structural properties of the skin layers. For example, shorter visible wavelengths such as violet and blue are more easily absorbed by melanin, making deeper lesions in the skin harder to image on darker skin

tones. On the other hand, Near-Infrared (NIR) light has a much greater penetration depth which allows for subsurface imaging, but without tailored customization to each skin tone it may miss surface level details that are important for accurate skin assessment. These crucial complexities are often overlooked and not properly addressed by current market solutions. As highlighted in related works later, VISIA and DermaSensor are the top skin imaging products that are not designed with inclusivity or baseline personalization in mind. [1, 2]

Clinical and social background is important to consider when understanding the motivation behind SkinLumina. Melanoma is frequently diagnosed at more advanced stages in nonwhite populations, contributing to significantly lower survival rates—66.7% for Black patients compared to 92.5% for white patients. This disparity, driven by a lack of inclusive diagnostic tools, education gaps, and limited access to care, is a key reason we are developing a device designed to support early skin abnormality detection across all skin tones. [3]

SkinLumina’s design is informed by the complex optical properties of human skin, which vary widely based on melanin concentration and skin structure. For example, melanosome volume fraction in the epidermis ranges from 1.3% in light skin to 43% in dark skin, significantly impacting how light is absorbed and scattered. Spectral imaging technology is particularly suited for skin analysis because it can capture both spatial and spectral data, allowing for more accurate and personalized identification of skin abnormalities.

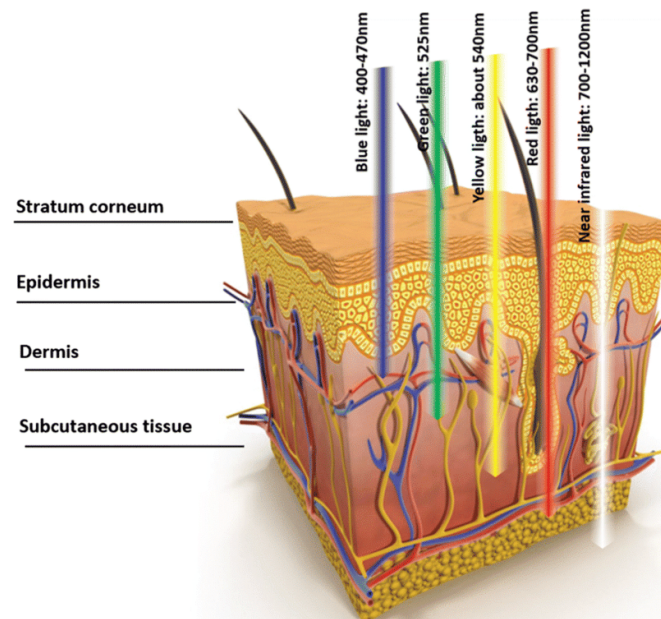


Fig 1 The penetration of light of different wavelengths in the skin. [4]

The 600–1300 nm spectral range is referred to as the “therapeutic window”. SkinLumina takes advantage of deeper light penetration, enabling noninvasive scanning of subsurface features across diverse skin types. Which can be seen in figure 1. This therapeutic

window is where light penetration is deeper due to minimal absorption by chromophores such as hemoglobin and water making it ideal for imaging structures below the surface. In a shorter range of wavelengths (e.g., 400-500 nm), light is scattered more and absorbed by melanin and hemoglobin, limiting penetration to the epidermis. As wavelength increases, scattering decreases and absorption shifts to deeper chromophores, allowing longer wavelengths. For SkinLumina, the therapeutic window is critical and selecting wavelengths within it enables the system to noninvasively capture high-contrast, spatially resolved information. This window enables clear imaging from varying depths and skin tones, supporting an accurate and inclusive skin condition assessment. [4]

Effective imaging for photodynamic therapy (PDT) and other diagnostic applications relies on understanding how light interacts with biological tissue at different wavelengths. Pretreatment imaging plays a critical role in noninvasively assessing target areas, such as tumors, lesions, or regions of abnormal tissue, especially when visual inspection is insufficient. The optical behavior of human skin is highly wavelength-dependent and varies with individual factors like pigmentation, tissue structure, and lesion depth.

Shorter wavelengths (e.g., blue or green light) tend to scatter more strongly and are absorbed heavily by melanin and hemoglobin, making them ideal for imaging superficial skin layers and vascular structures. Conversely, longer wavelengths (e.g., red and near-infrared) experience less scattering and absorption, allowing deeper penetration into subdermal tissue. Multispectral imaging leverages this wavelength-dependent penetration by capturing spatially-resolved data across multiple wavelengths, enhancing the ability to detect and characterize abnormalities at varying depths and across diverse skin tones. This spectral sensitivity makes it possible to visualize vascular patterns, identify areas of necrosis or disease infiltration, and support personalized treatment planning and dosimetry. [5]

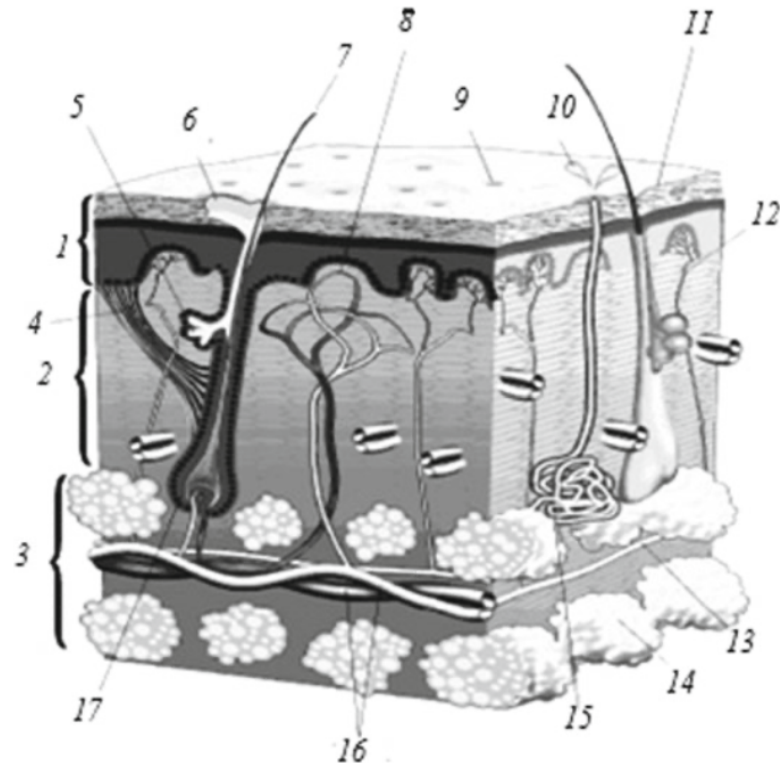


Fig 1.1 The biological structure of the human skin: 1 epidermic; 2 dermis; 3 hypodermis; 4 muscle; 5 oil gland; 6 fatty secret; 7 hair; 8 capillaries; 9 oscule; 10 sweat; 11 keratin (corneal layer); 12 nerve ending; 13 nerve; 14 fat lobule; 15 sweat gland; 16 blood vessels; 17 hair sac. [6]

The human skin is a multi-layered biological tissue that varies per person. As seen in figure 1.1, the epidermis (1), dermis (2), and hypodermis (3) are the skin components with individual optical characteristics. The optical components and light interactions in skin are influenced by factors such as water, melanin, hemoglobin and oxyhemoglobin. Melanin is concentrated in the epidermis and primarily absorbs in the UV and visible ranges. Hemoglobin is concentrated in the dermis and absorbs light in the blue to green spectral regions. Water is present in all skin layers but shows the most absorption in wavelengths near and reaching above 1000 nm.

An imaging system designed to operate within the optical therapeutic window ensures that light absorption by water in skin is low while allowing for deeper and safer light penetration. Staying within a 600-1300 nm spectral range maximizes imaging contrast for different skin features while avoiding the risks of tissue heating or photodamage. Varying wavelengths in a multispectral design allows a broader range of scans to accommodate varying optical properties of skin. This ensures effective imaging performance suitable for diverse skin tones and varying lesion depths each patient has. [7]

2.2.2 Explanation of the Multispectral and Hyperspectral Imaging Applications

Existing methods for diagnosing melanoma often struggle to detect skin cancer early and accurately in patients with darker skin tones. Due to this, researchers are developing new non-invasive imaging technologies that provide more detailed information about skin. Two of the most promising approaches are multispectral imaging (MSI) and hyperspectral imaging (HSI). These two approaches capture images at multiple wavelengths across the UV, visible, and near-infrared ranges.

Hyperspectral imaging systems use many narrow wavelength bands to collect detailed spectral data from the skin, allowing detection of small changes in tissue composition. Multispectral imaging systems use fewer wavelengths but still provide clear depth and pigmentation information while being simpler. [8] Both of these imaging types help reveal differences between healthy and abnormal tissue by analyzing how light is reflected at different wavelengths. Studies using these systems have shown improvements in melanoma detection and a direct reduction in unnecessary biopsies.

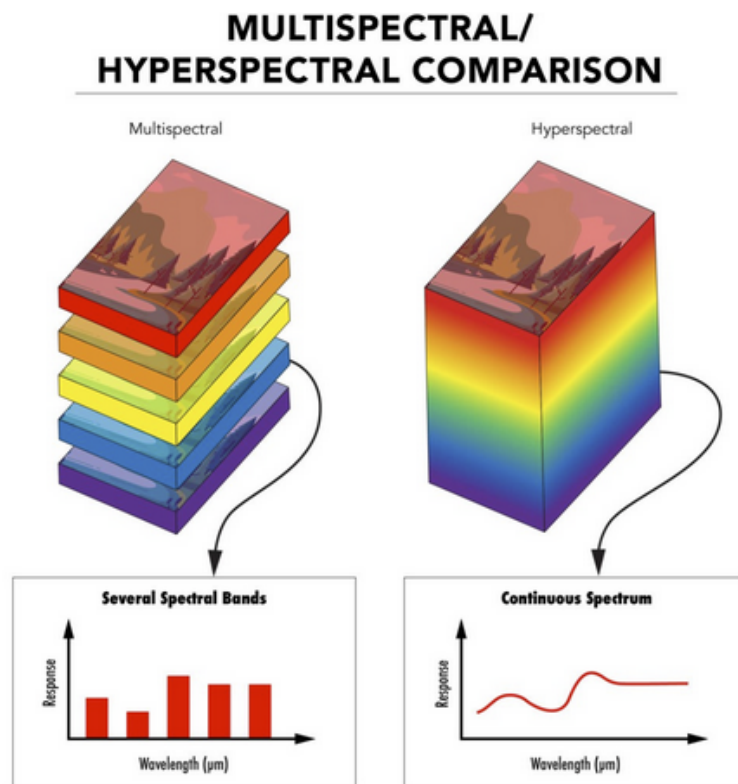


Fig 1.2 comparison of the image stacks in multispectral imaging, in which there are images taken in several different spectra, and hyperspectral imaging, in which there are images taken in many different spectra.

SkinLumina uses a multispectral imaging approach due to MSI having a balance between depth sensitivity, portability, and cost. This imaging method is shown in figure 1.2.

Hyperspectral systems that are larger and more expensive compared to MSI. The MSI

approach allows a target of specific wavelengths that penetrate different skin depths and work across a range of skin tones. This makes it ideal for SkinLumina's goal of creating an inclusive, non-invasive, and affordable skin assessment tool for detecting various skin abnormalities. [9]

SkinLumina's design is informed by the complex optical properties of human skin, which vary widely based on melanin concentration and skin structure. For example, melanosome volume fraction in the epidermis ranges from 1.3% in light skin to 43% in dark skin, significantly impacting how light is absorbed and scattered. Spectral imaging technology is particularly suited for skin analysis because it can capture both spatial and spectral data, allowing for more accurate and personalized identification of skin abnormalities. [4]

2.2.3 Consideration of Health Disparities in Dermatological Diagnostics

Dermatological diagnosis and skin type classifications are subjugated to current pigmentation categorizations like the Fitzpatrick Skin Type (FST) scale. The scale FST limits a patient to is 6 skin tone predictions as shown in figure 1.3. FST relies on patient self-reported data about ethnicity, sun exposure history, and UV sensitivity, making it prone to recall bias and inconsistent clinical evaluation. Existing computer vision models classify skin type based on RGB images are limited by their low spectral resolution and sensitivity to lighting variations. Studies have shown that these RGB-based methods often show weak correlation with FST categories, reducing their reliability for objective skin assessment.

Dermatological diagnosis and skin type classifications are subjugated to current pigmentation categorizations like the Fitzpatrick Skin Type (FST) scale. The scale FST limits a patient to is 6 skin tone predictions as shown in figure 2.1. FST relies on patient self-reported data about ethnicity, sun exposure history, and UV sensitivity, making it prone to recall bias and inconsistent clinical evaluation. Existing computer vision models classify skin type based on RGB images are limited by their low spectral resolution and sensitivity to lighting variations. Studies have shown that these RGB-based methods often show weak correlation with FST categories, reducing their reliability for objective skin assessment.

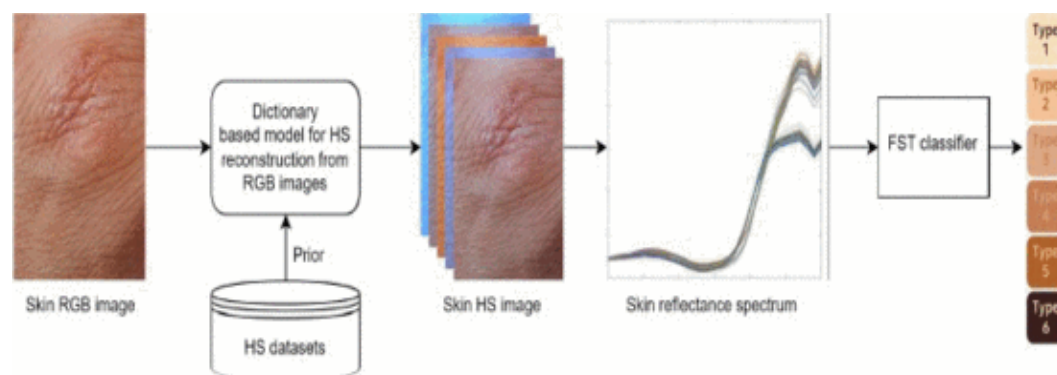


Fig 1.3 Flowchart outlining the process for estimating and predicting Fitzpatrick Skin Type (FST) classification. [10]

Recent research has focused on the use of hyperspectral imaging (HSI) for skin classification to overcome skin assessment limitations. HSI imaging captures detailed reflectance spectra across multiple wavelengths, allowing for a more accurate representation of skin tone and skin structure. Computational models trained on HSI data have demonstrated significantly better performance in predicting FST categories compared to RGB-based models. This highlights a need for more inclusive, non-invasive imaging solutions in dermatology that can provide accurate skin assessments for a patient. SkinLumina's use of multispectral imaging adopts this same principle by capturing targeted wavelength data to personalize and improve skin characterization and reduce diagnostic variability. [10]

As diagnostics have relied heavily on subjective visual inspection and, later, on invasive biopsy procedures, with histopathology becoming the diagnostic gold standard by the 20th century. Both methods present challenges in accurately assessing skin conditions across diverse skin tones. A greater amount of pigmentation can mask clinical signs, leading to underdiagnosis or misdiagnosis in individuals with darker skin. Studies show inconsistencies among clinicians when evaluating skin conditions. Diagnostics for melanoma vary widely in accuracy based on clinician experience. The reliance on subjective assessment has contributed to health disparities leads to delayed or inaccurate diagnoses. This growing recognition has driven newer research into non-invasive imaging and image processing techniques for dermatology aimed at improving diagnostic consistency and reducing bias across all skin types. [7]

2.2.4 Photobiological Safety of LEDs

The photobiological safety of LEDs revolves around the level of risks and potential harmful effects light sources can have. The photobiological safety studies often narrow down to the potential harmful effects optical radiation has on human tissues such as the eyes and skin. The severity of these effects depend on several factors including wavelength, exposure intensity, duration, and the specific tissue exposed.

LEDs that fall under the visible light source category have the primary concern in harming eye retina. The high intensity, lower wavelength 400-500 nm spectral range had the potential for photochemical damage to the retina from prolonged exposure. This is

called the blue light hazard where temporary effects like disability glare and reduced visual performance can occur. These effects are only a risk when eyes are directly exposed to the light source at close distances for extended durations of time. [11]

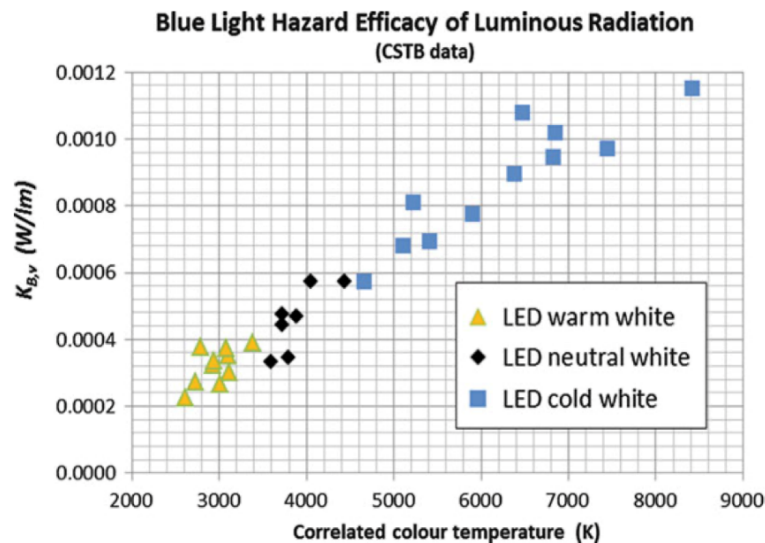


Fig 1.4. The penetration of light of different wavelengths in the skin. [11]

SkinLumina operates safely within the pre-determined therapeutic imaging window where we only use selected visible and near-infrared wavelengths that are within the photobiological exposure limits. The design of SkinLumina ensures that the light source is directed only towards the skin and not directly viewed by eyes during operation. Not using high-energy UV or short-wavelength LEDs, additional risks are avoided. These risks include thermal skin damage and phototoxic effects caused by irradiance levels above a certain threshold as seen in figure 1.4. Keeping within the guidelines outlined by the International Commission on Non-Ionizing Radiation Protection (ICNIRP) and IEC 62471 photobiological safety standards for lamps and lamp systems ensures a safe usage of LEDs. [11]

2.3 Goals and Objectives

The main goal of our project is to create a portable imaging system that can be used in medical diagnostics to scan and image the skin to provide analysis on skin abnormalities such as lesions, moles, scars, and discoloration, as well as detect subsurface cancers such as melanoma. Our main goals and objectives are listed below.

Basic Goals

- Build a multi-wavelength imaging system to detect skin abnormalities like bruising, scarring, discoloration, and melanoma.
- Create a 2-scan imaging process to provide an initial personalized baseline scan and a second scan to get more inclusive and accurate results across a wide-range of skin tones.

- Create an image processing algorithm to correlate the images and provide user's or dermatologists with insight into skin quality and health.

Advanced Goals

- Create a portable imaging system that can be used in real dermatologist settings to provide support in diagnosis and skin analysis.
- Enable basic user feedback via simple software.
- Integrate subsurface imaging techniques such as cross polarization to enhance contrast and visibility of subsurface structures.

Stretch Goals

- Create a companion software platform for real-time data visualization, such as a mobile app.
- Design a modular optical system, allowing us to easily change lenses, apertures, filters, etc.

Objectives

The SkinLumina Project is driven by the goals outlined above. We plan to achieve these goals by putting in place a structured and scalable set of objectives to give us a clear path to making our vision a reality. Our project at its core is defined by the 3 basic goals outlined above, with the first being to design and build a multi-wavelength system to detect skin abnormalities such as bruising, scarring, discoloration, and melanoma. To achieve this, we are going to design a structured optical stack with varying optical elements like mirrors and lenses to use in conjunction with the LEDs and a camera to give us this multi-wavelength system. The next main goal we are trying to accomplish is the notion of a 2-scan process to be more inclusive to all skin tones. This will be accomplished by having a set of white LEDs, as well as our colored LEDs to take a base image of the skin, in which we could then correlate with other known skin tone images to allow our machine to recognize this skin tone and adjust the brightness accordingly. Lastly, as far as basic goals go, we are looking to be able to process and correlate these images to give feedback to the user on the quality of their skin. For this we are going to have to either train our system using some sort of machine learning model or have an existing “database” in which our images could then be presented to a dermatologist for further analysis.

Building upon these foundational goals, our advanced system criteria aim to build upon the system's clinical viability, diagnostic capabilities, as well as improve the overall reliability of the images we collect. One way we aim to do this is to increase the portability of the machine with the end goal of our device being a handheld product that could be used in real-world dermatologist settings. To achieve this level of portability we first must create a consistent imaging system, in which we can then modify and scale down. To further enhance the ease of use and reliability of our imaging system in clinical settings, we aim to use features such as cross-polarization and other optical imaging techniques as well as aiming to create an easy-to-use software interface. This will be

done through strenuous optical design as well as software adjustments and improvements, giving clinicians an easy to use and reliable system.

Finally, the stretch goals of this project, as the name suggests, aim to stretch the scope of this project and make it more viable in the long term as the world and the medical field continues to evolve. This includes the development of a companion platform, such as a mobile app or computer software, this would allow for real-time data visualization as well as remote consultation. Additionally, we would like to design the system in the future to be modular in nature. This means that we would be able, or the dermatologist would be able to freely upgrade/customize the system for their specific needs. This would give our imaging system a more “tailored” feel as well as increase the system’s long-term viability. In sum, we hope that through these goals and objectives we ensure that SkinLumina provides a comprehensive skin analysis that is easy and reliable to use as well as stays adaptable for future use cases.

2.3.1 Optical System Architecture of SkinLumina

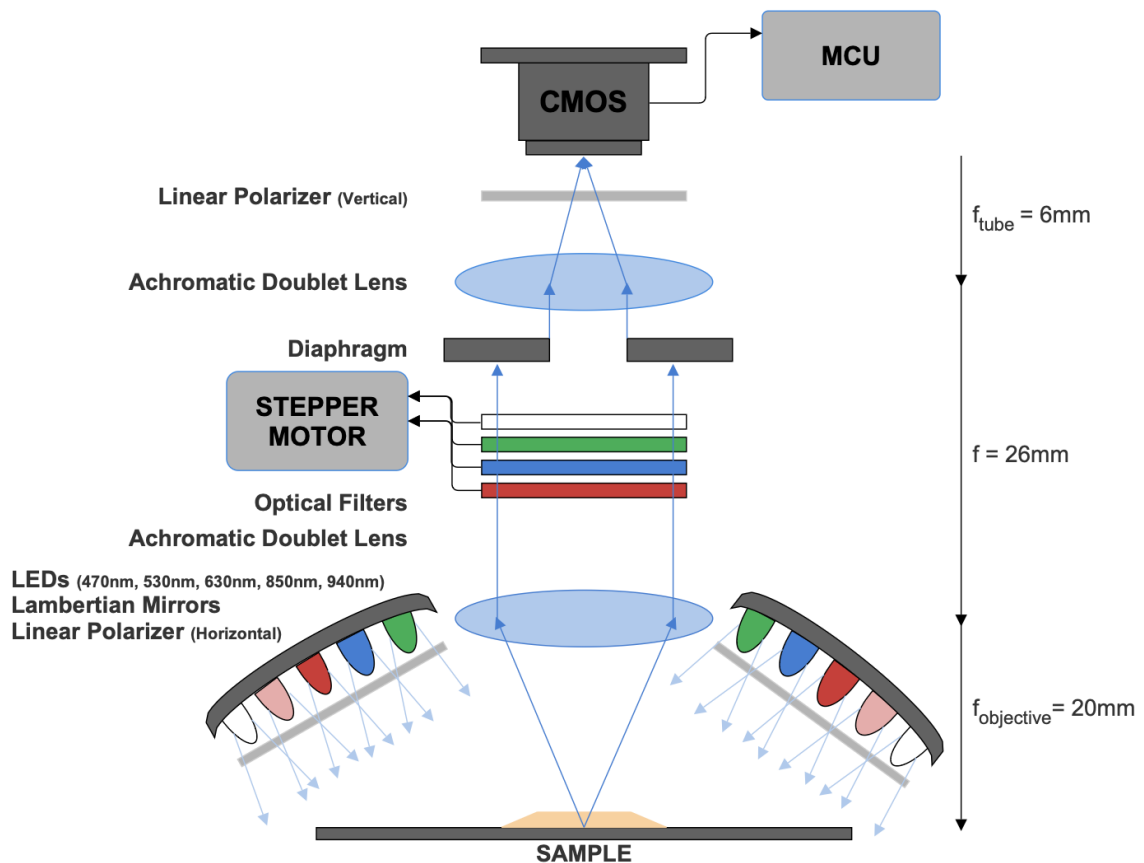


Fig 2 Optical System Layout

The optical system of SkinLumina is designed to enable high-resolution, multispectral reflectance imaging across both visible and near-infrared (NIR) bands, while minimizing optical aberrations and maximizing contrast for diverse skin types. As seen in figure 2,

the system is composed of a carefully aligned, vertically stacked optical path that integrates imaging optics, polarization control, spectral filtering, and structured illumination. At the top of the optical stack is a CMOS image sensor interfaced directly with the system's microcontroller unit (MCU). The CMOS sensor is responsible for capturing high-resolution images across various wavelength bands. It receives light through a multi-element imaging path that begins with a linear polarizer oriented to suppress specular reflection and surface glare from the skin sample, thereby enhancing subsurface contrast.

Following the polarizer is the primary relay optic, implemented using an achromatic doublet lens, commonly referred to in this system as the tube lens. This lens is designed to correct for chromatic aberrations across the visible and NIR spectrum, ensuring that the incoming rays are properly collimated and focused for spectral imaging applications. Next in the optical path is an adjustable iris diaphragm, which functions as a variable aperture stop. This component regulates the numerical aperture (NA) of the system and controls the amount of light reaching the sensor. Proper aperture adjustment is critical for optimizing image contrast, depth of field, and reducing optical flare. Beneath the diaphragm lies a motorized optical filter wheel, which houses a set of narrow-bandpass and long pass optical filters aligned with the center wavelengths of the system's LED illumination sources (470 nm, 530 nm, 630 nm, 850 nm, 940 nm, and broadband white). The filter wheel is actuated via a precision stepper motor, electronically synchronized with the camera's exposure timing to ensure that the correct filter is in place during each image acquisition cycle.

Immediately below the filter wheel is a second achromatic doublet lens, functioning as the objective lens. This lens focuses the filtered and collimated light onto the skin surface, forming a high-resolution image on the CMOS sensor with minimized chromatic and spherical aberrations. The focal length and placement of this objective are optimized for a fixed working distance and shallow depth imaging typical of dermatological inspection. Surrounding the lower periphery of the objective lens is a custom LED illumination ring. The LED array contains discrete emitters centered at the aforementioned wavelengths, enabling multispectral image acquisition. The spatial arrangement ensures uniform irradiance across the sample area, and the system supports both sequential and combined wavelength illumination modes.

To enhance diffuse and uniform lighting, the LEDs are embedded within a Lambertian reflective housing. This passive diffusion structure eliminates hot spots and promotes isotropic scattering of light toward the sample, improving the homogeneity of the illumination field. Just above the skin sample and below the LED array is a second linear polarizer, oriented orthogonally (cross-polarized) with respect to the first. This configuration implements cross-polarization imaging, a technique widely used in dermatological optics to eliminate surface glare and reveal subsurface features such as melanin distribution, hemoglobin absorption, and skin texture irregularities.

In summary, the SkinLumina optical system integrates a vertically aligned, modular configuration consisting of polarization optics, chromatic aberration-corrected lenses, a synchronized filter wheel, and multispectral LED illumination. This combination enables

high-fidelity, label-free imaging tailored for inclusive skin diagnostics across a wide range of skin tones and lesion types.

2.3.2 Core Functions

This project is centered around three core imaging functionalities that compose the technological foundation of the SkinLumina system: Multispectral Imaging, Baseline Scan Calibration, and NIR Depth Imaging. Each of these functions plays a crucial role in achieving the project's overall goal, which is to deliver a portable, inclusive, and efficient skin analysis tool to be used in real clinical settings.

Multispectral Imaging will enable the system to capture images at several visible wavelengths of light, which all interact with the skin in different ways, which will be highlighted in detail in a later section. By using a planned combination of red, blue, green, white, and NIR LEDs, the device will be able to gather reflectance and absorption data on skin features like bruising, moles, discoloration, scarring, as well as some subsurface features like melanoma. This will then allow us to create coherent and quality images of these features. This multiwavelength approach works by enhancing the contrast between different chromophores in your body such as melanin or hemoglobin which allows dermatologists to distinguish between healthy levels in your skin or skin abnormalities by showing lowered or heightened levels. These collected images are analyzed individually as well as in conjunction with the other images to provide a comprehensive spectral profile of the user's skin and features on their skin.

The next key aspect of our system is what makes our system adaptive and inclusive, that being the baseline scan. As mentioned above, in most current skin imaging systems they tend to adhere to traditional one-size-fits-all calibration settings which can often lead to diagnostic bias or even in extreme cases a misdiagnosis, especially for people with darker skin complexions. This is because darker skin tones have higher melanin content, which will lead to image washout or underexposure. To counter this notion, our project will implement an initial scan using white LEDs to determine the user's skin tone profile. This can then be used in later scans for that individual to adjust brightness if needed to get clear full contrast images regardless of the skin color of the individual. This feature will ensure inclusivity and customizability with each different scan which will increase the diagnostic and clinical accuracy of our product.

Lastly, SkinLumina plans to implement Near-Infrared Depth Imaging as well. This will add an additional dimension to the diagnostic power of the system by enabling subsurface visualizations. The system will use NIR wavelengths specifically in the 800 nm to 950 nm range, which have a greater penetration depth in the dermis due to the reduced scattering and absorption of melanin. This will allow for imaging of deeper lesions and subsurface structures which would not be feasible with just visible wavelengths. NIR Imaging is also critical in early melanoma detection as malignant (cancerous) tumors often form and originate below the surface. By operating in the "therapeutic window", which is 600 nm to 1300 nm, SkinLumina will be able to capitalize on this spectral range of light where it can travel deeper into tissue while retaining imaging contrast.

In summary, these three imaging functions form an integrated system that balances precision, adaptability, and inclusivity. They inhibit SkinLumina to operate efficiently in clinical settings as well as provide users with actionable insight into their skin health, regardless of skin tone or background.

2.3.3 Existing/Related Works

Existing skin imaging technologies with goals like our project often fall short in terms of inclusivity, portability, or accessibility for a broader range of users. By analyzing these systems, we gain valuable insight into design gaps that SkinLumina seeks to address through a compact, customizable, and cost-effective solution.

One reference system is the VISIA Complexion Analysis device by Canfield Scientific, as seen in figure 3, a global leader in medical imaging solutions. VISIA employs a combination of standard IntelliFlash, cross-polarized, and ultraviolet lighting to generate high-resolution facial skin analysis. However, the system weighs approximately 31 lbs. and is designed strictly for clinical, stationary environments, limiting its portability and accessibility for broader dermatological applications. [1]



REVOLUTIONIZE

Your Consultations

VISIA's capture module rotates smoothly around the subject to easily photograph left, right and frontal facial views.

The multi-point positioning system and live image overlay make it easy to capture perfectly registered images to document progress over time.

Simplify the imaging process while providing greater comfort for the client.

ELEVATE YOUR CONSULTS

Fig 3 VISIA clinical complexion analysis device. [1]

The VEOS system, also by Canfield, introduces more portability by integrating with a smartphone, as seen in figure 3.1, to provide AI-assisted dermatoscopic imaging. While VEOS is compact and user-friendly, it lacks multispectral illumination and personalized baseline calibration, reducing its effectiveness for analyzing diverse skin tones or subtle subsurface features. [2]



Fig 3.1 VEOS portable smartphone complexion analysis. [2]

Additionally, the DermaSensor device utilizes elastic scattering spectroscopy to detect potential cancerous lesions and has recently received FDA clearance. However, this system is a regulated medical device intended solely for clinical use and lacks the adaptability, affordability, and baseline-referenced analysis that SkinLumina aims to offer. [12]

In contrast, SkinLumina integrates multispectral LED illumination, optical filtering, and onboard image processing into a fully handheld platform. It is designed to adapt to a user's unique skin tone through an initial baseline scan and enables routine screening of skin abnormalities in a wide range of settings, not just clinical environments.

2.3.4 Engineering Specifications

Below in table 2.1 are listed numerical values for main features of each subsystem that encompasses the project. Beginning with the imaging/optical system. Its level of portability and weight are designed for easy convenience of use, and our sub-3-pound weight limit and near-handheld size well match our expectations. The drawing of power that is needed for each system helps exceed our portability constraint, as the maximum voltage and current needed for the project are able to be supplied through batteries or a small power cord system, and for temperature regulation, as not much heat is generated for this level of power consumption. Imaging for the project is a top priority, and our choice of imaging sensors is well suited for detailed analysis and visibility. Even to the capability of subdermal analysis through its NIR features.

Imaging/Optical System		
Requirements	Target Value/Range	Unit
<i>Portability</i>		
Weight	3	Pounds (lbs)
System Dimensions	8 x 6 x 6	Inches (in)
<i>Power</i>		
Battery Life	> 2	Hours
System Power	> 12	Volts (V)
System Current	3-4	Amps (A)
Luminous Intensity (adjustable)	0-30	% (varies per λ)
<i>Imaging Aspects</i>		
Camera Resolution	> 2	Megapixels
Pixel Size	< 2-3	Microns
Wavelength Bands	400-700, 850, 940	Nanometers (nm)
LED Switching Latency	< 100	Milliseconds (ms)
Image Processing Time	< 5	Seconds per scan (sec)
Field of View (FOV)	1.2 x 1.2	Inches (in)
<i>Light Penetration Depth</i>		
Visible Depth	$0.5 < x < 1$	Millimeters (mm)
NIR Depth	> 2	Millimeters (mm)
<i>Safety and Compliance</i>		
Skin Safe Power	<10	mW/cm ² (per LED array)
Operating Temperature	15 - 35	Celcius (C)

Table 2.1 Optical Engineering Specifications

The requirements for the electrical and software portion of this project are detailed in a visual table 2.2. Its contents show the individual subsystem along with its specifications and its numerical target value/range for optimal use. The requirements covered go into close detail about each aspect of the project that regards anything electrical and software.

Electrical/Software System		
Requirements	Target Value/Range	Unit
<i>Electrical Requirements</i>		
Image Capture Timing	< 100	Milliseconds (ms)
Connectivity	> 115200	Bits per Second (bps)
Error Handling	< 1	Second to report error
Data Storage	< 4	Megabytes per Image
Voltage Regulator	12	Volts (V)
Microcontroller	100-200	Milliamp (mA)
LED Clusters	5-12 @1-2	Volts @ Amps
Camera Module	3.3 @ 200mA	Volts @ Amps
Motor (stepper/servo)	1V @ 300-1000mA	Volts @ Milliamps
Filter Wheel Feedback Sensor	3.3 @ 50mA	Volts @ Milliamps

Table 2.2 Electrical/Software Engineering Specifications

The system design for the SkinLumina imaging device is represented through two primary architectural diagrams: the hardware block diagram and the software block diagram. These diagrams outline the functional components and data flow within the system and provide a clear division of responsibilities across the engineering team.

2.3.5 Hardware Block Diagram

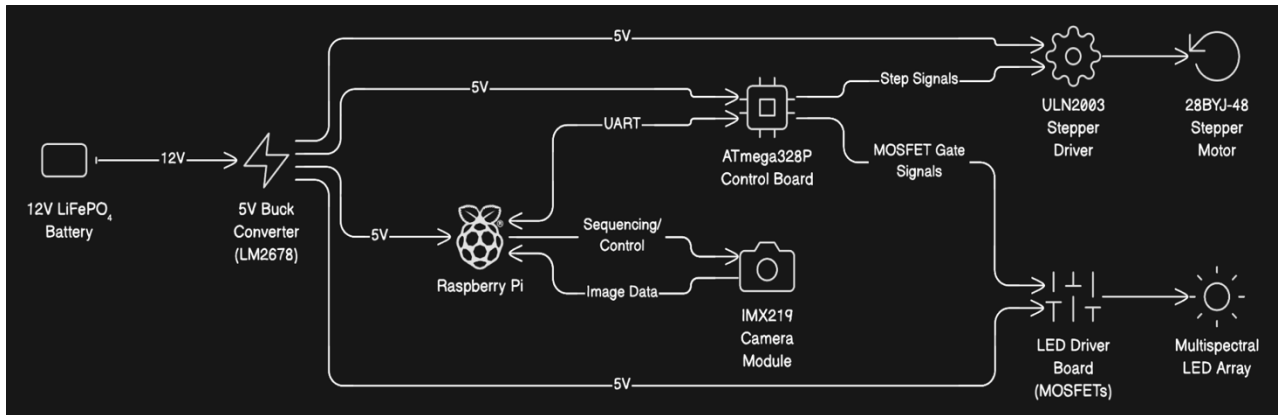


Fig 2.3 Hardware Block Diagram

The hardware block diagram in figure 2.3 encompasses the physical components required to operate and control the multispectral imaging system. Key elements include the power supply, microcontroller unit (MCU), printed circuit board (PCB), motor controller, Arduino, and CMOS camera sensor. Central to the optical subsystem is the optical stack, which includes the motorized filter wheel and multi-wavelength LED array, enabling dynamic illumination and spectral imaging. These hardware components collectively support the controlled acquisition of skin images under specific illumination conditions.

2.3.6 Software Block Diagram

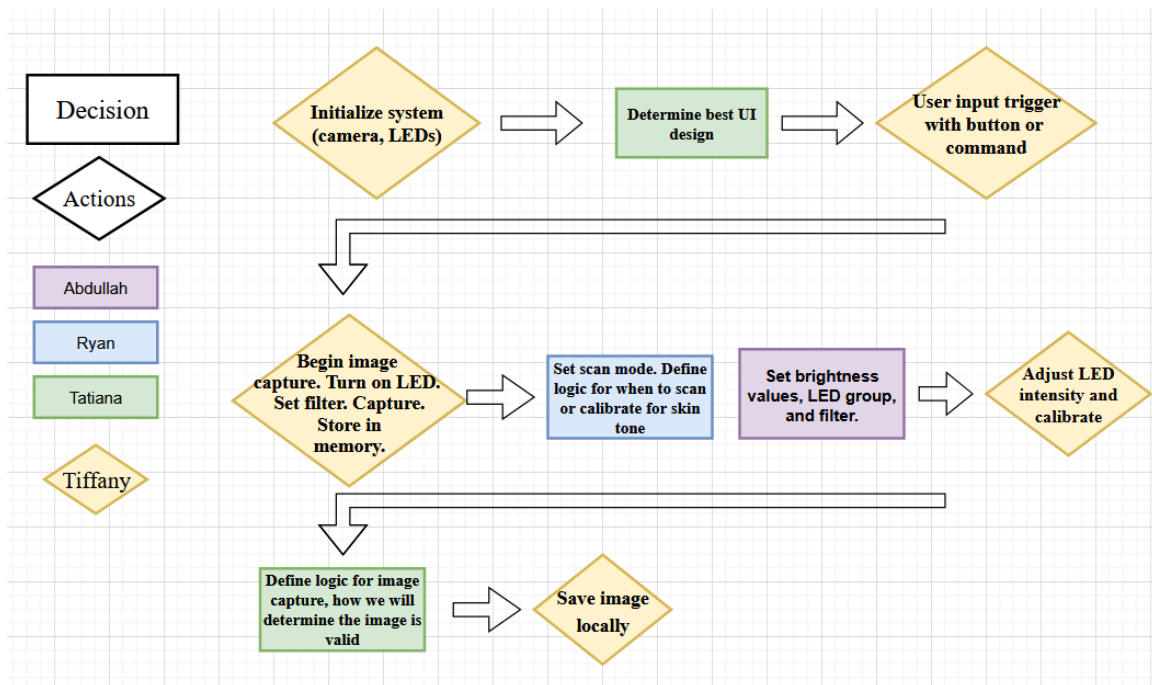


Fig 2.4 Software Block Diagram

The software block diagram in figure 2.4 defines the control logic and data-processing workflow of the system. It begins with a decision and actions block, responsible for initializing both the camera and LED system. Subsequent steps include selecting the optimal imaging configuration, triggering image capture, and storing raw data for analysis. The software pipeline then extracts RGB hex codes from the image and uses them to modulate LED brightness in real time, based on spectral characteristics. Finally, the processed image is saved locally for further diagnostic interpretation or machine learning analysis. These tasks are modularly assigned across the development team, enabling parallel progress in both embedded control and optical imaging functionality.

2.3.7 House of Quality

The House of Quality for this project shows four primary requirements: inclusivity, ease of use, reliability, and affordability. While also showing seven engineering metrics: portability, image resolution, image processing, safety and compliance, data storage, and cost. The table shows a strong proportional relation between ease of use and image processing and image resolution. It shows a negative relationship between cost and affordability. Further detailed qualities are shown below in figure 2.5.

3.1 Imaging Technology

As mentioned above, the core functionalities of our final product rely on a multispectral imaging system that can accurately capture both surface and some subsurface features on human skin across a broad range of skin tones. Therefore, choosing the appropriate imaging technology is crucial in our design process as it will directly impact our baseline image quality, power, and cost. We investigated 3 different imaging technologies: CMOS (Complementary Metal-Oxide-Semiconductor) imaging sensors, CCD (Charge-Coupled Device) sensors, and a smartphone-based imaging system.

CMOS imaging sensors are heavily used in modern electronics due to their low power consumption and cost-effectiveness. These sensors function by converting light into electrical signals directly at each pixel, which allows for parallel processing and faster readout times. This makes them especially great in real-time imaging and embedded systems as well as many imaging devices. These technologies have greatly increased in recent years as they have worked towards enhanced image sensitivity as well as global shutter capabilities which make them viable in a lot more settings.[13]

The next technology is CCD imaging sensors, which when compared to CMOS tend to be viewed as superior and the gold standard of precision imaging systems. They are known for their superior image quality, especially in lower light environments. CCD sensors work by transferring pixel charges sequentially through a shift register to a common output, which enables uniform signal processing. This system provides excellent signal to noise ratios and dynamic range, making these sensors super-efficient in applications like high resolution microscopy, astronomy, and other precision imaging methods. This increase in quality does have some drawbacks however, as CCD sensors tend to be much larger, have slower readout times, are more expensive, and a much larger power consumption. [14]

Lastly, we investigated using an existing smartphone imaging system and adding onto it to accomplish our multispectral imaging approach. Smartphone-Imaging systems have been increasing in popularity as the quality of smartphone cameras has increased. A smartphone-based imaging approach would leverage the high-resolution cameras integrated into standard commercial devices like iPhones. Systems like this offer exceptional accessibility and ease of use because it could be easily integrated with the phones software interface making imaging seamless. While these systems do benefit from large sensor sizes and great image processing algorithms, they lack control over the illumination source and make integrating hardware with the phone itself much more of a challenge. [15]

Technology	Pros	Cons	Selected?
CMOS Imaging	Low power compact	Lower low-light sensitivity than CCD	Yes

	cost-effective	Lower resolution than other two	
CCD Imaging	Better low-light performance Great image resolution	Power-hungry Bulkier Expensive	No
Smartphone Imaging	Portable user-friendly superior image processing	Limited control over optics and lighting Hardware harder to integrate	No

Table 3 Imaging Technology Constraints

Table 3 highlights a few of the pros and cons considered when choosing imaging technology to base the imaging system around. When choosing technology, it really came down to what we were the most constrained by, which are power consumption and cost. To keep both down to one achieve a safe portable imaging system as well as stay within our defined budget for this project. Furthermore, we did need to make sure that we have good enough image resolution to be able to actually image and capture the features of the skin we are targeting. Based on this analysis, we decided to use CMOS imaging for our system as this is a cost-effective and lower power imaging sensor that we can build the system we want around it. By choosing CMOS, we just need to make sure when we are choosing a camera and building the lens system that we target high enough resolutions ranging from 2 megapixels to 8 megapixels in order to maximize the effectiveness of CMOS.

3.1.1 Illumination Source

The next big technological component we needed to research is what light source we plan to use. Illumination plays a fundamental role in determining the contrast, depth, and fidelity of our images. As mentioned earlier, different wavelengths of light interact with the skin in numerous different ways, some absorb better than others, some scatter easier and some penetrate well. Due to this notion we are looking for a source that is power friendly and safe for the skin as well as provide a consistent multiwavelength light source for our imaging system.

At first, we thought of using an array of just white LEDs in order to do all of our imaging. White LEDs are good because they produce a broad-spectrum in the visible range by combining a blue or UV LED with a phosphor coating that emits in the yellow-orange region of the visible spectrum. This blends to create white light. This illumination source is very energy efficient, low cost, and good for general lighting and imaging. However, where its lacking in our use case is the fact that it is broadband. Meaning, it

really lacks that narrowband control that we are looking for to create our multispectral imaging. White LEDs are going to be useful for us in providing a uniform background illumination for our baseline scan but will fall short in our wavelength-specific diagnostic imaging where chromophore absorption varies sharply with light frequency. [16]

This leads us to our next source which would be using a multispectral LED array. This would contain various LED wavelengths of interest both in the visible spectrum as well as the near infrared. For applications in the dermatological sector, we are targeting wavelengths like blue (470 nm), green (530 nm), red (630 nm), and NIR (850 nm and 940 nm). Each wavelength in our array is a narrowband that we are using to target and subsequently highlight various optical properties of the skin. These arrays will allow for dynamic control over illumination by allowing us to selectively activate LEDs, often through pulse width modulation to control their intensity. This notion along with the fact that LEDs emit incoherent light and require less total power make for a nice fit in our SkinLumina system. [17]

Lastly, we also considered both laser-based and laser diode-based illumination systems. With Lasers, they produce very collimated, coherent, monochromatic beams of light. These qualities have their benefits as they allow deeper tissue penetration and very high spatial resolution, which can be very advantageous from a medical imaging standpoint. However, the main drawback with a laser approach is safety, as lasers often have much higher irradiance than LEDs. As we are trying to keep our system non-invasive and skin safe this approach would be hard to accomplish. Additionally, since laser light is highly coherent, it can cause lots of interference with skin tissue which can lead to noise and artifacts in the images. Switching to a laser diode approach would be a good middle ground between LEDs and lasers. Laser diodes are electrically pumped semiconductor lasers that will produce narrowband and coherent light in a very compact form. They offer better spectral selectivity and a greater penetration depth than LEDs, without being as complex and high powered as a traditional laser system. Again however, laser diodes have much greater irradiance than LEDs and also introduce thermal management concerns especially as we try and make the system portable. Additionally, they tend to be more costly and power hungry than LED-based systems. [18]

Strategy	Pros	Cons	Selected?
White LED Only	Low cost widely available	Poor spectral control lower contrast	No
Multispectral LED Array	High control Portable programmable	Requires LED driver circuitry	Yes
Laser-Based	High intensity, deep penetration	Expensive unsafe for skin bulky	No
Laser Diode-Based	Precise wavelengths, more portable than lasers	Thermal issues safety concerns	No

Table 3.1 Illumination Source Constraints

Table 3.1 highlights some of the pros and cons of all the illumination sources we have researched as a solution for this project. Ultimately, we decided to go with using a multispectral array in conjunction with white LEDs. We figured we could use the white LEDs to perform our baseline scan and imaging to determine the user's skin tone. Then follow up with subsequent imaging scans using our multiwavelength array to gather much more specific data on their skin features. This approach will allow us to stay below FDA power requirements while also being cost effective and programmable.

3.1.2 Filter Integration

Continuing with the design of our SkinLumina system, we next wanted to compare technologies for how we would be able to integrate a filter system into our design to accomplish the multiwavelength approach. We want to use filters because this is key in making sure that we are isolating the target wavelengths to be able to highlight the features we are trying to image. This is extremely important as different chromophores like melanin and hemoglobin absorb different wavelengths. We are considering many different options for our filtering system. The first being to have fixed bandpass filters in the optical path, another would be a motorized filter wheel, and lastly, we could use liquid crystal tunable filters.

First, we investigated using fixed bandpass filters of the various wavelengths in the optical path. These bandpass filters are passive optical elements that could be placed in front of the imaging sensor or in the illumination path. These filters would allow a narrowband typically between 10-50 nm of light through the filter while blocking out wavelengths outside the range. The filters are very widely available and relatively inexpensive and often have very high transmission efficiency. The only main downside is we would have to manually swap out each filter on each iteration of an image to swap imaging wavelengths which makes this setup very inflexible. After some thinking, we realized we could use these same types of filters but make a motorized mechanism that will iterate through each different bandpass filter to get rid of the negative of having to switch out each filter manually. We could use a stepper or servo motor to properly position the desired filter in the optical path. This would add a little extra cost to the project but still this option would be cost effective because it would just add a little bit more mechanical and software complexity to the backend. [19, 20]

Lastly, we considered the notion of using LCTFs (Liquid Crystal Tunable Filters). These are electronically tunable filters that make use of liquid crystal birefringence to modulate to the transmitted wavelength. These filters, much like the regular bandpass filters, provide narrowband transmission but offer continuously tunable transmission typically across a broad range of wavelengths. These liquid crystal filters contain no moving parts and therefore are very compact and provide switching speeds as fast as 10-50ms. This would make our multispectral approach super-fast and efficient. The main drawback to these filters is that they are quite costly, ranging from 3000 to 10000 dollars. They also require very heavy control circuitry to tune, making this a very complex method for our filter setup. [21]

Filter Type	Pros	Cons	Selected?
Motorized Filter Wheel	Programmable Modular low-cost	Mechanical and software complexity slower switching	Yes
Fixed Filters	Simple Cheap reliable	Manual switching limited flexibility	No
LCTF	No moving parts Fast highly tunable very fast switch speeds	VERY Expensive lower transmission complex control circuitry	No

Table 3.2 Illumination Source Constraints

Based on the table 3.2, it would be best to use a mechanical filter wheel. This would offer us the best tradeoff between imaging speed and affordability. We even considered not using a filter wheel at all and just hard coding the LED iterations to turn off selected colors and only have one on per scan. However, we ultimately went with the motorized filter wheel as it adds optical design to our project, whilst also lessening the load we need from our software and electrical engineers.

3.2 Additional Supplemental Technologies

Another main issue with our project is that the skin often comes in many various “states”. What I mean by this is that skin could have wrinkles, be very hairy, be very oily, have tattoos, etc. Most of these will affect the images in some way, shape, or form. They can greatly impair image quality and possibly obstruct certain diagnostic information. So, we need to look at a technological solution to help mitigate most of these negative effects and abnormalities produced by the differences in skin.

One solution when researching is the notion of “cross polarization”. The principle of cross polarization is that it involves placing two polarizing filters in the optical system, one in front of the illumination source and the second in front of the image sensor or camera. The key with this effect is you want one linear polarizer, typically the one in front of the LEDs, to be 0 degrees linearly polarized while the second linear polarizer is positioned 90 degrees or orthogonal to the first polarizer. When light from the source hits the skin, most specular reflections preserve their polarization so are thus blocked by the cross-polarization effect whereas the reflected light that has interacted with the tissue is depolarized and thus will pass through both polarizers and reach the imaging sensor. This technique would allow us to mitigate unwanted reflections from the surface due to oily,

hairy, or wet skin. If we did not have this mechanism under these circumstances our images would be saturated and it could even mask deeper features, we are trying to image. This is even more important for the near infrared wavelengths as they have a greater penetration depth where if we didn't have this technology implemented surface reflections would end up dominating the image. We are still looking into other either hardware or software methods to possibly continue to reduce surface reflections and increase image fidelity for tattooed and wrinkly skin. [22-24]

3.2.1 Use of Lambertian Reflectors in Diffuse Illumination Systems

Lambertian reflection is a method of diffuse reflection where light is scattered equally in all directions from a surface. Visually demonstrated in figure 3, we will be using Lambertian reflection to maintain a constant radiance when illuminating the skin sample for more consistent imaging in SkinLumina.

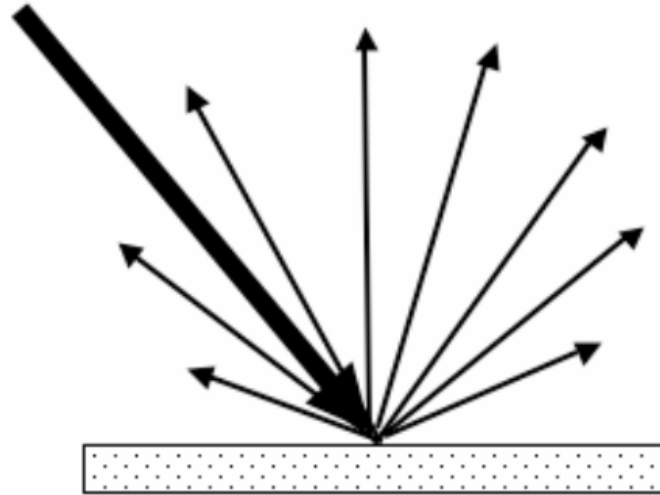


Fig 3. Lambertian reflectors scatter incoming light uniformly in all directions, independent of the angle of incidence.

Achieving spatially uniform illumination is critical for dermatological imaging when using multispectral light delivery architecture. The reflectors scatter incident light uniformly in all directions according to Lambert's cosine law. The Lambert's cosine law states that the radiant intensity observed from the surface is proportional to the cosine of the angle θ is given using equation 1.

$$I(\theta) = I_0 \cos(\theta) \quad (1)[25]$$

Light emitting diodes (LEDs) typically have non-uniformities due to the unstructured illumination dispersion. Principles previously established in backlit display systems determined that hot spots and directional biases in illumination occur when using LEDs. Using near-Lambertian reflectors eliminates these common lighting issues when using

LEDs and ensure a more consistent lighting source for imaging across various skin tones and complex surfaces.

Benefits in performance when using high reflectance material as a Lambertian reflector around a light source are shown in radiometric efficiency and optical uniformity. Comparable optical systems have shown when using a reflective cavity lined with materials exceeding 99% reflectance can retain over 95% of the incident luminous flux. When using a cavity lined with only 95% reflectivity, only 80% of the incident luminous flux is retained. By using multiple high-efficiency reflections, Lambertian geometry maximizes the photon delivery and minimizes power consumption at the same time. Having a less power-reliant system benefits an illumination system with more compact design.

The addition of a feature that removes illumination inconsistencies directly benefits multispectral imaging quality. Having a more consistent imaging performance enhances the system's ability to capture clear subsurface tissue analysis across diverse patient populations. This supports the core goal of SkinLumina to broaden the scope of inclusive and equitable diagnostic imaging.[26]

3.3 Comparative Analysis of Imaging Methods and Design Strategies

An investigation of imaging artifacts in varying skin types and improvements to this start from addressing a problem in the current technology and choosing the best solution based off of various research studies. Adjusting the focus of SkinLumina into improving performance across varying skin tones to segment and classify lesions accurately is what makes it stand out from other imaging devices on the market. The use of multispectral imaging in dermatology has shown promising diagnostic capabilities, yet imaging artifacts in melanin-rich skin remains a persistent challenge. High melanin concentrations in darker skin types lead to increased absorption in the visible spectrum, particularly below 600 nm. This can result in underexposed regions, reduced signal-to-noise ratio, and loss of lesion boundary contrast. These artifacts impair the segmentation and classification of dermatoses, especially when superficial pigmentation masks deeper pathological structures.

To address these limitations, it is important to extend the spectral coverage into the near-infrared range, where melanin absorption is significantly reduced. Incorporating wavelengths such as 850 nm and 940 nm, multispectral imaging systems can probe deeper dermal layers while preserving signal integrity across a broader range of skin tones. In the first comparison study by Iliesanu et al. (2023), the authors recommend computational approaches when using multispectral imaging systems. This includes exposure normalization, adaptive illumination control, and contrast enhancement algorithms to dynamically compensate for pigment—induced attenuation. These strategies collectively contribute to more inclusive and accurate diagnostic performance in multispectral imaging systems, supporting the need for device designs such as SkinLumina. Incorporating a larger spectrum and more custom controls to image with a device that is sensitive to phenotypic variability in skin optics.[27]

An additional improvement multispectral imaging devices could improve upon is their ability to segment and classify lesions accurately. To do this, investigating into the study by Delpueyo et al. (2018) highlights how to improve upon lesion segmentation and classification in skin cancer diagnostics. The system uses selected wavelengths from 414 nm to 1613 nm to detect differences in chromophore absorption, especially in melanin and hemoglobin. This spectral sensitivity helps distinguish lesion borders, pigment irregularities, and vascular patterns linked to malignancy. Multispectral imaging enables more accurate identification of features including asymmetry, atypical vasculature, and melanin distribution.

Multispectral imaging had been proven to perform well across a broader range of skin tones in comparison to using a single wavelength. In skin with a higher melanin distinction, contrast is reduced under visible light. The addition of near-infrared wavelengths improved penetration and contrast similarly to the previous imaging system when investigated. This inclusion helps reveal deeper structural features that may be hidden in standard imaging. This study also combines multispectral imaging data with machine learning tools to increase classification accuracy. Overall, the use of both visible and NIR light makes multispectral imaging systems more inclusive, sensitive, and reliable for diagnosing skin lesions.[28]

A comparative analysis of polarized and non-polarized imaging modalities was the final investigation when designing SkinLumina's imaging system. A observational study by Benvenuto-Andrade et al. (2007), showed polarized light dermoscopy versus non-polarized contact dermoscopy. The polarized and non-polarized methods were systematically compared to evaluate their diagnostic capabilities and differences in visualizing skin lesion features. Across 90 lesions assessed by two experienced dermoscopists, the study demonstrated several diagnostically significant features were modality-dependent. Notably, vascular structures and shiny white streaks were significantly more apparent under polarized light, while milia-like cysts and comedo-like openings were more consistently observed using contact dermoscopy. This contrast highlights that the polarizes method offers superior visualization of deeper dermal features due to its ability to suppress surface reflection and capture polarized light scattered from within the skin. In contrast, the non-polarized imaging method was shown to be more effective at revealing superficial epidermal features aided by direct skin contact and immersion fluid. Direct skin contact and immersion fluid helps reduce skin surface scattering. Importantly, diagnostic agreement between the two techniques was high confirming their complementarity rather than redundancy. The others of this study conclude that utilizing both imaging modalities in clinical practice provides a more comprehensive assessment of skin lesions. This indicates that non-contact demoscopy utilizing cross-polarized light reduces surface glare while giving visualization of deeper dermal structures. This is especially useful in assessing vascularized lesions, fibrosis, and potential malignancies such as melanoma. [29]

3.4 Part Selection

When it came to designing the SkinLumina system, we had to do careful and considerate research into which actual components we were going to use as well as calculate the specifications so that we are able to meet our performance, cost, and other system

requirements. We have evaluated every component against our technical specifications such as resolution, power consumption, complexity, and cost. The following subsections detail the comparison of proposed parts with the ultimate selection of these parts subsequently following, as well as explaining their integration into the overall SkinLumina system.

3.4.1 Camera Selection

To start, we wanted to take a look at possible cameras we could use in our system as this is the central core component of the imaging acquisition system that ultimately determines most of our resolution, sensitivity and wavelength range for our system. Given the fact that we are trying to take high resolution skin images across both the visible and near-infrared spectrums, we evaluated possible camera module options based on several key specifications:

Resolution (≥ 2 MP recommended for diagnostic skin analysis)

Pixel size (smaller pixels offer better spatial resolution but lower sensitivity)

IR sensitivity (important for imaging subsurface features at 850–940 nm)

Interface compatibility (SPI, USB, or MIPI CSI for MCU integration)

Form factor and mounting options (board-level or standalone modules)

Cost and power draw, considering the system’s battery-powered design

After extensively searching for camera sensors that would fit the above specifications, we narrowed our possible solutions down to 3 camera modules: the OV2640 (ArduCam), Sony IMX219 (Sony Pi Camera), and the Arducam Mini 5MP. All these cameras fit the bill for the minimum specifications we are targeting for our system, with each of them having their own benefits and drawbacks that we had to consider. Below in table 3.3, shown is that what compares the cameras based on our key specifications.

Camera Module	Resolution	IR Sensitivity	Interface	Cost (USD)	Selected?
OV2640 (Arducam)	2 MP	Moderate	SPI	~\$10	No
IMX219 (Sony)	8 MP	High	MIPI CSI	~\$25	Yes
Arducam Mini 5MP	5 MP	Moderate	SPI	~\$18	No

Table 3.3 Camera Comparison

After much consideration, we decided to go with the Sony IMX219 camera module. We ended up choosing this camera because it met all of our baseline specifications but also gives us a substantial upgrade in imaging quality and resolution, with the only two major drawbacks being it is on a harder code interface, and it costs slightly more than the other

options. We feel that this camera will allow us to achieve our systems imaging goals and objectives whilst still prioritizing cost and portability.

3.4.2 Filters

The next component we wanted to look at is using bandpass optical filters to be able to filter out multiple wavelengths. And focus on one at a time per image. These filters are key in our image acquisition process as without these we would have to develop complex software image processing algorithms to try and mimic this filter component. We need these filters to have high transmission for the given narrowband wavelength we are targeting that way we maintain image clarity throughout. These filters must be carefully selected as they directly affect image contrast, signal-to-noise ratio, and spectral accuracy.

Most narrow bandpass filters that are used in the biomedical field work through interference, using multiple dielectric layers that are designed to reflect and transmit certain wavelengths using constructive and destructive interference. Below are some of the key defining characteristics that are useful in helping us select what filter we are going to be using.

Center Wavelength (CWL): The peak wavelength of transmission (e.g., 470 nm for blue).

Full Width at Half Maximum (FWHM): The spectral width over which transmission exceeds 50% of the peak, typically is around 20-50nm. We need ours to be narrow to ensure separation between bands.

Peak Transmission: The percentage of incident light transmitted at the CWL, typically >85–90%. For SkinLumina specifically we are targeting 90% as this will directly impact our image clarity during acquisition.

Blocking Range (OD): The optical density (OD) in the rejection band (OD4 = 0.01% transmission), ensuring minimal signal leakage.

Angle of Incidence Sensitivity: Interference filters shift CWL depending on the angle of incoming light — typically blue-shifting at off-normal angles. This must be controlled in optical design.

When it comes to what filters we are going to be needing specifically for the SkinLumina project, we are targeting specific biomolecules like melanin, hemoglobin, and water content. Therefore, we are going to need filters that fit the absorption characteristics of these molecules. These absorption characteristics are shown below:

Melanin strongly absorbs in the 400–600 nm range.

Hemoglobin has peaks near 542 nm and 577 nm.

Water and deeper tissue layers absorb in the NIR (700–1000 nm), allowing subsurface exploration at our proposed NIR wavelengths; 850 and 940 nm.

In terms of filter selection, we are targeting bandpass filters that give us modularity, affordability, and meet our portable design. Therefore, each of our bandpass filters must have small optical diameters, which can be achieved using off the shelf parts, or custom buying filters, or cutting the filters ourselves. We also need these filters to have a narrow FWHM (20 nm to 40 nm), to ensure that during image acquisition we can distinguish all our wavelength bands. Lastly, they must have high peak transmission to avoid losses, minimize LED output power, and keep our image resolution high. We also explored the possibility of using dual-band and triple-bandpass optical filters. These filters are often coated to obtain multiple transmission peaks using a single optical filter whilst avoiding interference between peaks. [30]

Filter Slot	Wavelength Bandpass	Possible Filters	Peak Transmission	Notes
Blue (~470 nm)	460–483 nm	MidOpt BP470, Thorlabs FB470-10	$\geq 90\%$	Enhances surface contrast, matches LED band
Green (~530 nm)	535–565 nm	MidOpt DB550/850, BP550	$\geq 85\%$	Targets hemoglobin, vascular visibility
Red (~630nm)	~630–660 nm	MidOpt TB550/660/850 or DB660/850	$\geq 85\%$	For pigmentation and mid-depth imaging
NIR (~850nm and 940nm)	830–870 nm	Knight Optical BP850, MidOpt DB850	$\geq 90\%$	Reveals subsurface tissue features

Table 3.4 Optical Filter Comparison

We have decided to use start our initial design using the MidOpt single band optical filters for all of our visible wavelengths. This will allow us to simultaneously allow the targeted visible light to pass through while also blocking the unwanted NIR wavelengths. For our white LEDs we decided to use no filter at all so that we can get a equal baseline image that is the same across all skin tones. Lastly, for the NIR wavelengths at 850 and 940nm, still trying to find a dual-band option that has peaks around our two target wavelengths. This setup combine with the notion that our filter components will incur losses in intensity this will make sure we have a safe yet effective imaging system for what we are trying to accomplish. Our final optical filter decision is shown in table 3.4.

3.4.3 LED Specifications and Background

In multispectral dermatological imaging, the choice of LED illumination wavelengths directly influences the system’s ability to capture diagnostically relevant contrast across different skin layers and conditions. SkinLumina’s design is rooted in the principle that each spectral band contributes uniquely to the detection, characterization, and monitoring

of a wide range of skin abnormalities. Rather than relying on broadband illumination, SkinLumina incorporates a carefully selected array of discrete visible and near-infrared (NIR) wavelengths to optimize both spectral specificity and tissue penetration depth. This approach enhances sensitivity to key chromophores such as melanin, oxyhemoglobin, and deoxyhemoglobin, as well as structural and functional changes associated with inflammation, fibrosis, neoplasia, and wound healing.

The visible spectrum offers high resolution and contrast in the epidermis and superficial dermis, where chromophore concentration is highest. Blue light provides excellent sensitivity to superficial inflammation and microbial activity, while green light enables simultaneous visualization of melanin-rich pigmented regions and hemoglobin vascular patterns. Red light, with its moderate penetration and lower hemoglobin absorption, captures deeper vascular changes and early remodeling in the upper dermis. These visible bands are especially critical for delineating lesion boundaries, identifying early pathological transitions, and enabling effective segmentation particularly in skin types with varied pigmentation.[31]

Extending beyond the visible range, SkinLumina integrates NIR wavelengths to probe deeper structures that are less accessible through conventional imaging. LEDs in the 850 nm to 940 nm range penetrate into the reticular dermis and superficial subcutaneous tissue. This is where imaging can detect vascular remodeling, collagen degradation, and chronic inflammatory processes that do not manifest as clearly at shorter wavelengths. Unlike visible light, NIR is minimally absorbed by melanin, making it ideal for use across diverse skin tones and for visualizing subsurface abnormalities that may otherwise be obscured. The combination of visible and NIR bands enables SkinLumina to acquire both spectral and spatial data across skin depths, improving diagnostic accuracy and enabling quantitative lesion assessment.[28]

This multispectral strategy supports SkinLumina's broader goal to create an inclusive, portable, and noninvasive imaging platform that adapts to varied skin phenotypes while maintaining high diagnostic performance. The following sections will explore each wavelength range in detail, discussing its optical properties, biological relevance, and contribution to imaging contrast within the context of real-world dermatological applications.

Imaging with Blue Light

The blue light range is wavelengths falling within 400 nm to 500 nm. This light is seen as blue in the visible spectrum and provides specific advantages in skin imaging due to its interactions within human skin. Blue light has been shown to have stronger interactions with superficial chromophores and a high absorption by hemoglobin, cytochromes, and flavins when compared to other wavelengths. These interactions make it suitable for imaging skin features within the epidermis and upper dermis range. The chromophores that absorb blue light strongly serve as functional and structural markers of skin conditions including acne, inflammation, superficial vascular changes, and early-stage wound environments. In imaging systems using a multispectral setup benefit from incorporating a light source within the blue light range enables clinicians to enhance

diagnostic contrasts of these features when imaging skin. One of the LED wavelengths dermatologists use due to standing out when showing high contrasts within this range is the 470 nm light. This wavelength specifically targets superficial vascular and inflammatory features that are less distinguishable under broadband and other light sources.

When working with 470 nm blue light, research has shown that when interacting with key mitochondrial chromophores has an effect that stands out from other blue light. When 470 nm interacts with critical components of the electron transport chain such as cytochrome c and cytochrome c oxidase, these molecules exhibit increased photoactivity. When an increase in photoactivity takes place, cellular respiration and alteration of redox balance within the tissue is enhanced. These biochemical activations lead to measurable changes in optical scattering and absorption. The chromophore Protoporphyrin IX amplifies the sensitivity of these mitochondrial structures to blue light. This interaction and sensitivity intensifies the optical contrast associated with metabolically active or inflamed tissue.

These molecular interactions impact skin imaging by modifying the local concentrations of ATP, ROS, and mitochondrial density. This results in a change in light absorption and autofluorescence signatures within target regions. A change in light absorption and autofluorescence signatures are detectable changes through multispectral imaging systems. Enhancing the differentiation between normal and pathological tissues increases the imaging contrast in areas of subtle inflammation, hyperplasia, and early neoplastic activity. The influence of blue light on fibroblast metabolism can produce variations in light backscatter and surface texture additionally contributing to a clearer diagnostic and lesion margin definition in captured images.

The diagnostic utility of 470 nm when imaging is further reinforced by its ability to visualize inflammation-related phenomena. Blue light has been shown in research to stimulate macrophage polarization and promote tissue regeneration. This tissue transition accompanied by angiogenesis and dermal remodeling leads to observable changes in vascular density and collagen architecture. Both of these are key imaging targets in dermatological diagnostics. The high absorption of blue light by hemoglobin enhances the visualization of capillary loops, telangiectasias, and sebaceous gland activity aiding in the differentiation of certain skin conditions. These skin conditions include, but are not limited to rosacea, psoriasis, and inflammatory acne. This stands out in comparison to using other wavelengths outside of the blue light range when imaging dermatological skin features. [31]

Imaging with Green Light

The green light range is ranging from wavelengths falling within 500 nm to 565 nm. The incorporation of green light in a multispectral imaging system is driven by its ability to enhance optical contrast between vascular and pigmented skin features. Optical absorption characteristics of endogenous chromophores, particularly oxyhemoglobin and melanin. These characteristics have been shown to exhibit distinct profiles when using the green spectral range illumination improving lesion discrimination. As outlined in the optical modeling review by Jacques et al. (*J. Biomed. Opt.*, 17(9), 090901), hemoglobin

exhibits two key absorption bands centered around 540 nm and 575 nm. These wavelengths are responsible for the strong attenuation of green light in blood-rich regions of the skin. The absorption features localize mainly within the papillary dermis, where microvascular structures such as capillaries and venules reside. When skin that has these features is imaged under green light, these structures result in reduced reflectance and an increased absorption contrast. This can be used to visualize the vascular density and distribution in a range of skin tissue conditions including inflammation, angiogenesis, and neoplasia.[28] Some of these skin conditions can be recognized as bruising, irregular borders of redness or swelling, vein patterns, dot vessels, and new capillaries visible under the skin's surface.

Further evidence from Delpueyo et al. (*Sensors*, 2018, 18(5), 1441) supports this wavelength range having diagnostic evidence. Noting in their multispectral imaging system, 545 nm LEDs were selected to illuminate and assess the blood content in skin lesions. In this paper, reflectance intensity at 545 nm was compared to reflectance intensity at 660 nm where hemoglobin absorption is minimal. These wavelength 545 nm is absorbed by blood more than 660 nm to create a ratio when imaging. This is useful due to skin cancers, such as melanoma, having a higher blood concentration than in less dangerous benign nevi lesions. Lesions with neovascularization or increased blood flow demonstrated greater absorption at 545 nm, which was associated with malignant progression. Adding a green LED into SkinLumina's spectral band selection further supports classification algorithms sensitive to hemodynamic changes within lesions.

Green light additionally provides meaningful interaction with epidermal melanin and maintains a continuous absorption profile across the visible spectrum. This absorption supports the precise outlining and identification of pigmented lesion margins, particularly in melanocytic nevi and early-stage melanoma. The combined sensitivity to both melanin and hemoglobin allows the 530-545 nm band to target optical differences across multiple skin layers. The diagnostic use of a 530 nm light source when imaging offers a dual-contrast advantage within a single illumination channel. The increase in ability to visualize vascular structures, segment lesion boundaries, and capturing spatial and spectral features are critical when imaging broad ranges of skin types and melanin concentrations.[32]

Imaging with Red Light

The visible red light spectrum falls between 620 nm and 750 nm with one of the most commonly used LEDs being 630 nm. 630 nm red light is strongly supported in skin imaging systems due to its optical penetration characteristics and diagnostic sensitivity to dermal features. As demonstrated in the radiative transfer modeling by Barun et al. (2007), red light around 630 nm exhibits a low absorption by hemoglobin when compared to shorter wavelengths in the green light spectrum. This reduction in absorption allows photons to penetrate more deeply into skin layers reaching the upper and mid-dermis. In the upper and mid-dermis is where critical targets such as capillary networks, inflammatory infiltrates, and fibrotic tissue reside. Rosacea, chronic sun damage, eczema, contact dermatitis, psoriasis, and thickened skin from scarring are examples of these possible targets. In comparison to highly absorbed wavelengths like 530 nm, red visible light provides enhanced access to deeper structures without being

significantly scattered or absorbed in the epidermis skin layer. This is shown in figure 3.1. where the absorption rate of water, melanin, and hemoglobin varies according to wavelength of light. This makes it more ideal for reflectance-based imaging systems. Imaging systems that rely on contrast generated by differential absorption and scattering in both healthy and pathologically altered tissue benefits from the addition of a red light source.[33]

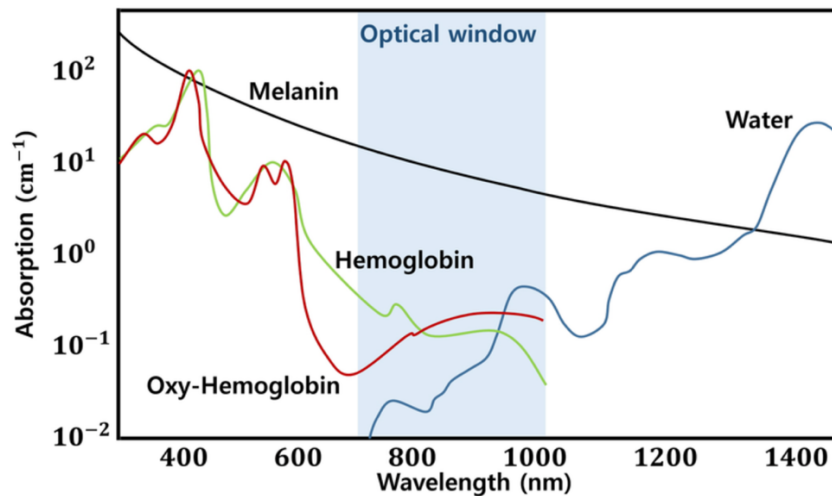


Fig 3.1 Graph showing the absorption spectra of water, melanin, and hemoglobin as a function of light wavelength. [34]

Red light supports imaging through its interaction with vascular and metabolic markers. Although the hemoglobin absorption is lower at this wavelength range, it remains sufficiently responsive to variations in blood content and tissue health. These variations are especially shown in inflamed or neoplastic tissue where vascular remodeling occurs. This makes a wavelength of 630 nm highly suitable for identifying features such as neovascularization, inflammatory foci, and collagen degradation. All of these features alter tissue optical properties in ways that are detectable when using multispectral imaging. Research on LED-based therapies indicate that 630 nm red light influences biological processes such as fibroblast activation and collagen synthesis. These biological processes are not only therapeutic in nature, but exhibit as spectral and textural changes in imaging. When red light that contains these benefits is incorporated into imaging systems, the ability to enhance contrast and detect certain abnormalities is important when expanding the imaging spectrum. Red light at 630 nm specifically assists in highlighting subsurface lesions, assessing dermal remodeling, and delineate vascular involvement. This brings a balance between penetration depth and contrast generation in a non-invasive, label-free diagnostic process.[4]

Imaging with Near-Infrared Light

Near-infrared (NIR) wavelength range spans from about 800 nm to 2500 nm, but 850 nm to 950 nm is part of the most commonly used range in multispectral skin imaging. The integration of NIR wavelengths within this range offer diagnostic advantages enabling

deeper tissue visualization and improved characterization of dermal pathology. Demonstrated in a study by Delpueyo et al. (*Sensors*, 2018), longer NIR wavelengths such as 950 nm provide significantly enhanced penetration in to skin layers compared to shorter wavelengths. Scattering increases with tissue depth, but the relative attenuation of absorption by melanin and hemoglobin allows photons at these wavelengths to reach the deep dermis and superficial subcutaneous tissue. In this study's imaging of melanocytic lesions, the researchers observed a stronger contrast when using 950 nm to observe melanomas. This suggests that deeper structural alterations and disruptions below the skins surface can be detected more effectively in the NIR region. This research highlights the unique capability of NIR imaging to visualize pathological changes beneath the superficial skin layers. It proves critical structural information that aids in differentiating between lesion types.[28]

Evidence supporting the utility of 820 nm to 950 nm wavelength band is presented in the comprehensive review by Marti et al. (*Photodermatol Photoimmunol Photomed*, 2023). This paper highlights both the optical and biological benefits of NIR within this spectral window. The authors reported that wavelengths in this range when applied at clinically safe irradiances can penetrate to the papillary and reticular dermis. A safe irradiance range around 15 mW/cm² to 25 mW/cm² can uncover key features such as collagen fibers, vascular plexuses, and fibrotic tissue. In addition to its physical depth of penetration, NIR light has been shown to stimulate collagen and elastin production and promote tissue remodeling in both clinical and preclinical studies. These remodeling processes lead to measurable changes in tissue optical density and scattering profiles. Using these optical changes in NIR reflectance imaging can identify subsurface fibrosis, angiogenesis, and structural heterogeneity. Importantly, these changes occur without damaging the epidermis and ensures that using NIR wavelengths is suitable for safe and repeatable imaging.

The inclusion of 850 nm and 940 nm wavelengths are fundamental in addition to the contrast provided by visible light which is often limited to superficial pigmentation and hemoglobin signatures. By extending the spectral range into the NIR, the system is capable of probing deeper dermal layers. This allows for capturing of information including vascular perfusion, tissue oxygenation, and collagen matrix changes. This data plays a pivotal role in diagnosing and monitoring dermatological conditions such as melanoma, chronic inflammation, and scarring. The ability to asses these features across a broader spectral profile enhances the sensitivity of multispectral classification algorithms. Expanding into the NIR wavelength range supports SkinLumina's mission of providing inclusive, noninvasive diagnostic imaging for diverse skin types and clinical needs. [35]

The table 3.5 displays all of the wavelengths we are going to use and why exactly each wavelength was chosen. It presented what each LED is useful in imaging on the skin as well as how they are useful to the overall system. When looking at actual LED components we can use in our system we made sure to prioritize FDA compliance and staying under 10mw per cm squared. This ensures that our device remains compliant and non-invasive in nature. We also are making sure the LEDs we choose have enough radiant flux to image through filters and with losses as well as their peak wavelengths should match the filters we have selected as well.

Wavelength	LED Model	Peak Wavelength	Power Output (mW/cm ²)	Viewing Angle	Selected?
Blue	Nichia NSPB500S	470 nm	6–8 mW/cm ²	120°	Yes
Green	Cree C503B-GCN	530 nm	7–9 mW/cm ²	125°	Yes
Red	OSRAM SFH 4550	630 nm	8–10 mW/cm ²	120°	Yes
NIR 1	Lite-On LTE-302	850 nm	9.2 mW/cm ²	130°	Yes
NIR 2	Vishay TSAL6400	940 nm	9.8 mW/cm ²	100°	Yes
White (baseline)	Everlight 67-21	Broadband	6–9 mW/cm ²	120°	Yes

Table 3.5 LED Comparison

Table 3.5 highlights all the wavelengths of LEDs we plan to use and shows wavelength, output power and ensures they are compatible with the filters we have also chosen. Using the LEDs above will give us enough light power to be able to get clear images in the visible and near-infrared.

3.4.4 Lens Selection and System Design

For our SkinLumina project, our imaging system needs a lens setup that is capable of capturing images with high contrast and high resolution, whilst imaging across a broad spectral range. Our system also must have wavelength consistency, minimized 1st order aberrations, and be modular in nature. We are designing the system to use an infinity corrected optical setup centered around two achromatic doublet lenses.

In a system that is infinity-corrected, the first lens in the system, or the objective lens, collimates the light that comes off the sample, making the light parallel rays. There is then a second lens placed at the sum of the two lenses focal lengths, known as the tube lens. This lens is responsible for focusing the light on our imaging sensor. Using an infinity-corrected system will also allow us to place other optical elements like the filter wheel and aperture in the space between the two lenses because the light is collimated so the rays will not be interfered with. The proposed optical lens system can be shown in the schematic figure 3.2 below.

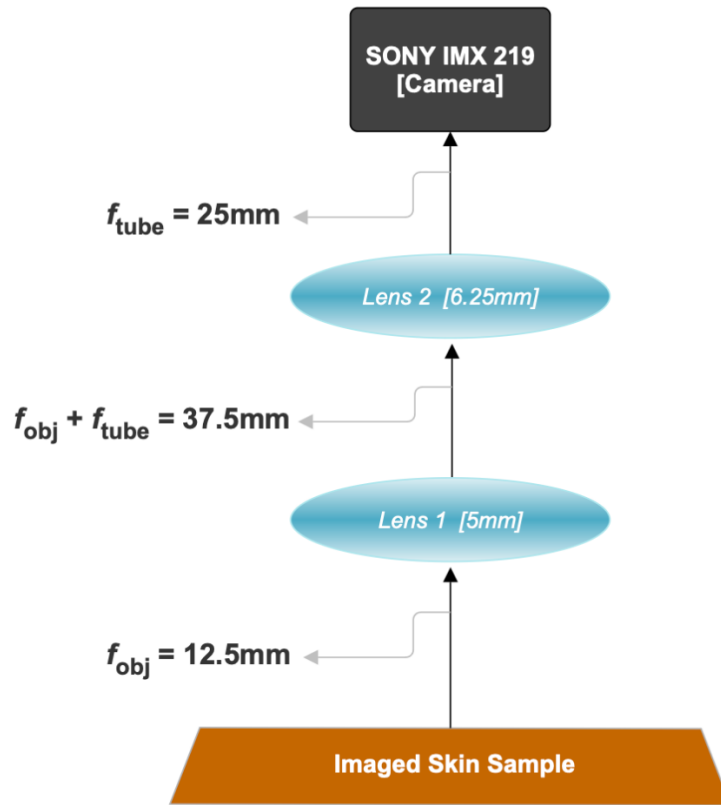


Fig 3.2 Optical lens schematic

Our choice in achromatic doublet lenses is fairly important as we chose this lens specifically for its optical properties as it pertains to bio-photonic imaging processes. An achromatic doublet lens is usually made from two different pieces of glass compounded together, often a crown and a flint. The bonding of these two types of glass forms a lens that is great at correcting both chromatic aberration and spherical aberration. When compared to traditional singlet lenses, doublet lenses offer key advantages such as significantly improving image sharpness, color accuracy, and particularly important when imaging across a broad spectral range. Without the use of these lenses, we would not be correcting first order aberrations which would cause shifts in the focal length and imaging plane; leading to lesser resolution and image differentiation especially for the features we are targeting exceedingly difficult. [36, 37]

We want an Imaging FOV of 10mm x 10mm

$$\text{Magnification } (M) = \frac{\text{Sensor Diagonal}}{\text{Object Diagonal}} = \frac{f_{\text{tube}}}{f_{\text{obj}}}$$

$$\text{Sensor Diagonal} = \sqrt{(3.68\text{mm})^2 + (2.76\text{mm})^2} = 4.6\text{mm}$$

$$\text{Object Diagonal} = \sqrt{(10\text{mm})^2 + (10\text{mm})^2} = 14.14\text{mm}$$

$$M = \frac{4.6\text{mm}}{14.14\text{mm}} = 0.325 \cong 0.333$$

This is the lowest magnification we can have to be able to image in our FOV the features of the skin we are targeting.

Now to calculate focal lengths:

First, we chose an appropriate objective lens focal length that is reasonable for goals of our system; $f_{\text{obj}} = 12.5\text{mm}$

$$f_{\text{tube}} = M * 12.5\text{mm} = 0.333 * 12.5\text{mm} \cong 4.2\text{mm}$$

Since commercial lenses at our minimum calculated focal length are very expensive and hard to find off the shelf, we decided to target a 2x magnification for our system giving us a focal length for the tube lens at 25mm.

Fig 3.3 Mathematical proof of concept: magnification and focal lengths

The above figure 3.3 details mathematically how we calculated our proposed magnification and focal lengths for the objective and tube lenses given that we want an imaging field-of-view of 10 by 10 millimeters. We plan to use lenses with these focal lengths to test the working principles of our imaging system, as using lenses with larger focal lengths will make testing much easier. When we eventually build the final prototype for our system we are aiming to have the whole optical lens system stay under 30mm. We are also still researching and deciding what magnification would be best for our system; whether that's using a demagnified or magnified system. This would directly affect our lens focal lengths so that is currently still to be decided.

Lens Model	Focal Length	Diameter	AR Coating	Transmission Range	Selected?
Thorlabs AC127-019-A	19 mm	12.7 mm	VIS-NIR (350–700 nm)	400–700 nm	No
Thorlabs AC080-010-B	10 mm	8 mm	NIR (650–1050 nm)	650–1050 nm	No
Edmund Optics #49-778	10 mm	6.25 mm	Broadband (VIS-NIR)	400–1000 nm	Yes
Edmund Optics #49-883	40 mm	12.5 mm	Broadband (VIS-NIR)	400–1000 nm	Yes

Table 3.6 Optical Lens Comparison

The above table 3.6 shows a few lens options we could use in our system from the best commercial vendors in the optical component market. We decided to use the highlighted lens above from Edmund Optics as it provides high broadband transmission across both the visible and NIR spectral ranges. Using these lenses would also allow us to easily use commercially available M12 or C mounts to hold the lenses or even custom 3D print our lens mounts. This would help maintain the modular nature of the SkinLumina system.

3.4.5 Lambertian Reflectors

Another technology we are proposing for this project design is the use of Lambertian reflectors, essentially a mirror like material or object that will allow us to increase the light intensity from the LEDs onto the region of interest we are trying to image. This setup will also allow us to increase the illumination efficiency and light uniformity of our multispectral LED arrays. These reflectors will aid in redirecting off-axis light toward the imaging target on the skin. This will effectively increase the amount of useful light emitted from the LEDs, whilst preserving the spatial characteristics needed for high-contrast biomedical imaging. In LED systems, a lot of the light exits the emitter at wide angles which reduces the intensity directly in the conventional straight direction. If we surround the LEDs with a reflective mirror-like cavity or film this previously wasted light is now redirected to increase the brightness at the plane, we are imaging at. This concept is super important for our imaging in the near-infrared wavelengths, as LED intensity in this range is typically weaker and we need greater intensity to penetrate further into the skin and maximize the NIR LEDs full absorption range.

Lambertian reflectors conceptually work by exhibiting diffuse reflections, this is where light is scattered uniformly in all directions regardless of the incidence angle. For our SkinLumina project specifically we have researched two possible types of reflectors:

Diffuse white reflectors: (PTFE, sintered Teflon, or white-coated polymers) for a Lambertian effect, excellent for uniformity towards the region of interest and minimizing hotspots.

Specular mirrors: (aluminized film, polished foil, acrylic mirror segments) for maximum beam collimation and directional gain. Which can be useful when aiming to penetrate deeper into tissue; super important for NIR.

Both of the above options have been deeply researched and considered in use for our system. We are thinking of shaping the reflectors into hemispherical or conical cavities around the LED arrays. This will help in optimizing the LED intensity while keeping the same illumination profile across the imaging region of interest. What we end up deciding to use between diffuse and specular reflectors depends on our idea of balancing the uniformity of the LEDs compared to the peak intensity profile. [38]

Reflector Type	Material	Reflectivity (VIS–NIR)	Geometry	Uniformity	Selected?
White PTFE Sheet	PTFE (Teflon)	~95%	Cylindrical well	High	Yes

Silver Mylar Film	Aluminized PET	~98%	Faceted cone	Medium	Still in Consideration
Acrylic Mirror Segments	Polished PMMA	~92–94%	Planar tiles	Low	No

Table 3.7 Lambertian Reflector Comparison

The table 3.7 compares diffuse and specular reflector materials and geometries suitable for this application. For our SkinLumina project we have decided to go with a highly reflective white PTFE sheet. This is a plastic Teflon material that is highly reflective between 250 nm to 2500 nm. This reflector material also incurs only about 5% loss in our spectral range, making it a great option to increase the uniformity of our LED arrays. As mentioned above, we are looking into how we can increase the effective intensity of our NIR LED arrays to boost their penetration depth for subsurface imaging. One possible solution for this would be to use something like a silver- mylar film. This has very high reflectivity and is great at enhancing and reflecting NIR radiation. We think this would be good to use in our design to increase our systems subsurface imaging capabilities without going to longer IR wavelengths. We just need to figure out when it comes to designing and implementing the LED arrays, how we could implement both the Teflon sheets and the mylar sheets for their respective LED groups.

3.4.6 Polarizers

The next component we need to implement is polarizers, specifically using a “cross polarization” technique. This will be crucial to our overall system’s performance as this will help to reduce surface glare and enhance the subsurface features we are looking to image. As mentioned previously, this technique involves placing a linear polarizer in front of the LEDs and a second polarizer orthogonal to the first polarizer that is placed in front of the camera. This will block specular reflections that maintain the polarization of incident light while allowing the depolarized scattered light that has passed through the tissue to reach the camera. This is important because when imaging oily or wet skin the specular reflections off the surface will not reach the camera and allow for clear subsurface imaging.

We are looking to use a polarizer with a high extinction ratio, aiming at >800:1. The extinction ratio is a measure of how good the optical component is at blocking light with a specific polarization. This will ensure that we are effectively suppressing the reflective light rays off the surface of the skin while still prioritizing high optical transmission across a broad spectral range. We looked at a few possible options for components when it comes to polarizers; we could use sheet-based polarizers or standard optical mounted lens-style polarizers. Sheet-based polarizers would offer us a lot of versatility in our system’s design as we could easily integrate them into our flat LED array design and camera. They are also a very cost-effective option as traditional polarizers tend to be a substantial uptick in cost; thus why we are leaning towards using sheet based polarizers.

Polarizer Model	Type	Spectral Range	Extinction Ratio	Form Factor	Selected?
-----------------	------	----------------	------------------	-------------	-----------

Thorlabs LPVISE100-A	Linear Film	400–700 nm	>1000:1	100 mm × 100 mm sheet	Yes
Edmund Optics #88- 240	Linear Film	400–700 nm	~500:1	50 mm diameter unmounted	No
Knight Optical LPVIS-BB	Broadband Linear	400–950 nm	>800:1	25 mm diameter mounted	Yes

Table 3.8 Polarizers Comparison

The table 3.8 categorizes the polarizers considered for implementing cross-polarization in the SkinLumina system. These components were selected based on their spectral range, extinction ratio, and physical format, all of which affect their ability in reducing surface glare and preserving subsurface imaging contrast. We ultimately decided to use both a film style polarizer for in front of the LED array mainly for its design versatility as well as, a traditional lens style polarizer in front of the camera as it will be much easier to implement in the optical stack.

3.4.7 Aperture

In many optical imaging systems like the one detailed in this paper, the aperture play a huge role in being able to control the system's depth of field and directly effects image contrast. By using an aperture, we are essentially able to limit the amount of light that enters the imaging optics of our system and will therefore lower the risk of aberrations and improve focus especially on uneven surfaces. This is super important when doing things like dermatological imaging like this project is trying to accomplish, as many surfaces like moles, scars, and other lesions can vary greatly in their skin topology.

One thing that is important to note when it comes to an aperture is balancing the trade-off between spatial resolution and signal strength. For example, a smaller aperture increases depth of field and will reduce chromatic and spherical aberrations but will subsequently reduce the output light intensity. On the contrary, a larger aperture allows more light. This will improve SNR but decreases the depth of field and could introduce image blur. This is why choosing a proper aperture for our system to balance these tradeoffs is key. Since our system uses an infinity corrected system, the aperture can be placed anywhere in the collimated light space between the two lenses. This also gives us a little more play in our aperture size as we can also move the aperture within the collimated space to adjust. We researched three different types of possible aperture types for our system described briefly below:

Fixed Iris Disks: Simple laser-cut or machined apertures with a specific diameter. This solution is very cost effective and easy to incorporate into our system but lacks adjustability.

Manual Iris Diaphragms: Adjustable ring-style diaphragms allowing real-time tuning of the aperture size. These are a little more expensive than fixed disks but offer adjustability which would be great for testing and initial prototyping.

Electronically Controlled Iris: Motorized apertures for programmable control. These apertures typically are not cost-effective and much larger in size but do offer the highest precision of control. [39]

Aperture Model	Type	Diameter Range	Adjustment Method	Size/Form Factor	Selected?
Thorlabs ID12/M	Manual Iris	1.0 mm – 12.0 mm	Manual ring	M12 mountable unit	Yes
Edmund Optics #36-395	Fixed Aperture	2.0 mm	Static	25 mm disk	Yes
Thorlabs SH05R/M + SM1D12D	Motorized Iris	0.8 mm – 11 mm	Stepper motor	Large (SM1 tube-based)	No

Table 3.9 Aperture Comparison

The following table 3.9 outlines the apertures we researched for integration in the SkinLumina optical system. Apertures are essential for controlling light throughput, depth of field, and image contrast. The ideal aperture must balance compact size, adjustability, and compatibility with an infinity-corrected optical system. This is why we ultimately went with two actual apertures as of right now. We wanted to use Thorlabs ID12/M initially for prototyping and testing throughout the first half of senior design two. Doing this would allow us to easily tune and adjust our imaging system to get the desired output images. We then also would like to end up using the Edmund Optics fixed aperture rings, where we end up using the fixed ring size that performed the best during testing with the manual aperture. Although this proposed two aperture approach should work just fine, if money and time allow, we would like to switch to an electronically controlled aperture as this would really level up the customizability and modularity of our SkinLumina system.

3.4.8 Microcontroller Platform

Choosing a microcontroller is one of the most key integral parts, as this is the backbone of the SkinLumina project. This project needs a microcontroller to handle heavy-load, semi-complex hardware systems, controlling and handling them in an efficient manner. This microcontroller should handle LED timing, sensor interfacing, and motor control. We have considered several alternatives for the low-level control layer that best gives the availability for ports, which allows for further additions to the project and simplistic design; low-level hardware timing accuracy for the many sequences that work in tandem, which all gives the most optimal results and performance; and wireless integration for display of information and sending results to an external display for a flexible and easy user interface. To compare, we chose three platforms that give great coverage for all the requirements we had: the Arduino Uno, the STM32, and the ESP32.

The microcontroller's responsibilities begin with driving the multispectral LEDs using pulse width modulation and must not have any issues with high-precision timing. Controlling the filter wheel via the stepper motor, which communicates through a driver

connected to the board itself. The microcontroller itself (whichever platform is chosen) communicates to the higher-level controller (the single computer, i.e., Raspberry Pi) for image sequence synchronization via UART while supporting deterministic timing with extreme accuracy. The different routines held separate from the microcontroller and the SBC make timing complex as instructions are being sent across to each but allow for better symbiosis and efficiency as the microcontroller and the SBC handle their own routines, which fit their architecture.

The project specifications give a clear minimum functional requirement based on the subsystems and their extensions. From the LEDs we have determined that we need at least 4 digital outputs for the individual channels (red, green, blue, NIR). We have determined 4 outputs for the stepper motor driver connecting to the microcontroller and 2 lines for serial communication between the SBC and board. The board must support sub-millisecond pulse durations for the fast-timing LEDs along with timer interrupts.

The final discussion and group consensus decided on the dual combination of both the Arduino board and the Raspberry Pi. The Arduino itself is known for its simplicity to program and work with. It works perfectly for the low-level hardware while delegating tasks to all the hardware under its architecture (i.e., LED pulsing and stepper sequencing). As with all systems, the Arduino has its drawbacks, but none of them are detrimental or hindering to the project. It has no built-in wireless, and while its limited GPIO number of pins is lower compared to the other, it still has more than enough for the project. As shown in table 3.10, the Arduino compared to the others, has a better platform for easy access and software design while offering superior timing capabilities for its key communication to other subsystems. This dual-processor architecture (MCU + SBC) mirrors a master-slave-time model where the Raspberry Pi is the imaging master and the Arduino is the real peripheral slave.

Feature	Arduino Uno/Nano	STM32F103 / F401	ESP32
Clock Speed	16 MHz	72–84 MHz	160–240 MHz (Dual-Core)
GPIO Pins	~14 Digital, 6 Analog	37+	30–34
Timer Resolution	~4 μ s	<1 μ s	<1 μ s
Hardware PWM Channels	6	10–16	16

ADC Resolution	10-bit	12-bit	12-bit
Native Wireless	No	No	Yes (Wi-Fi + BLE)
USB Serial	Yes (Native)	Yes (via ST-Link or USB)	Yes (Native)
Idle Power	~40 mA	~10–15 mA	~20 mA idle
Voltage I/O	5V Logic	3.3V Logic	3.3V Logic
Ecosystem / Libraries	Strong	Moderate	Good (some gaps)
Development Environment	Arduino IDE	STM32CubeIDE/PlatformIO	Arduino IDE / ESP-IDF

Table 3.10 Microcontroller Comparison

3.4.9 Single Board Computer

Only using a microcontroller for the SkinLumina multispectral biomedical imaging system is not enough to manage the complexity of the different routines and operations, such as the image capture, data storage, and machine vision-based decisions (most of the complexity comes from the imaging subsystem). A single-board computer provides a higher level of processing to properly execute the complex operations with efficiency, along with different modules camera interfaces to the camera module, different peripherals, and data storage.

The SBC responsibilities begin with additional camera peripheral interface support to have proper instructions executed for the entire imaging subsystem, but the key aspect is sequence. Data storage is an overlooked but key aspect. As it contains all the information stored and calculated for our results, a micro SD and USB support system help with storage capabilities and reducing a large amount of error. Along with USB support for the data storage but also for the hosting of any additional peripheral systems that rely on the SBC. A UART communication system helps communicate with the MCU for proper instructions given from the master board to the slave MCU as shown in table 3.11.

Feature	Raspberry Pi 4	Jetson Nano	BeagleBone Black	Intel NUC (Entry)
---------	----------------	-------------	------------------	-------------------

CPU	Quad-core 1.5 GHz ARM	Quad-core ARM Cortex-A57	AM335x 1GHz ARM Cortex-A8	Dual/Quad-core Intel x86
RAM	2–8 GB LPDDR4	4 GB	512 MB	4–16 GB
GPU / AI Acceleration	VideoCore VI (Basic)	NVIDIA Maxwell 128-core	None	Integrated Intel UHD
Camera Interface	CSI + USB	USB only (no native CSI)	USB only	USB only
GPIO	40-pin Header	40-pin Header	72 pins (Complex Use)	Not Standard
OpenCV & Python Support	Fully Supported	Accelerated	Limited	Advanced (Overkill)
Power Consumption	5–7 W	10–12 W	3.5 W	15–30 W
OS Support	Raspbian (Debian-based)	Ubuntu-based Jetpack	Angstrom, Debian	Windows/Linux
Price (Approx. USD)	\$35–\$75	\$99–\$150	\$60–\$70	\$150+

Table 3.11 Single-Board Computer Comparison

The Raspberry Pi is an ideal choice due to its balance across processing, cost, camera interface, and software environment. The Raspberry Pi supports low latency and high-quality cameras, like in our case, the CMOS. It allows for USB support if there are any additional peripherals. Also, including a great software environment for additional libraries and support for subsystems. It also is extremely compatible with the Arduino due to its flexibility and energy efficiency as shown in table 3.12.

Function	Handled by SBC (Raspberry Pi)?
----------	--------------------------------

LED Timing and Synchronization	No (Handled by Arduino)
Motor/Filter Wheel Control	No (Handled by Arduino)
Image Acquisition	Yes (via Pi Camera or USB Camera)
Image Processing	Yes (Contrast Enhancement, ROI Analysis, Storage)
Communication with Arduino	Yes (Serial Commands over USB)
Data Logging	Yes (CSV, Image Logs, Time Stamping)
User Interface (GUI or App Host)	Yes (Tkinter, Flask, or PyQt GUI)

Table 3.12 Raspberry Pi Comparison

3.5 Power Regulation and Safety

The power architecture of the SkinLumina Project is key, as it is the limiting factor for the entire portability of the said device. Due to its delicate nature, any failures in the power system can ruin the entire project or at least lead to image sequencing errors and data corruption, microcontroller resets, breakdowns in communications between SBC and MCU, and potential harm to patient and operator while in use. All of which are not to be tolerated at all, as this is a biomedical device to be used by all personnel who can afford this cheap alternative in skin analysis. Therefore, power regulation and safety methods are key to ensuring the system's durability and reliability. The primary safety specifications for this are shown in table 3.2.

The proposed topology of the power architecture begins with the battery pack, which supplies all components connected. Using the many safety methods proposed is a sure way to greatly reduce any faults or hazards from this potentially dangerous power system. Using resettable fuses in the beginning ensures a secure hardware solution to voltage spikes, and with its combination of a transient voltage diode and a bulk capacitor along the power line, it greatly ensures power stability. Following this, the 12V goes through 2 buck converters, which lower the voltage from 12V to 5V. Ferrite beads along the path are used to absorb any fleeting electromagnetic field from the high voltage as it travels to not corrupt any systems connected. Both the TVS diode and fuse are a sure combination to stop any spikes or surges coming from the power system for stability. The bulk capacitors are another method to stabilize any minor peaks in the already stabilized voltage leaving the diode.

Component	Typical Voltage	Current Draw (Peak)
Raspberry Pi 4	5V	2.5–3A
Arduino Uno/Nano	5V	50–250 mA
LED Array (RGB/NIR)	3.3–5V	20–200 mA per LED
Filter Wheel Motor	5V or 12V	150–400 mA
Camera (USB/CSI)	5V	250–500 mA

Table 3.2 Power Architecture Safety Comparison

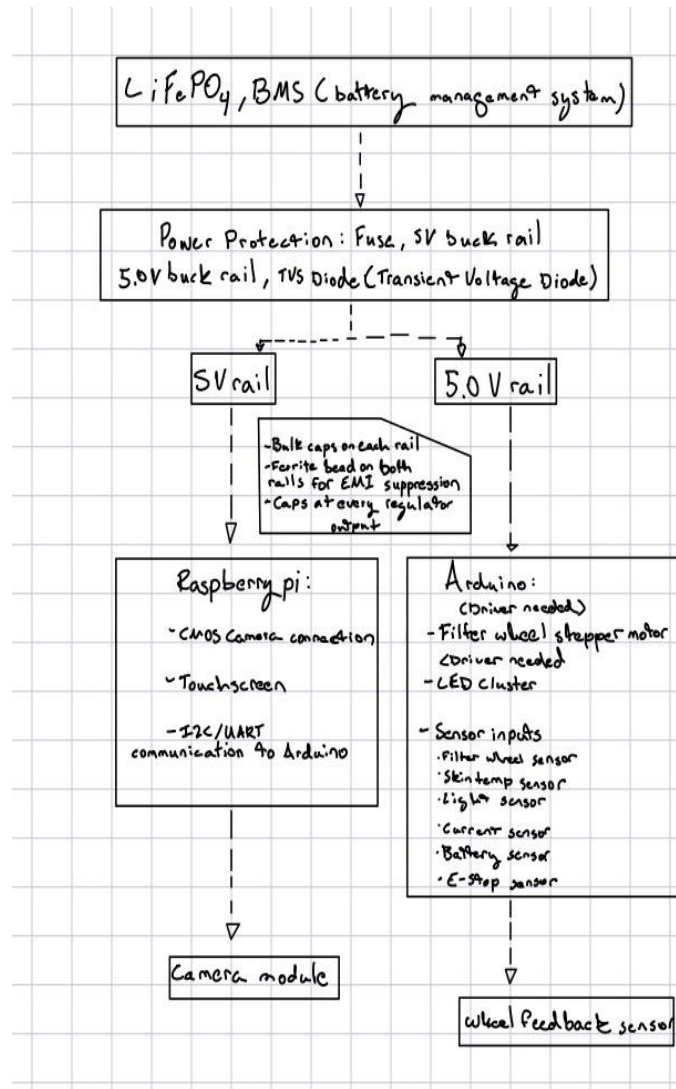


Fig 3.4 Battery management system

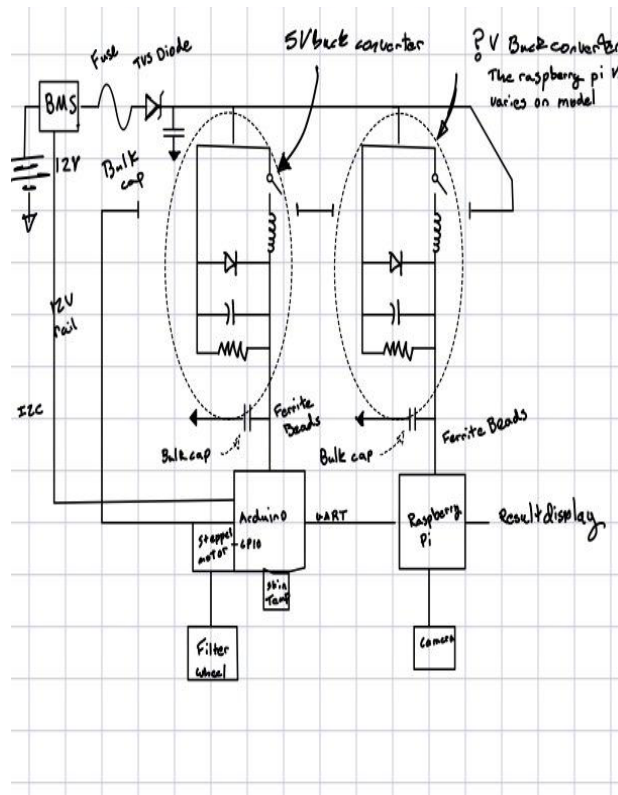


Fig 3.5 Circuit schematic and ground plans

Following figure 3.4, figure 3.5 shows the circuit schematic and ground plans for a PCB to system layout. This includes a single star ground tie point at a 12 V input protection. The digital ground under the MCU is shown alongside drivers and the communication system. The Analog ground layout will be under sensors and ADC. A note is that the tie DOND and AGND are at the star ground tie point only.

Power System Load

There are a total of 4 systems that act as a load from the power system: the ATM328 board, the stepper motor board, and the LED board. The LED driver board draws approximately 1.80 A, while the stepper motor and ULN2003 driver add another 0.25 A. The ATmega328P control board consumes about 0.05 A, and the Raspberry Pi requires up to 3.00 A under full load. Altogether, the system reaches a total maximum 5-volt current draw of approximately 5.10 A, which can be rounded to about 5 A for design calculations. The power system design has to maintain tight voltage regulation, low ripple, and a fast transient response because of the rapid switch of multiple high-power LEDs and the motor causing transient spikes. Any distortion from noise or voltage sag can affect LED brightness, camera stability, and data performance, all of which are reasons for a needed clean, stable power source.

Power System Expectations

A system like this needs a highly stable DC source that can give out sustained continuous current, can handle transient spikes, and can deliver stable voltage, all the while being safe as well. Several different types of systems were considered.

Wall adapters can provide stable voltage but cause excessive heat and remove the portability aspect of the project. Its poor efficiency at high current is not suited for this mobile system. Lithium ions are known for their high energy density and capable delivery. Their lower thermal stability and voltage drop under load spikes make this candidate too volatile for our biomedical device. Nickel-hydrogen battery systems are safe but bulky and have a poor discharge rate.

A lithium iron phosphate battery system was the top choice to follow through with. Its long life cycle and excellent thermal stability are a great combination for the desired features of a biomedical imaging device. Different from regular lithium-ion chemistry systems, lithium iron phosphate maintains a flat discharge rate for consistent output and excellent stability. This is a good safety measure to prevent voltage sag that would otherwise affect other peripheral systems on its load. The chemistry's safety, reliability, and voltage consistency make it the best option available.

Power System Regulation

The 12V battery pack system is designed to be stepped down to deliver clean and well-regulated power to the peripheral systems. This 5V regulator must produce at least 5A, handle fast load transitions, maintain low ripple, be efficient enough to prevent heat buildup, and support high-frequency switching for better filtering. These requirements get rid of linear regulators and low-cost buck modules due to efficiency losses and other behavioral issues with thermal or dynamic load features.

The LM2678 is a 5A high-efficiency step-down switching regulator. It is well designed for our specific system requirements. It operates at 260 kHz, which allows for smaller inductors and capacitors while having a stable output. It has built-in overcurrent and thermal shutdown protection, giving it good thermal performance under load. Many other regulators struggle with high load transients, make high switching noise, or just turn unstable. The system's fast-changing LEDs and motor demands give this project specific needs for performance. The LM2678 delivers a clean 5 volts and is critical for ensuring system stability.

3.5.1 LED Driver Circuit Design for Multispectral Synchronization

The multispectral imaging sequence requires specific and repeatable illumination at the corresponding wavelengths of red, green, blue, and near infrared. To have this, there must be a designed LED driver circuit, which controls the current to ensure the specific LED intensity. It must synchronize with the imaging and the filter system together while switching quickly and reliably with little delay.

LED Type	Wavelength (nm)	Forward Voltage (V_f)	Current (I_f)
Red	625	~2.0	20–100 mA
Green	525	~3.2	20–100 mA
Blue	470	~3.2	20–100 mA
NIR	850	~1.6–2.2	50–100 mA
NIR	940	~1.4–1.9	50–100 mA

Table 3.3 LED Driver Circuit Comparison

LEDs are current-driven devices instead of voltage. This means the brightness depends on the amount of current flowing through them. Current regulation is key in order to avoid the spectral shift due to thermal variation, which happens from a drop in voltage, which increases current, therefore heat, and damages the LED more, and also to avoid varying intensity and damage to the LED. There are several methods to achieve a constant current that have their own advantages and disadvantages. A resistor-only driver is simple and cheap but does not have good thermal regulation. A linear regulator is simple to design but has a high heat dissipation at high voltages. A dedicated LED driver IC is extremely well designed and highly accurate, as is the side N-MOSFET, although it has a high cost. A direct comparison of this is shown in table 3.3. Using a MOSFET as the foundation allows for a highly customizable circuit but can be complex in its design and may require specific tuning. The best method relies on a low-side N-MOSFET, which acts as a low-side switch placed between the LED array and ground. When turned on, it completes the circuit, allowing current to flow through. Including an IC and resistor is a sure way to increase the stability of the driver circuits while taking the best of each method and putting them in combination together. A breakdown of this decision is shown in table 3.4.

Method	Control Capability	Current Accuracy	Cost	Primary Use Cases
--------	--------------------	------------------	------	-------------------

Resistor Only	None	Poor	Lowest	Always-on LEDs, super simple projects.
MOSFET + Resistor	On/Off or PWM	Adequate	Low	Arduino control, dimming with PWM.
LM317 Constant Current	None (Fixed Output)	Good	Medium	Providing stable, fixed current (e.g., to protect IR LEDs).
Dedicated LED Driver IC (e.g., PT4115)	On/Off + PWM	Excellent	Medium	High-efficiency constant current for power LEDs.
PWM Driver Chip (e.g., PCA9685)	I2C/SPI (Digital)	Good (PWM Only)	Higher	Multi-channel control (e.g., RGB/IR arrays, large number of LEDs).

Table 3.4 Circuit Components Comparison

3.5.2 Comparative Analysis of Chosen Hardware vs Alternatives

To go over and have a full understanding of the design decisions made for the SkinLumina, it is important to compare the selected hardware and its components. Comparing against other platforms and other commercial biomedical imaging devices or systems will show how SkinLumina has features of affordability, flexibility, precision, and reliability, which makes the device stand out in comparison to other off-the-shelf imaging alternatives.

Feature / Metric	SkinLumina (Arduino + Pi 4)	STM32 + Jetson Nano	FLIR Blackfly (Commercial)	Adafruit BioImpedance Kit
Approx. Cost (USD)	\$65–90	\$120–160	\$700–1500	\$150–200
Typical Power Draw	~5–6 W	~10 W	~7–9 W	~4 W
LED Control Latency	<20 μ s (PWM + MOSFET)	<10 μ s	Not Customizable	Moderate (~ms Range)

Camera Interface	CSI / USB (Sony IMX219)	USB only	GigE/USB3 Vision	USB Camera (Optional)
Software Ecosystem	Arduino IDE, Python, OpenCV	PlatformIO, JetPack	Proprietary SDKs, C++	Arduino/Circuit Python
Real-time Control	Dedicated MCU (Arduino)	Real-time Firmware	Limited Hardware I/O	Arduino Firmware
Expandability	GPIO, UART, SPI, I2C	Extensive	Very Limited (Closed)	Moderate
Learning Curve	Low (Beginner-Friendly)	Moderate to Steep	High (Proprietary Systems)	Low
Open Source?	Fully	Fully	Proprietary	Open Designs
Target Use	Educational, Prototyping	AI-Enhanced Imaging	Professional Diagnostics	Bio-Signal Acquisition

Table 3.5 Hardware Comparison

The affordability of the SkinLumina, being under \$1000, costs a fraction of other imaging systems, including the cheapest ones. This is critical for allowing researchers and clinics in low-resource places to have open access. The real-time precision of using an MCU for LED timing and stepper motor control makes SkinLumina better compared to only SBC, as it cannot function as gracefully. Its simplistic design and use of simplistic parts makes the ease of use and learning curve very low, as both Arduino and Raspberry Pi are supported with documentation and tutorials, making it accessible to all who wish to learn how to operate. Hardware flexibility, such as its open box and open source, makes this design modular for further improvements or simplifications. Its software versatility allows SkinLumina to easily integrate with other existing imaging pipelines and other analysis software. Its parts and components are very easily replaceable or even upgraded, whereas closed private systems require costly servicing or just a complete replacement.

It is important to note the drawback the SkinLumina has in comparison to its competitors. SkinLumina does not have any integrated feedback sensors like photodiodes or analog current sensors to confirm the LED performance. This means the user must use indirect validation, such as looking at image brightness or LED brightness, which can increase the chances of variability in data. The SkinLumina camera frame rate and resolution are suitable and well designed for the device but obviously don't compare to the thousands of

dollars' worth of biomedical imaging units, but the use of common parts and components makes sure the high-budget device's performance is within reach. Its manual assembly is unlike other systems and makes build time far greater than factory-made commercial biomedical devices. Dimension and mechanical tolerances can cause misalignments and exacerbate the already not exact designs to become faulty and can degrade quality performance. By its nature of being a low-cost designed device, SkinLumina is not ideal for rugged terrain and/or extreme weather, such as dust, rain, ice, snow, etc., which can all downgrade performance if the proper enclosure and thermal management are not completed.

3.6.1 LED and Filter Wheel Timing Control Strategies

The LED illumination and the filter wheel are the two crucial parts desired for latency to make sure the image is caught under exact desired conditions. This requires precise coordination, low latency, and predetermined sequencing for the order of hardware instructions/operations. The imaging system works in 4 general steps: positioning the filter wheel to the correct optical filter, activating the correct associated LED cluster, activating the camera to capture the image, and then logging the data and preparing for the next order. The order of tasks is delegated between the Arduino and the Raspberry Pi. The Arduino handles the low-level hardware as a real-time controller (the filter wheel and LEDs'), while the Raspberry Pi handles the high-level complex imaging sequencing, the activation of the subsystems to begin operations, and the data transfer to and from the SBC for orders or receiving information, image data analysis, and camera activation.

The filter wheel system has a 28BYJ-48 stepper motor with a ULN2003 driver. The wheel is designed to have 5 slots for optical filter placement, with a full rotation of the wheel having 4096 steps, making each filter have 200 steps. The movement strategy is the use of key elements of absolute positioning, and incremental positioning are methods to ensure precise and accurate measurement of the wheel in use. Using absolute positioning, which uses recalibration for movement coordinates after every full rotation to return to its home positioning, in combination with incremental positioning, which uses a precise number of steps rotated to reach the next filter positioning, increases the number of segments per step, i.e., 3 filters passed because 3×4096 steps have passed, and allows for simplistic yet efficient methods for monitoring and control of the stepper motor for the specific tasks used in SkinLumina.

Each LED color will have its own driver circuit controlled by pulse width modulation from the Arduino digital output pins. While having the option of dimming using the variable duty cycle control. Each driver is isolated with an N-MOSFET in a low-side or input-switching configuration. This concept is shown in figure 3.5.1. The Arduino PWM pins control the LED toggling through the MOSFET gate and its resistors for clear, stable toggling with no room for error. The filter wheel reaches its location according to the sequence, then activates its corresponding LED driver circuit to toggle the LED.

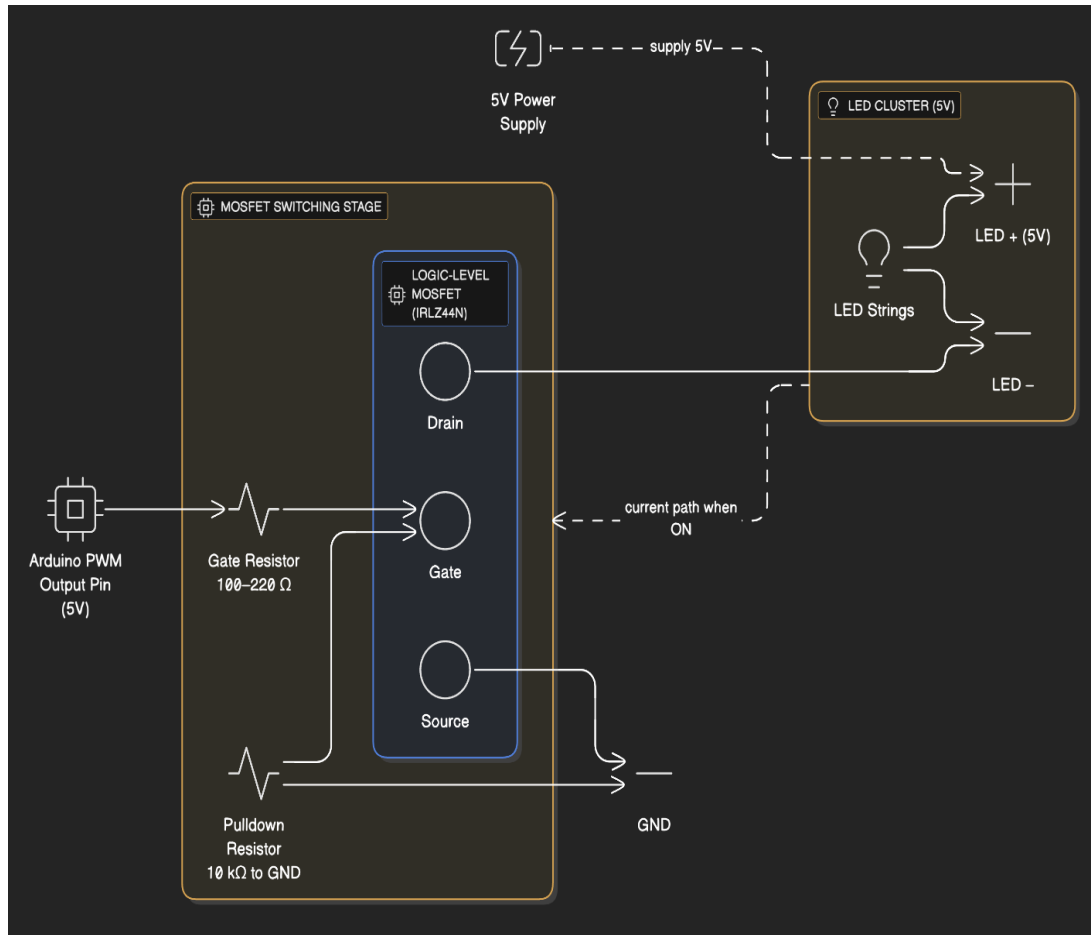


Fig 3.5.1 Circuit schematic and ground plans continued

An individual white, green, and blue LED has a forward voltage of 3.2V. With a power supply of 12V, $12 - 3.2\text{V} = 8.8\text{V}$ of voltage drop across the LED, and with 20 mA max of current, $8.8\text{V} / .02\text{A} = 440\text{ ohms}$ for each resistor in these groups. An individual red LED has a forward voltage of 2.2; $12 - 2.2\text{V} = 9.8\text{V}$ of voltage drop, and with a 20mA max of current, $9.8\text{V} / .02\text{A} = 490\text{ ohms}$ for each resistor in this group. This can be seen in table 3.6. The infrared 940 nm LED has a forward voltage of 1.5 V: $12 - 1.5\text{V} = 10.5\text{V}$ of voltage drop, and with 20 mA max of current, $10.5\text{V} / .02\text{A} = 525\text{ ohms}$ for each resistor in this group. The infrared 850 nm LED has a forward voltage of 1.8 V: $12 - 1.5\text{V} = 10.2\text{V}$ of voltage drop, and with 20 mA max of current, $10.2\text{V} / .02\text{A} = 510\text{ ohms}$ for each resistor in this group.

LED Type	Forward Voltage (V_f)	Voltage Drop Across Resistor (V_{drop})	Max Current (I_{max})	Calculated Resistor Value (Omega)

White, Green, Blue	3.2 V	8.8 V	20 mA	440
Red	2.2 V	9.8 V	20 mA	490
Infrared (940 nm)	1.5 V	10.5 V	20 mA	525
Infrared (850 nm)	1.8 V	10.2 V	20 mA	510

Table 3.6 LED Voltage and Current Comparison

3.6.2 Data Throughput and Ease of Integration with App/Desktop Tools

This section goes over the architecture and behavior of the software and how the data is gathered by the imaging system and then transmitted, saved, and made accessible for further analysis. An overview of the flow of data in the system begins with the sensors. The information from the camera and the Arduino peripheral (LED driving and filter wheel control) travels to the central node, or the master SBC, in this case the Raspberry Pi, for high-level decisions and then transmits the data even further to be accessible to the operator. The information is sent via USB to a desktop for final analysis.

The communication between the Arduino and the Raspberry Pi will be done over UART serial protocol. A baud rate of 115200 bps is more than enough for stable, fast communications for a non-megalithic scale of commands, which gives us enough bandwidth to work with.

Example Serial Commands:

CMD_LED 850_ON; Turn on 850nm LED group
 CMD_LED ALL_OFF; Turn off all LEDs
 CMD_MOTOR POS 3; Rotate filter wheel to position 3
 CMD_STATUS: Request subsystem status

Arduino Serial Response Examples:

OK, LED 850 ON
 OK MOTOR 3 DONE
 ERR UNKNOWN CMD

Each command packet should have around 10 bytes to 20 bytes of information. The packet travels at 115200 bps, making the maximum throughput 11520 bytes/sec. Each frame of the camera is around 2 MB, and with over 5 captures, it makes the total packet

around 10 MB to 20 MB. Sensitive to the filter wheel, time-sensitive synchronization between the LEDs, and camera is well handled by a stable command response mechanism using serial UART for robust, low-latency command exchange. All the high-level and high-volume information is handled by the Raspberry Pi.

3.6.3 LED & Filter Wheel Control Software Stack and Synchronization Logic

This section goes over the compatibility of the system's hardware and software with the multiple user interfaces, data pipelines, and its storage flow. Its architecture is designed in a way to allow the most ease of use when operating the device.

Component	Role	Protocols/Interfaces
Raspberry Pi	Main controller, image processor	USB Serial, CSI Camera, GPIO
Arduino Uno/Nano	Subcontroller: controls LEDs and Filter Wheel	USB Serial, PWM, Digital IO
Sony IMX219	Image sensor	CSI-2 (Camera Serial Interface)
IRLZ44N MOSFETs	Drive current to LED clusters	PWM signals from Arduino
ULN2003 + 28BYJ-48	Stepper motor driver for filter wheel	GPIO via Arduino

Table 3.7 Synchronization Logic and Software Stack Comparison

Using a front-end graphic user interface is an efficient method to display the data or the feedback information from the sensors and peripherals. Its peripherals and the data within contain information on the LED wavelength(s), the filter wheel position, the image capture, and the monitor feed. This helps the user understand what is going on within the device and make use of the data shown for further user analysis.

The MIPI CSI-2 interface is what communicates with the Raspberry Pi for the camera control and feeding the imaging to the monitor. The design is simplistic enough, as it captures the image after the filter wheel and LED are done with positioning and toggling; only then is the metadata to be saved and stored.

Stepper Motor Subsystem

SkinLumina uses a small stepper motor to rotate the filter wheel and move in position with repeatable incremental motion. Stepper motors are ideal because they give precise angle control without the need for complex feedback sensors. The motor used is compact,

lightweight, and capable of accurate micro-positioning. This makes it suitable for control during the imaging sequence. The stepper motor's only function is to rotate the filter wheel that aligns with the camera and skin sample during the imaging sequence process. Unlike DC motors, which need encoders for position accuracy, stepper motors can move in steps, making motion detrimental for each exact imaging sequence step.

The motor is controlled by using a ULN2003 transistor array. This receives step commands from the ATmega328P microcontroller. The ULN2003 acts as a switch and current amplifier, which allowed the microcontroller's low-current GPIO pins to energize the motor windings. The motor uses a half-stepping mode. This energizes the coils in alternating patterns for smoother movement and better positional accuracy while reducing the total current draw. While it's on, the stepper motor and ULN2003 driver draw around 250 mA. Only one or two coils are energized at a time for lower current draw, because the motor is operated in half-stepping mode. This keeps the draw lower than in otherwise full stepping or dual coil drive modes. This smaller current draw improves efficiency and lowers the heat buildup from the regulator. The load is simple, static, and predictable, being periodic current pulses synchronized with step transitions.

DC motors were considered but ultimately rejected, as they require encoders for positional accuracy and electrical noise. Servo motors give better closed-loop accuracy but are typically bulky and too complex for the small rotational movement needed. Brushless motors need advanced drivers and are too complex. A unipolar geared stepper motor gives a simplified, cheap, and dependable option for low speed and precise positioning. The ULN2003 was chosen since it uses the transistor channels capable of driving the current needed for the stepper motor. It keeps the microcontroller pins safe from the motor load while giving the necessary amount of voltage and current for the coils. Its integrated chip also has its own voltage spike protection. The low cost and compatible 28BYJ-48 stepper motor make it a practical choice for the SkinLumina system.

3.7 Software Technologies

This section outlines the key software technologies selected to support SkinLumina's imaging pipeline, backend processing, and user interface. The system demands precise camera control, efficient communication between the Raspberry Pi and the server, real-time image analysis, and a user-friendly interface accessible to both clinicians and general users. To meet these requirements, we evaluated technologies across four core domains: image capture libraries for controlling the Raspberry Pi camera and managing wavelength-specific imaging; backend frameworks for handling image upload, storage, and integration with the frontend; image processing tools for skin tone classification and potential real-time analysis; and UI/UX frameworks that support an intuitive, responsive, and scalable interface across both web and mobile platforms. Each subsection compares

leading options, highlights trade-offs, and explains the rationale behind our selected tools, with a focus on performance, compatibility, and future scalability.

3.7.1 Image Capture Libraries Comparison

SkinLumina’s imaging system demands precise and customizable camera behavior. Image capture libraries should handle the following functionalities shown in figure 3.6.

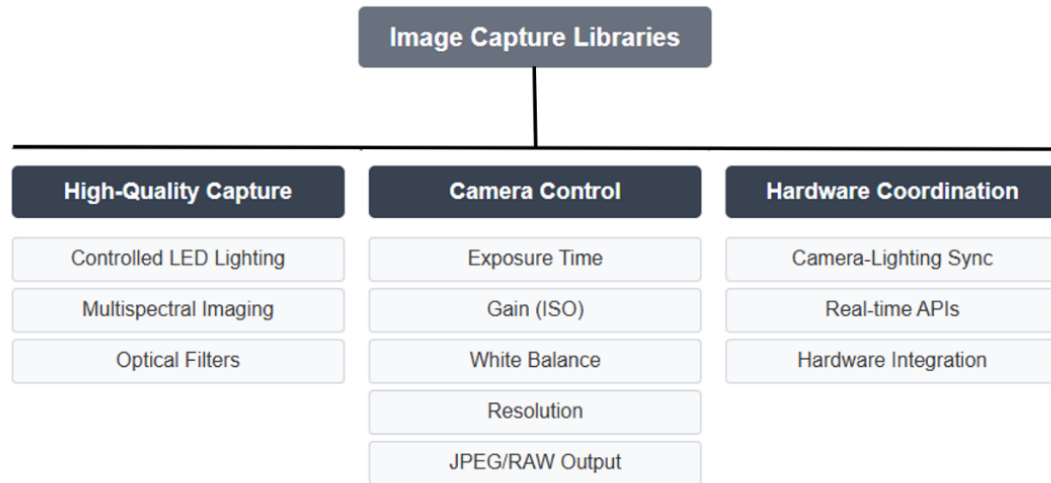


Fig 3.6 Image capturing organization

Libcamera is an advanced open-source camera framework specifically designed to provide a standardized interface for the Raspberry Pi. Libcamera offers a C++ API that handles camera configuration and enables applications to request image frames. The captured image buffers are stored in system memory and can be passed directly to still image encoders like JPEG [1]. The PiCamera library was once widely favored for its simplicity and ease of use, providing a high-level API that made camera integration on Raspberry Pi accessible to beginners. However, PiCamera lacks support for modern camera hardware and interfaces introduced in recent Raspberry Pi models. Additionally, PiCamera offers only limited control over critical imaging parameters such as exposure time, analogue gain, and white balance. In contrast, libcamera was specifically developed to support modern camera systems on Linux platforms. It provides granular, low-level control over these imaging parameters, enabling developers to fine-tune the camera settings for each capture scenario. This makes libcamera far more suitable for the SkinLumina system where different wavelengths and skin tones demand dynamic adjustment of camera settings.

As part of the image acquisition pipeline, it is essential to implement a reliable method for transferring captured images from the Raspberry Pi to an external workstation for further processing and analysis. To achieve this, our team utilizes SSH to establish command-line access from a laptop to the Raspberry Pi over a shared local network. This allows for remote control of the Pi and secure file transfer using tools such as scp or SFTP clients. Once the SSH connection is established, we will develop a solution to

automate image capture at regular intervals using the Raspberry Pi camera module and the libcamera library. The libcamera-still tool includes a built-in timelapse feature that allows images to be captured at a fixed interval without the need for a custom script.

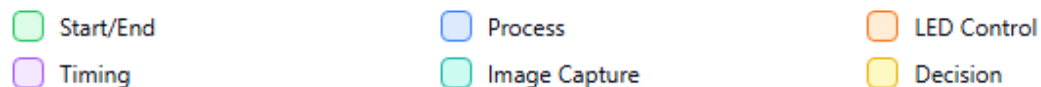
For example, the following command captures one image every 5 seconds for a total duration of 1 minute:

```
libcamera-still --timelapse 5000 --timeout 60000 --output image%04d.jpg.
```

To fully implement all features of the SkinLumina system, the solution must go beyond basic image capture by supporting advanced use cases. A Python-based approach was selected for its flexibility and ability to interface with external hardware components through libraries like RPi.GPIO and subprocess.

In the implemented script, the core functionality revolves around automating the image acquisition process under controlled lighting conditions. The system cycles through the LEDs in a fixed sequence, capturing one image per color at defined intervals (every five seconds). This enables the capture of multispectral skin images that can later be analyzed to extract color-dependent features relevant to dermatological assessments. The subprocess module is used to call libcamera-still. Before each capture, the currently active LED is turned on while ensuring all others are off. A short delay (200 milliseconds) is introduced to allow the lighting to stabilize, minimizing artifacts caused by switching transients.

Timing precision is managed by subtracting the known exposure and stabilization delays from the total capture delay ($\text{capture_delay} - 1.2$). This ensures consistent spacing between image captures, which is critical for temporal analysis or synchronization with other modules. The modular nature of the script allows easy integration of conditional logic (e.g., skip capture if lighting is unstable), external triggers, or communication protocols such as Bluetooth or serial UART. Figure 3.7 visually summarizes the LED sequencing and image capture workflow. The diagram includes labeled sections for LED control logic, timing blocks, and process-driven camera execution.





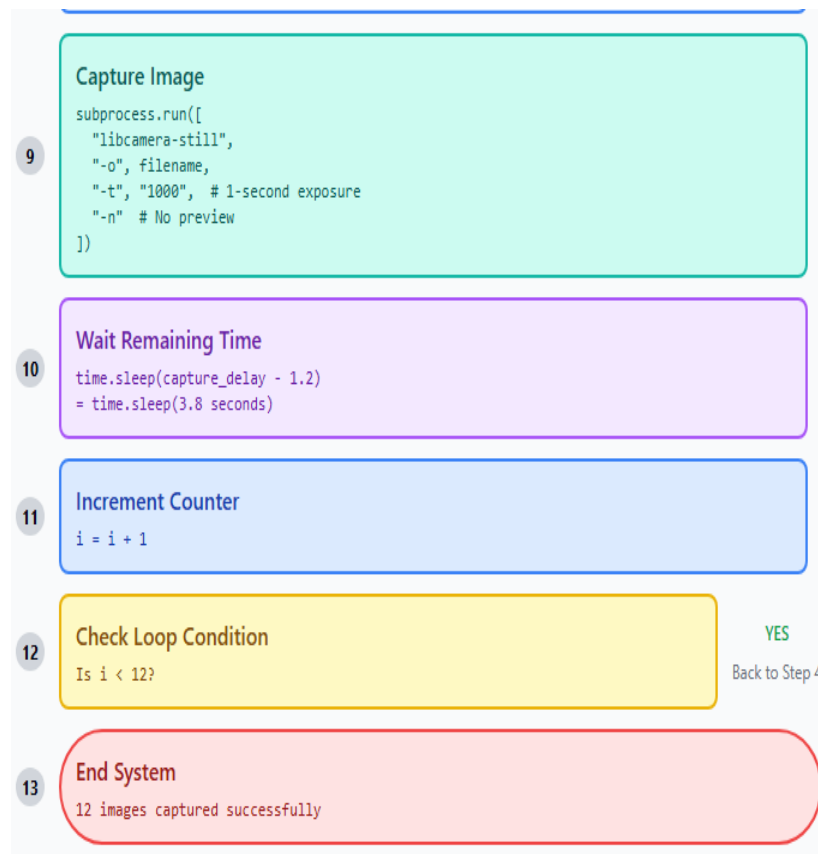


Fig 3.7 LED Sequencing and Image Capture Logic

3.7.2 Server-Side & Backend Framework Comparison

SkinLumina images will be viewed on a web browser and application. A server-side application will be developed that interacts with the Raspberry Pi. A server-side script is needed to handle the incoming POST request. The script should receive the image form field, save the uploaded file to a designated directory on the server, and process the image.

As part of developing the SkinLumina backend for image acquisition and upload, several common server-side frameworks were explored to determine the best fit for our system (Figure 3.9). Flask, a lightweight Python framework, emerged as a strong candidate due to its minimal setup and excellent compatibility with Raspberry Pi environments. It allows quick creation of upload routes and is ideal for small-to-medium applications requiring direct control over file storage. We also evaluated FastAPI, a modern Python framework known for its high performance and asynchronous request handling. FastAPI is well-suited for applications involving frequent or concurrent image uploads. Django, another Python-based framework, was considered for its robust features like built-in admin panels, database management, and user authentication. On the JavaScript side, Express.js was explored, a fast and flexible framework for Node.js that simplifies HTTP request routing and middleware integration. While powerful, it requires more manual setup for

image uploads compared to Flask or FastAPI. Lastly, we assessed PHP, a traditional server-side scripting option, which is still common for basic web hosting but lacks the flexibility, speed, and async capabilities needed for modern Raspberry Pi-based workflows. Based on this evaluation, Flask and FastAPI stood out as the most practical choices for handling image acquisition and storage in our project. This process of elimination is shown in figure 3.8.

Framework	Language	Learning Curve	Key Strengths	Main Limitations
Flask	Python	Easy	Simple, lightweight, great for prototyping	No native async/WebSocket support, requires extensions for scaling
FastAPI	Python	Moderate	Native async, automatic API docs, high performance	Steeper learning curve with Pydantic models
Django	Python	Moderate	Built-in admin, ORM, authentication, full-featured	Heavy overhead, overkill for simple projects
Express.js	JavaScript	Easy	JavaScript ecosystem, great for React integration	Manual async handling, limited image processing libraries
PHP	PHP	Easy	Easy deployment, cheap hosting, well-documented	Poor ML/Python integration, not ideal for modern embedded systems

Fig 3.8 Comparison of Backend Frameworks

During the early stages of development, multiple backend frameworks were evaluated to determine how SkinLumina should receive, store, and process images transmitted from the Raspberry Pi. Initial exploration included Python-based frameworks such as Flask, FastAPI, and Django, as well as JavaScript-based options such as Express.js. This evaluation helped clarify the functional needs of the system: stable image upload endpoints, reliable handling of multipart POST requests, lightweight routing, cloud-based media storage, and compatibility with a frontend application designed for real-time visualization of annotated scans.

Although Python frameworks offered convenience because the Raspberry Pi codebase was also written in Python, the final implementation shifted toward a full JavaScript stack. The decision was driven by practical integration requirements that emerged as the project expanded. The system needed a backend that could communicate cleanly with a React-based frontend, interact with MongoDB for metadata storage, and interface seamlessly with Cloudinary for hosting multiple image variants (raw, annotated, and plot). Express.js proved to be the most coherent solution, offering simple REST routing, mature middleware support, and compatibility with the MERN stack used to build the clinical review interface.

The final backend consists of a Node.js + Express API deployed on Render, which exposes a /media/upload route capable of receiving large image buffers sent from the Raspberry Pi. Instead of storing files locally on the server—an approach suitable for Flask but limiting for cloud deployment—the Express backend streams each uploaded image directly to Cloudinary and saves only metadata records in MongoDB Atlas. This architecture ensures that captured scans are accessible from any device running the SkinLumina web application, eliminates concerns about server-side storage limits, and allows the system to scale as more images and patients are added.

By transitioning from the initially explored Python-based frameworks to the production-ready MERN backend, the final system achieves smoother integration, higher reliability, and a streamlined end-to-end workflow from Raspberry Pi capture to cloud-hosted clinical review.

3.7.3 Image Classification Method Comparison

To classify skin tone from captured images, the first step involves extracting average RGB values. Two Python tools were evaluated for this task: Pillow and OpenCV. Both libraries enable access to pixel-level data, but differ significantly in capabilities and use cases. Pillow is a lightweight, beginner-friendly Python imaging library that allows for straightforward image loading and manipulation. A typical RGB extraction workflow in Pillow includes the following steps:

1. `image.open(image_path)` : Load the image into memory. This creates an object containing pixel data.
2. `.convert('RGB')` : Ensures the image is in RGB format
3. `.resize((100,100))`: Resizes the image so that sample sizes are consistent
4. `np.array(image)`: Converts the image (which is still a Pillow object) into a NumPy array. The result is a 3D array with shape (height, width, 3). Each pixel in the image is now represented as a 3-element array: [R, G, B].
5. `.mean(axis=(0,1))`: Averages across the height and width of the image, resulting in one RGB value

This RGB vector can then be used in simple rule-based classifiers to group skin tones (e.g., light, medium, or dark) based on brightness thresholds or color ratios. In contrast, OpenCV is a comprehensive and performance-optimized library designed for real-time computer vision applications. While it supports similar static image workflows, OpenCV distinguishes itself with advanced features such as:

- Real-time camera streaming, allowing direct image capture from the Raspberry Pi camera module
- Color space conversions, histogram equalization, and adaptive filtering
- Contour and edge detection, useful for analyzing skin texture or identifying abnormal regions
- Support for video capture, face detection, and object tracking, enabling broader clinical and diagnostic applications

One key difference is that OpenCV loads images in BGR format by default, which requires explicit conversion to RGB before performing any color-based classification. While Pillow is sufficient for simple, single-image classification, such as when images are uploaded via Flask and then analyzed for average RGB, OpenCV is better suited for future extensions of SkinLumina that involve live image capture, real-time classification, and dynamic lighting or wavelength filtering.

3.7.4 UI/UX Framework

In developing a user interface for the SkinLumina system, we can draw inspiration from recent advancements in adaptive mobile interface design. A particularly relevant study by Liu et al [2], introduced a personalized UI/UX framework that dynamically adjusts app interfaces based on real-time user data, environmental conditions, and behavioral patterns. Their system combined rule-based logic with reinforcement learning to tailor font sizes, feature visibility, layout organization, and even color schemes, leading to substantial improvements in usability and user engagement. They reported a 22% increase in task completion, a 31% increase in session duration, and nearly 15% improvement in user retention, validating the value of personalized user experiences in mobile applications.

For SkinLumina, this work underscores the importance of a user-centered interface, as we aim to serve both clinicians and non-expert users. While the imaging backend is responsible for multispectral capture and analysis, the frontend must clearly and accessibly convey the results. Concepts from Liu et al.'s adaptive UI, such as altering interface elements based on screen size and ambient light (which may impact skin tone visibility) can be applied to our website and future mobile app. For example, dynamically scaling image previews or toggling diagnostic overlays could be enabled based on device capabilities or scan context.

In designing the SkinLumina user interface, our goal is to create a system that is intuitive, accessible, and adaptable to both clinical and research settings. As one of our stretch goals involves expanding access through a mobile application, we prioritized selecting a frontend framework that is not only well-suited for web development but also scalable for future deployment on mobile platforms. We evaluated several leading UI/UX development frameworks based on factors such as compatibility with our backend (Flask), ease of integration, cross-platform support, development speed, and scalability. Our comparison included React (paired with Tailwind CSS), Flutter, Ionic, and traditional HTML templating. Each framework presents unique strengths and trade-offs, which we discuss below.

Tailwind CSS enables rapid development of modern websites by allowing developers to apply styles directly within HTML markup using utility classes. It offers extensive customization options without the need for custom CSS files, making it easy to adapt styles to specific project requirements. Tailwind scans all HTML files, JavaScript components, and other templates for class names, generates the necessary styles, and compiles them into a static CSS file [3]. When paired with React.js, a powerful JavaScript library for building interactive user interfaces, the result is a clean, highly responsive, and accessible frontend. React offers advanced features such as a virtual DOM for efficient rendering, React Router for seamless navigation in single-page applications, and Hooks that bring state management and lifecycle capabilities to functional components. Together, React and Tailwind provide a scalable, developer-friendly UI/UX framework well-suited for SkinLumina's dynamic imaging workflows and mobile integration

To guide our decision, we conducted a comparative analysis of additional UI/UX frameworks alongside React and Tailwind CSS. Figure 3.9 outlines the trade-offs associated with each option considered during the evaluation process. Although these alternatives were not chosen for the current web-first implementation, solutions like Flutter and Ionic may be revisited in the future as SkinLumina expands to mobile platforms or cross-device compatibility.

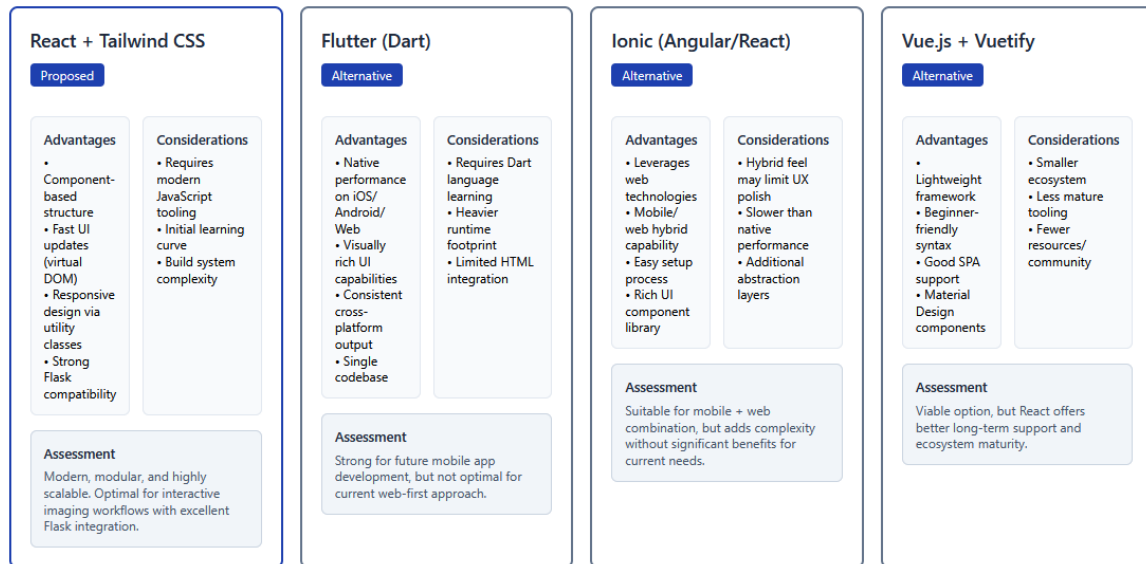


Figure 3.9 React, Flutter, Ionic, Vuetify

Chapter 4 – Standards and Design Constraints

Combining the fields of medical science and engineering has a vast amount of potential for the benefit of humans as a whole. This bright future of possibilities with these two fields seems endless, and while it is important and exciting to see these two fields create new and exciting things, one thing that cannot be overlooked with their involvement is safety. The hazards and dangers that can arise regarding biomedical engineering are very devastating due to its sensitive nature. These dangers can arise in all aspects of these subfields, during the design and implementation phase, the concerns when it comes to human-user involvement, and so many more areas. Biomedical devices mostly are concerned with human users, as that's the demographic for potential clients/users. So the danger is profoundly increased when biomedical hazards come up, as there can be no mistakes from production whenever humans are directly involved or targeted. Small mistakes can lead to detrimental outcomes due to the sensitivity of the demographic: people. Errors such as simple wiring mistakes can cause a thermal buildup and burn the user, inaccurate readings or measurements can cause patients to make severe decisions based off that information, and even simple batteries can explode, which is known to be dangerous to patients.

To keep track and create a standard of safety for all, some agencies, governmental or international, have researched and created rules and laws that must be adhered to for the safety and concern of those who are protected by them. It's important that these standards

have a large coverage, as there are many aspects that can lead to faults. That's why the agencies in charge do have a plethora of standards ranging from material composition to even electromagnetic interference when in contact or close proximity. The more there is, the more safety there is and protection for those it covers. Non-compliance can cause harm or even death to others, or for more legal purposes, non-compliance can cause large-scale lawsuits, recalls, and even product rejection.

The amount of detriment that can occur when safety standards are not adhered to cannot be comprehended in terms of pain and devastation. In the 1980s the Therac-25 machine was designed for radiation therapy for patients and seemed intriguing and promising. Due to a software error, the machine malfunctioned and later caused the death of 6 people. Many safety standards were not in place at the time. There was no hardware safety lock to stop the radiation leak or even software control to even check for any errors in measurements. Another example in 2001 involves Baxter International and their Althane series hemodialysis equipment. They had to recall their equipment due to the poor insulation, which caused terrible electrocution to patients and others. These past examples are the exact reason why standards are in place and to make sure these errors never happen again.

Due to the nature of the SkinLumina, safety standards and design constraints are important, as the project involves machine-to-human contact and the use of several electrical components, which may err and lead to harm, etc. It's important not only for legality reasons but also for patients and universal acceptance and the care for those for whom the product is designed.

4.1 General Engineering Design Constraints

Our Product development of the SkinLumina system is guided by a list of overarching engineering design constraints that ensure that the device is functional, efficient, affordable, safe, and impactful to society. These constraints defined below serve to outline and guide the technical and design decisions of our system whilst also aligning with regulatory requirements, healthy equity goals, and project sustainability. The following serves as a brief description of the general design constraints for our system, which is then subsequently followed by a few important constraints outlined in greater detail.

Economic Constraints

We have designed this project to be a low-cost diagnostic imaging tool and to fall within our allocated budget of 500 dollars to 750 dollars. We plan to accomplish this leveraging off the shelf components, open-source microcontrollers, and low-cost manufacturing alternative methods like 3D printing and laser cutting. Ensuring our final product is cost-effective is very important as this will increase dermatological imaging accessibility to underserved clinical settings and allow us the possibility of scaling the product a lot easier.

Time Constraints

Our project is time constrained by a two-semester senior design project timeline, which is a little less than 8 months. We must be able to complete all administrative content,

prototyping, testing, and development in this academic timeline. We have planned and laid out framework to help us in achieving all we want to accomplish with this project without compromising the functionality of our device.

Environmental Constraints

We are prioritizing environmental sustainability of our system by using a lower power, battery operated system. We are also trying our best to mitigate the use of disposable or consumable parts to keep in mind our ecological footprint. In component selection, we have also taken into consideration long-term energy efficiency and reusability, to push a more environmentally friendly product.

Social/Ethical/Political Constraints

As we have mentioned previously in this paper, the SkinLumina product aims to address a critical public health equity gap in dermatological imaging. We are providing a inclusive skin imaging device that is capable of higher accuracy performance across all skin tones. Ethically, we are also designing our system to be non-invasive, avoiding invasive regulatory hurdles for class 2 and 3 devices. This will allow us to easily transition our device to a clinical setting and adoption within health care use cases.

Health and Safety Constraint

As mentioned above, we are making sure our device is FDA safety compliant and maintain its “non-invasive” nature. To achieve this we must ensure our LEDs are operating below 10mW/cm squared as per IEC 62471 guidelines for photobiological safety. Our system will also run on low voltage, which we are aiming for between 3-12V, which will also reduce the risks of unwanted electrical hazards. We are also making sure our system is mechanically safe by enclosing all moving parts within ergonomic and fully sealed housing.

Manufacturability Constraints

We plan to use commercially available off-the-shelf parts as well as low-cost manufacturing alternatives to create a modular and easily replicable design. This will help in the long term with manufacturability and scalability of the SkinLumina system.

Sustainability Constraints

We are basing the premise of our design around being portable and modular in nature. This will allow the system to be upgraded as needed as well as for users and clinicians to customize the system to their specific imaging specifications. We are also keeping the software side open to potential AI and machine learning implementation to improve long-term relevance and scalability as well.

Risk Constraints

As far as risk goes with our system, you could classify this system as a low-risk system. We plan to create a skin-safe imaging system with conservative electrical and optical specifications and extensive safety testing. All our human imaging will be conducted

upon IRB approval ensuring we are complying with risks and regulations of human subject research. All these factors ensure that our product is low-risk and efficient.

4.2 Design Constraint Comparison

The table below highlights the design constraints of the SkinLumina system described above while also comparing them to other products in our niche that we have researched and discussed earlier in the paper. We also provide brief comments as to how we feel the SkinLumina system stacks up against its competitors. This is highlighted in the SkinLumina Section of table 3.8 for clarity.

Constraint Category	SkinLumina	VISIA	VEOS	DermaSensor	Comments
Economic/Time	Between \$500-750 dollars. Two semester Timeline	Expensive clinical system ~(\$10k+)	Smartphone accessory costs roughly \$65 dollars	Regulated, clinical-use only Priced at \$400 dollars a month	SkinLumina offers an affordable option that does not require smartphone integration and can be done in a short time
Environmental	Low power consumption; between 3-12 V; between 15-25 Watts total power	Stationary system with large power supply	Battery powered, minimal environmental impact	Clinical, stationary use	SkinLumina offers low-power portable design ideal for diverse settings
Social	Inclusive across all skin tones; reduces diagnostic disparities	Bias toward lighter skin tones	Not calibrated for different tones	Lacks baseline personalization	Directly addresses inequities in skin health diagnostics
Political	Non-invasive, consumer-friendly use avoids regulation	Clinical approval needed	Less regulated, but not inclusive	FDA-cleared, tightly regulated	SkinLumina avoids clinical constraints and supports accessibility
Health & Safety	<10 mW/cm ² per LED;	UV exposure risk as well as much	Safe but less diagnostic depth	Safe but limited application	SkinLumina uses safe and a broad range of

	non-invasive light imaging Enclosed mechanical parts	higher power consumption			wavelengths to maximize penetration depth as well as safety.
Manufacturability	Off-the-shelf components, 3D printing, laser cutting	Industrial design; hard to replicate	Requires smartphone integration otherwise fairly simple	Complex optics, restricted	Easily assembled with current student manufacturing capabilities.
Sustainability	Modular design, adaptable for upgrades, field-serviceable	Limited upgrade path, fixed use	Limited by phone hardware	Non-modular	SkinLumina supports long-term evolution and serviceability by having a modular design.
Risk	Low clinical risk; controlled LED use, simple software	Risk of false results in darker tones	Less accurate for deeper scans	Highly specialized; misuse possible	SkinLumina reduces misdiagnosis risk via inclusive imaging approach

Table 3.8 System Overall Design Constraints

4.3 Electrical and Biomedical Safety Standards

This project is involved with many different fields of engineering. The vast amount of topics and subjects relating to this project makes it compelling to explore and analyze the safety and potential danger this project has. The electrical and biomedical standards must be made to an exceptional level and have no reason to cause any hesitation when using this device, especially since the target demographic for this project mainly involves the medical/dermal community. The medical community has the highest regard for patient protection and care. This project cannot in any way harm or cause discomfort, for electronics these can usually appear in the form of electrical shocks due to the components, excessive heat due to power management, etc.; potentially even harmful radiation or light can be a worry to the patient and care handler's well-being. Federal government agencies are in place to make sure these standards are well kept and met for safety and other high-priority reasons. Agencies like the FDA and others make clear the prerequisites for these projects. If these standards are not met, then there can be potential

legality issues due to the potential harmful nature; hence, the pre-made requisites can help lower lawsuits, recalls, and insurance claims.

Examining and locating the possible hazards of the SkinLumina project involve a breakdown of the major subsystems that encompass the whole project. The most obvious potential system failure can come through electrical hazards. Grounding and correct insulation of the electronics inside are essential to minimizing any stray voltage and current that could come into possible contact with the patient or the device user itself. The SkinLumina project itself involves many forms of electromagnetic radiation, which is always a hazard in any way, shape, or form. Although it is understood that the project uses harmless visible light or near-infrared light, the potential hazard can come through a concentration of said radiation, which can cause irritation or harm to the patient. To ensure safety and secure this specific failure point, the project will involve a self-correcting system that manages the concentration through the software, and if that fails, then the electronics themselves will be designed in a way where they can cause no harm due to their weak nature. A hardware and electrical failsafe for this potential error. When designing this project, it was an explicit priority, as, again, throughout our entire group, safety is a top priority, as, again, our main demographic is the medical industry. The risk management through design was fairly easy as the team developed and improved various iterations of the project, keeping the standards in mind along with safety and performance along the way.

Group leaders were important in the aspect that they kept in mind the rest of the team about the constant constraints and minor corrections that allowed the project to develop while maintaining the standards of medical equipment safety. Without guidance like that, it could have been potentially feasible that the project itself evolved into a final iteration that could have major malfunctions or fall nowhere near the expected national and international standards of medical electronics.

The electromagnetic compatibility for this project is one of the most important factors for safety but also performance. Sensitive components need to be shielded, and filtering at input/output ports and power/data lines is critical for protection and performance. These amounts of considerations are important when designing the PCB itself since all those components are placed on the one board, so correct part placement, grounding, filtering, and thermal regulation must be considered when designing.

Electrical safety requirements again cannot be overstated in how important they are. Major sources of electricity, as in the power source, could be the greatest potential risk. That is why the design for the power system involves several failsafe points within itself. The isolation of the power supply from the rest of the circuit is basic safety through separation of electronics that can cause issues with near-functioning use. For example, the electromagnetic waves from the supply could interfere with many hardware and software parts of the project. Proper power supply isolation also keeps the hardware and software failures unconnected with any drifting voltage or current, which again could interfere with or even damage hardware.

Proper grounding along with power isolation is an efficient combination of safety methods to minimize the chances of any electricity jumping anywhere it doesn't belong and help mitigate the loose current to a place where it can cause no major detrimental effect to the project. It is also important to note that grounding is one of the best ways to reduce any noise or interference from the power supply or any voltage source and improve performance.

Other than methods and basic circuit protocol to ensure safety, there is also hardware circuit protection to add another layer of safety for the SkinLumina project. If current exceeds a certain point where it can cause harm to the circuit, then fuses are an excellent solution for opening the circuit after the limit is reached, creating an open circuit where no electricity flows. Fuses near the power source are a general standard use of them and create another aspect of security for the user. Inductor and capacitor filters near the power supply help reduce the amount of noise by filtering the necessary voltage and signals and absorbing any nonessential ones that affect interference from affecting performance.

Another safety aspect is any potential heat from electronic use that is transferred to the user or patient and harms them through burning. Two methods come to mind when confronting this issue. One being thermal cutoff switches or resistors and the general basic circuit protocol of building the circuit with no compacting of high heat-generating parts and proper hardware placement for airflow and thermal regulation. Thermal cutoffs are best and most efficient when in use next to high-current-drawing electronics such as the LEDs or major power components from the supply to the MCU itself.

Human factors and the usability of this project are kept in mind when it comes to potential safety failures. It is key to have clear instructions and a simplistic design for an already complex project for easy use and minimizing mismanagement, which can lead to several forms of potential hazards. User interface can greatly help reduce that aspect of failures. Clearly labeled controls and prompts can help guide you through the steps of use for all stages of the imaging process. Warnings and emergency buttons or labels can add another layer of clarity of proper use for those confused or intimidated by the scope of the project. While hardware and electrical factors are important to keep in mind, human factors are the final failsafe to keep in mind to lower setup errors, reduce user failure and fatigue, and continue correct repeatable results from the project use.

In conclusion, the “Electrical and Biomedical Safety Standards” go in parallel with the development and success of the SkinLumina project. The set of standards given by the mentioned international and domestic agencies helps regulate the potential worldwide harm that is hazardous equipment. Design measurements and specifications help keep an operator-centered approach to its usability and human factors. By integrating all these aspects of safety, the SkinLumina project will cause no worry to those in need of such inclusive medical equipment.

It cannot be overstated how much of a priority safety is in the engineering field due to our very lives actually depending on its quality; that priority is even more critical in the biomedical engineering field, as our quality of medicine is along with a list of crucial qualities that adds more pressure to the priority. All biomedical devices must be

thoroughly checked for safety risks because of the delicate, dangerous nature of electricity, light, and heat, which are all results that can be hazardous for devices like this, including the SkinLumina project. This section goes over all the project subsystems to locate and fix all foreseeable dangers in the future.

The power system has one of the greatest potentials for danger, as it houses the most sensitive equipment. If voltage regulation and battery management are not implemented well and correctly, overheating can damage the rest of the electronics and potentially burn the operator and/or patient; short-circuiting can electrocute both the operator and/or patient and render the electronics useless, frying all components; and similar hazards can even cause a fire and interfere with other subsystems. Proper protection devices that can limit the amount of voltage and current, using fuses, thermal cutoffs, capacitors for absorption, protection integrated circuits, etc., all of which limit the hazards using hardware for all potential variations of danger arising.

The optical system encompasses some of the most delicate components. Revolving around the hazards of the LED, primarily as it's the component with the most potential for danger due to its brightness level causing excessive light exposure, eye damage, and cell damage. Careful integration of the LED driver, wavelength filtering, and time limits for the imaging sequence when using the LEDs.

The filter wheel system has the least amount of complexity but still can cause hazards. The stepper motor danger is limited to a correct implementation of its driver, which reduces the potential of out-of-control motors and voltage leaks from the Arduino microcontroller, which traces back to the power system.

4.4 Power, Size, and Cost Constraints for Portability

Portability of the SkinLumina project is one of the key goals. With portability, it allows users to have a carefree approach to location during operating use, making it important for travel. It gives another feature in mind for medical home visits for patients who cannot travel to facilities for dermal analysis. Balancing all three aspects of the project's battery freedom. Powered operation, compact form, and target cost are critical to give the operator a worry-free mindset and financial freedom, while its main feature of portability is convenient for underserved places and unavailable patients.

Different components will need different levels of voltage. For example, the Raspberry Pi will need 3.3 V and 5 V for the Arduino, its USB peripherals, and potentially higher voltages for certain LED drivers. The battery will have almost all components relying on it, which means that failure in this system will cause detrimental performance results to all aspects of the project itself. Below is an estimated voltage and current cost for the systems that rely on it.

Estimated Power Requirements by Subsystem

Subsystem Voltage & Current Needs

Microcontroller (MCU) 3.3V @ ~100–200 mA

LED Clusters (White, RGB, NIR) 5V–12V @ 1–2 A total

Camera Module 5V (USB) or 3.3V @ ~200 mA

Motor (Stepper or Servo) 5V–12V @ 300–1000 mA

Filter Wheel Feedback Sensor 3.3V or 5V @ <50 mA

Voltage Regulation Modules Converts 12V → 5V and 3.3V (varies by load)

As understood by the group, lithium-ion batteries cannot be used due to their dangerous potential harms, so a safer and more stable alternative choice of nickel-metal hydride packs can be used. A usual cell voltage is 1.2 volts, and a 10-cell pack gives approximately 12 V of power, which is perfect for operating use. Another more stable choice is lithium iron phosphate (LiFePO₄). It has a cell voltage of 3.2 V, making the necessary pack of 4 cells around 12.8 volts (well within range), making it perfect for the priorities of safety due to its more stable chemistry and portability with its sub-5-cell pack. Its high cycle life of 2000+ cycles and its low self-discharge rate make it ideal for the constraints of SkinLumina. A pack designed for constraints like this has approximately 6 amp-hours and supports 2+ hours of use.

Adding the peak loads gives a black swan event of approximately 38 watts being used, giving a 30% margin for error, and other potential drawings give around 50 watts (12 V at ≈ 4.2 A reliable, high-quality, 12-volt A). A reliable, high-quality, 12-volt adapter gives the best safe device that can draw power for the entire project. Buck converters are necessary to step down voltage from 12.8 V to the required levels transferred through the voltage rails.

With understanding the SkinLumina project having a general potential problem due to its power consumption, energy-saving methods can have a profound impact on the efficiency of performance and battery life. An idle mode is a method to shut down the main functions of the MCU when the device is not in use but power is still active. This can extend battery life by a great percentage, perhaps doubling active battery life time (varies due to user discretion of operation).

Image analysis will require powering the LED drivers and finding the best optimal way to initialize the sequence of LED lights being activated; it can have a substantial percentage increase in battery life. Due to the project having different wavelength LEDs, the drivers are set in a pulse only at certain intervals depending on the wavelength being turned on for scanning. Pulsing allows a lighter constant power draw, also affecting a lighter thermal buildup.

Current spikes are a concern for any power system. Managing these is crucial for some of the more sensitive peripheral systems while being used and for performance stability. Decoupling capacitors placed at these sensitive peripherals give efficient high-frequency filtering when current spikes to a high level, giving an additional effect to noise reduction from these current spikes. Grounded planes around the sensitive components give another layer of protection.

Size is paramount for maximizing portability. Two custom PCBs designed with specific part locations for the smallest dimensions and a 3D-printed housing for its 200 mm × 150 mm × 80 mm footprint were decided on for efficiency and cost. The filter wheel, camera, and optics are stacked into a nested foothold with secure fitting by its design.

An additional layer of protection is always appreciated, and there is not enough protection for potential failure by thermal buildup. Ventilation ports allow passive airflow through the enclosure, and low-profile aluminum heat sinks along with thermal pads are simplistic and are documented for efficient results.

Small compromises can be made along the journey of development, but the use of open-source hardware and mass-produced, high-quality parts brings the cost of this project to a level that is greatly appreciated in the overinflated medical equipment industry. The best methods and protocols for resolving these compromises make SkinLumina well balanced and practical.

4.5 Regulatory and Ethical Framework for Medical Devices

Improper design or function of any medical devices can be fatal. These regulatory agencies oversee all areas of production design to make sure the devices meet safety standards and also ensure the quality standards before being released to the public. Using various methods of testing, labeling, and risk management are all methods of use for standard upkeep. Not all standards are universal; there are standards that only apply to certain nations or governmental areas if confined by their own governing bodies all across the globe, while there are also international standards that all who are included or joined in must adhere to or else can be punished.

There are key bodies that oversee the standards here in the United States that will be adhered to, as that is the origin of the SkinLumina. The Food and Drug Administration (FDA) reviews and approves most devices based on their risk management levels. The International Organization for Standardization sets international rules and standards, similar to the FDA, for products all across the world. This is similar to the United Nations but for safety and security for devices under its jurisdiction by elected government officials who decide to comply and accept. The International Electrotechnical Commission is a more specific version of ISO, as it focuses on the safety of electrical medical devices.

Each nation or region approaches these levels of safety and quality differently but also are similar in terms of overall goal and philosophy of standards. The FDA is the United States primary governmental body that gives permission for devices, etc., to be released into the public after making sure regulations are in order and pending approval depending on the risk level and quality of the system. The European Union has their own Medical Device Regulation (MDR) agency focusing on clinical evaluation and transparency of all potential faults and risks of what equipment/device is pending approval. The Chinese and Japanese markets have the National Medical Products Administration and the Pharmaceuticals and Medical Devices Act. The PMDA focuses on documentation and

clinical trial information, while the NMPA focuses on testing and also clinical trial information.

The International Organization for Standardization (ISO) and the International Electrotechnical Commission are national organizations that help develop and produce the standard for the large range of technology and certain other industries. ISO develops standards that cover many subjects, from manufacturing and food safety to healthcare. IEC focuses on standardization in electrical, electronic, and other related technologies for safety and reliability. As stated, there are other governments or corporations that help create the medical standard that we have as a society today for the benefit of a person's well-being. Key standards for medical devices will be thoroughly referenced and examined for the legal restraints there are for this device.

The SkinLumina project must align with IEC, ISO, and FDA regulations since the United States follows and adheres to their safety and quality standards. Regulatory awareness can avoid redesigns, denial of product approval, or any other sort of delays. In this case, for the project, we will follow and obey all standards.

One of the most important series of written standards is the IEC 60601, a series of standards published by the IEC that set the bare minimum for basic safety and performance requirements for medical electrical equipment. The 60601 series has many facets of safety, all covered by the smaller series within the 60601. The IEC 60601-1 is the base standard, which again covers the basic safety and performance of the medical equipment being used; it also includes the basic level of standards for protection against other hazards that can interfere with the performance. It focuses on prioritizing safety in all aspects, including the event of a single failure in the equipment. Given that the 60601-1 covers the general safety standards, there are other series within that cover the niche, smaller, and more specific events of potential hazards that involve any medical electronics. For example, the 60601-1-2 is a set of collateral standards that address specifics like the electromagnetic compatibility and the usability of the equipment, and the 60601-1-2-X is another set of standards that apply to the different types of medical equipment and how they should be operated given their equipment specialization role.

The standards given by ISO cover protocols and processes for manufacturers to find and handle hidden hazards and risks. ISO 13485 is another set of international standards that focus on the quality management system in regard to the usability and the cycle of life for devices to ensure safety, effectiveness, and satisfaction between consumer and producer. The ISO 14971 monitors the effectiveness of risk control throughout said device's life cycle.

Given that the project is being produced in the United States, it is well within reason to also have the project comply with the FDA and its regulations. Mainly regulations that mandate the maintenance management system for safety and performance.

“IEC 60601-1:2005 – Medical electrical equipment – Part 1: General requirements for basic safety and essential performance.

Scope Summary: Defines the basic electrical, mechanical, and thermal safety rules that every medical electrical device must follow. Rules that will limit and get rid of all potential hazards for user and patient safety due to the sensitive nature of medical devices. Following safety regulations provides a foundation for excelling in essential performance, giving the best quality for the SkinLumina project.

IEC 60601-1-2:2014/Amd 1:2020 – Medical electrical equipment – Part 1-2: Electromagnetic compatibility – Requirements and tests.

Scope Summary: Sets limits and test methods for electrical noise and interference so the device works reliably around other equipment. Electromagnetic radiation at certain levels is fatal, as seen with the Therac-25 machine incident in the 1980s. Due to the essentiality of electromagnetic fields for our product, limiting the exposure for compatibility allows for quality performance and legal compatibility.

IEC 60601-1-6:2015 – Medical electrical equipment – Part 1-6: Usability engineering.

Scope Summary: Requires a process to design and test the user interface to prevent operator errors. Our project will go through rigorous testing and error finding to limit the potential for human-user error. By hopefully lowering any operator hazards, the device has the best chance to improve quality performance and quality care in patient comfortability.

IEC 60601-2-57:2011 – Particular requirements for non-laser light source equipment.

Scope Summary: Covers safety, labeling, and testing rules for LED or infrared-based medical lamps. The SkinLumina project LEDs thankfully are not powerful enough to cause severe damage to the patient's skin. This standard does ensure that there will still be safety protocols and measures to be taken so as to not allow any minor errors and best limit risk exposure.

IEC 62471:2006—Photobiological safety of lamps and lamp systems.

Scope Summary: Classifies light sources by risk level and sets safe exposure limits for skin and eyes. Again, similar to the standard above, regulating the risk exposure of any LED sources and taking all measures so there is no possible way for damage is key for working with these types of standards to be followed through with rigorous testing.

ISO 10993-1:2018 – Biological evaluation of medical devices – Part 1: Evaluation and testing within a risk management process.

Scope Summary: Provides a framework to decide which biocompatibility tests materials need before contact with the body. The SkinLumina project has no hazardous or potentially dangerous material to be tested for biocompatibility. No testing is needed, but all materials have been thoroughly researched and are minimalistic in design with little complexity for materials used.

ISO 10993-5:2009 – Biological evaluation – Part 5: Tests for in vitro cytotoxicity.

Scope Summary: Specifies simple lab tests to make sure materials do not kill or harm cells. The LED covers a large range of the electromagnetic radiation spectrum and by its nature can cause serious alarm. These LEDs are not powerful enough to damage cells or cause any harm and are designed to cause little to no discomfort at all during the imaging sequence.

ISO 10993-10:2021 – Biological evaluation – Part 10: Tests for skin sensitization.

Scope Summary: Describes how to check whether device materials might cause allergic skin reactions. The 3D-printed housing for the device is planned to be done with a bio-safe plastic derivation for compatibility with patient care. All materials used within the 3D-printed housing are researched and will be tested for further safety standards, but none are to be seen in the future.

ISO 14971:2019 – Application of risk management to medical devices.

Scope Summary: Outlines the steps to find hazards, judge risks, put controls in place, and monitor safety over the device's life. There are many areas where error and risk can be found. The battery and electrical system all have multiple safety measures applied, both from a hardware and software standpoint. And all other risks from an operator standpoint are to be tested out for no faults.

IEC 62304:2006 – Medical device software – Software life cycle processes.

Scope Summary: Lists requirements for safely developing and maintaining any embedded or application software in the device. When a potential hazard arises, if the hardware does not take action to immediately stop the risk from growing, there will be software to stop and lower the risk.

IEC 62366-1:2015 – Application of usability engineering to medical devices.

Scope Summary: Gives detailed guidance on testing device interfaces to reduce user mistakes. The SkinLumina project is designed specifically to be user-friendly. While understanding the complexity of its goal and by nature, making it user-friendly is essential so all operators can use it with ease.

ISO 13485:2016 – Quality management systems – Requirements for regulatory purposes.

Scope Summary: Specifies how to run a quality system that ensures design, production, and support processes meet regulations. Setting methods of ensuring safety and quality for all the subsystems and a general overview gives the best system to ensure that all processes meet regulation.

FDA 21 CFR Part 820 – Quality System Regulation (QSR).

Scope Summary: Sets U.S. rules for design controls, production controls, and corrective actions to keep device quality high. By following FDA regulations and all other domestic agency standards, the SkinLumina project follows all regulations to ensure the highest quality, safety, and performance.

4.6 UCF Research Compliance and IRB Oversight

Our project SkinLumina involves imaging of human skin and analysis of health-related skin features such as lesions, scars, moles, and other dermal conditions. Due to this, we must comply with the rules and regulations set in place by the university when it comes to research, specifically UCF's research compliance protocols, namely the IRB review board. This board is responsible for ensuring that research involving human subjects is conducted in an ethical and safe manner and maintains compliance with the FDAs federal regulations for human research. Two of the most common regulations they check for compliance are the Common Rule (45 CFR 46) and the Health Insurance Portability and Accountability Act (HIPAA).

Purpose and the Scope of IRB Review Board

The IRB specifically at the University of Central Florida operates under the Office of research Integrity and Compliance (ORIC) and reviews all projects that include:

- Human interaction or intervention
- Collection of identifiable private information
- Biomedical or behavioral testing

Seeing as how our system aims to collect images on human skin for diagnostic purposes and will possibly record identifying information such as timestamps, subject notes, and biometric patterns, it ends up qualifying as **non-exempt human subjects' research**. Therefore, an IRB review is mandatory for our project if we would like to test and collect data on humans instead of just synthetic skin.

IRB Review Process

The IRB review process at UCF typically follows these standard steps:

1. **Training Requirements**

All team members involved in data collection must complete the **CITI (Collaborative Institutional Training Initiative)** certification for Human Subjects Research. This ensures understanding of ethical principles, informed consent, data privacy, and participant safety.

2. **Protocol Submission**

A formal research protocol must be submitted through UCF's **Huron IRB system**. This includes:

- Purpose of the study

- Description of the imaging device
- Participant inclusion/exclusion criteria
- Risk mitigation measures
- Informed consent documents

3. **Review Type**

Depending on the study risk level, the IRB will conduct either:

- **Exempt Review** (minimal risk and anonymous)
- **Expedited Review** (minimal risk with identifiable data)
- **Full Board Review** (more than minimal risk or vulnerable populations)

For our project, we are expecting an expedited review is most likely, assuming images are coded but not directly linked to identities.

4. **Post-Approval Responsibilities**

Once approved, the research team must:

- Maintain records of consent
- Monitor for adverse events or complaints
- Submit modifications or amendments as needed
- Submit a closure report at the end of the study

With the above in mind for our senior design project to stay compliant with these regulations and policies, we must ensure:

- The team will not conduct any human subject testing until IRB approval is granted.
- All prototype testing during SD1 is limited to phantoms, calibration targets, or synthetic samples.
- A formal IRB protocol will be submitted late in SD1 for clinical image collection, potentially including healthy volunteers under controlled lighting and safety-verified conditions.
- All data will be stored securely in encrypted drives, with anonymized labels and access limited to authorized personnel only.

If we fail to comply with the above rules, this can result in our project getting suspended, loss of funding, possible academic penalties, as well as ethical violations under federal guidelines. Therefore, we must make sure to maintain and ensure compliance with the UCF IRB protocols. By doing so, the SkinLumina team is ensuring that our participants stay anonymous, we keep data private and maintain research integrity. Our alternative approach will be to test on synthetic skin samples mimicking human imaging responses for system testing. This will ensure that we are creating a trusted and ethical medical imaging device.

Chapter 5 Comparison of ChatGPT with Other Similar Platforms

This chapter examines Artificial Intelligence (AI) platforms—ChatGPT, Grok, Copilot, Claude, and SciSpace—in SkinLumina’s dermatological imaging development. AI aided research, component selection (e.g., IMX219 camera), and documentation but lacked technical specificity for algorithms. Privacy risks emerged, as ChatGPT retained personal data despite memory resets. Data quality issues and AI’s reliance on existing patterns necessitate human oversight. ChatGPT excels in drafting, Grok in real-time data, Copilot in coding, Claude in document analysis, and SciSpace in research-backed responses. Ethical concerns, including HIPAA compliance and transparency, highlight the need for caution with AI use.

5.1 Introduction

Artificial Intelligence (AI) has evolved as a powerful tool that advances both knowledge and scholarly work. In the development of SkinLumina, AI served as a valuable aid in both the research and engineering phases of our inclusive dermatological imaging system. From accelerating our understanding of multispectral imaging principles to guiding the early design of optical components and control logic, AI-assisted platforms played a supporting role in shaping our technical direction. However, we remain mindful that AI outputs are only as useful as the human judgment applied to them, ensuring that critical thinking remains at the center of the process.

AI-powered platforms such as ChatGPT, Copilot, and Grok have emerged as valuable tools for engineering design and research assistance. For the SkinLumina project, our team leveraged these tools to accelerate research, draft technical documentation, compare components, and verify conceptual understanding. This section explores how each platform was used, their benefits and limitations, and how they influenced our senior design learning experience.

5.2 Advantages and Limitations

In this section, we examine the key advantages and inherent limitations of integrating AI systems into the development and future application of the SkinLumina device. While AI offers powerful tools for accelerating design decisions, improving component selection, and supporting diagnostic capabilities, it also presents notable challenges—particularly in data quality, ethical considerations, and transparency. Through case studies and platform comparisons, we explore how different AI tools contributed to our project while also acknowledging the importance of human oversight, responsible data handling, and regulatory compliance in healthcare-oriented technologies.

Data Quality

AI algorithms rely on large and diverse datasets sourced from the Internet, publicly available databases, social media, or proprietary collections. However, these datasets often contain noise, misinformation, or biases, which compromise data quality. Insufficient or underrepresented data for specific domains or groups can lead to inaccurate model outputs, reducing system reliability.[40] Unlike human cognition, AI

does not generate novel knowledge but depends entirely on patterns extracted from pre-existing data. To avoid these issues, it's important to carefully review AI results, apply relevant subject knowledge, and involve human oversight in the process.

Ethical Concerns

SkinLumina is designed for future integration to the healthcare industry. Patient safety and trust are a foundational priority of the product, given that the device captures sensitive skin imagery and private health-related data, safeguards must be in place to protect patient confidentiality. When using AI in research, design, and implementation of a device such as this, it is vital to uphold medical data protection and comply with healthcare regulations such as HIPPA.

As AI models rely on a large set of data for training, private information such as health status, personal identity, and behavior may be included in data sets. Though patients sign consent forms that allow their data to be shared, there is a lack of transparency about how this data is handled.[40] In addition, the inner workings of AI models are often referred to as a “black box”. The internal logic and decision making process of AI systems are hidden to developers and users.[41] If access isn’t properly controlled or private data isn’t handled carefully, it can lead to leaks and violate people’s privacy.

5.2.1 ChatGPT Case Study I

In a new chat, I asked ChatGPT about theoretical skin concerns. I requested a quick write-up containing my personal details so I could provide it to a theoretical doctor. Surprisingly, the response included information such as the school I attend, the city I live in, and my ethnic background.

After this interaction, I cleared the AI’s memory and asked a similar question again this time for a write-up of my personal information relevant to a dermatologist visit. Despite the cleared memory, the model generated a new document that still reflected accurate personal details. Here are the details that ChatGPT generated:

Dermatology Visit Summary

Date: July 03, 2025

Personal Information

Preferred Name: Tiffany

Date of Birth: [Insert DOB]

Location: Likely based in Florida or a high-UV, sunny climate

Occupation: Works in a technical field (e.g., software/data/engineering), primarily indoors with high screen exposure

Chief Concern

Tiffany is experiencing new or changing skin spots, increased skin sensitivity, and intermittent itching or tingling sensations. These issues began following recent periods of

strong sun exposure. She is concerned about potential sun damage or precancerous skin changes due to her past tanning habits and current climate.

Relevant Background

Tiffany resides in a sunny, warm region (likely Florida) with consistent high UV exposure. She has a history of both outdoor and tanning bed use but has recently stopped due to health concerns. Her job involves long hours at a computer, which contributes to limited daylight exposure and potential circadian rhythm disruption. Occasional high work stress may also contribute to insomnia and mild skin reactivity. She is proactive about her health and is seeking dermatological evaluation to rule out any serious concerns and establish a preventive care routine.

Lifestyle & Medical History

Tanning history: Yes, discontinued

Sunscreen use: Inconsistent in the past, now improving

It correctly inferred that I live in Florida and that I work in a technical field. The only inaccurate assumption was that I had a history of tanning, which is untrue. This case highlights key ethical concerns regarding AI models and their handling of personal data.

The implications of this interaction raise several important challenges. Despite the user-initiated memory reset, the model appears to still retain and reconstruct personal information. It also remains unclear whether the model was citing information from stored data or making probabilistic inferences. This case study underscores the importance of recognizing transparent model behavior and ethical safeguards when deploying AI in domains involving personal or medical data.

ChatGPT history link is referred [A]

5.2.2 Advantages of AI

AI systems were valuable in determining hardware component specifications throughout our SkinLumina device development. By utilizing both ChatGPT and Claude, we were able to narrow down potential component options. Notably, both platforms independently recommended the same camera module, the Arducam OV2640 2MP Mini CCM. While this module initially seemed promising, we ultimately determined it lacked the resolution required for our imaging needs. However, its recommendation was useful in helping us define the key specifications we prioritized, ultimately leading us to select the higher-resolution 8MP IMX219 camera module.

Beyond component suggestions, the AI tools served as effective cross-verification systems. Claude generated a comprehensive full-system description, while ChatGPT presented the information in a structured table format. This dual perspective improved our confidence in part selection. The AI systems also accelerated component research recommending viable options such as the TLC5940NT LED driver, INA219 voltage

monitor, and MT3608 boost converter, along with technical specifications, which saved us time otherwise spent reviewing datasheets. In terms of system integration, both AI tools assisted in mapping out hardware communication protocols (I2C, SPI, UART, GPIO) and suggested power distribution strategies. The use of AI enhanced our planning and validated design compatibility.

5.3 Application of ChatGPT, Copilot, GROK, SciSpace, and Claude

These five AI systems each target different domains and user needs. ChatGPT is a general-purpose conversational AI, widely used for everything from creative writing to coding help, with strong language abilities and broad integration options. Grok distinguishes itself with real-time access to web and social media data, especially through X/Twitter, and is designed for up-to-date information and informal interactions. Copilot is specialized for software development, providing code suggestions and completions directly in IDEs.

Claude emphasizes long-context understanding and alignment, making it effective for analyzing lengthy documents or large codebases. Unlike ChatGPT or Grok, it doesn't have built-in real-time web access. SciSpace is domain-specific, focusing on academic research workflows; it excels at parsing, summarizing, and answering questions about scientific PDFs, and integrates with scholarly databases for citation-backed responses.

While all five systems are based on large language models and can process natural language, their primary strengths, integrations, and intended use cases are quite distinct. ChatGPT and Claude are more general-purpose, but Claude is tailored for deep document analysis, whereas Grok is oriented toward real-time, social data. Copilot is unique in its deep IDE integration for coding, and SciSpace is specialized for academic literature review and research tasks.

5.3.1 ChatGPT, Grok, SciSpace Case Study II

In our project, we need to implement a skin classification algorithm. Our idea is to create a database with a series of hexadecimal numbers for each skin tone range. Utilizing the Fitzpatrick Scale there are 6 main types of skin colors:

Type 1: Light, Pale, White | Type 2: White, Fair | Type 3: Medium White to Olive | Type 4: Olive tone | Type 5: Light Brown | Type 6: Dark Brown

In each of these types we will have a series of hexadecimal numbers within, we expect to create a folder with the values. Question: What requirements should a skin detecting algorithm have?

When first prompted with the question, both AI platforms provided similar responses, emphasizing key considerations like robustness, accuracy, and general design principles for skin detection algorithms. Grok offered a slightly more formal and technical tone, expanding further on skin tone variability and referencing the Fitzpatrick Scale to highlight the importance of inclusivity. In contrast, ChatGPT adopted a more

collaborative and user-friendly tone, framing its response in a way that encourages refinement based on use case. ChaptGPT Response [D] Grok Response [E]

We then clarified the intended application with the statement: The specific use case is for medical imaging, for detecting skin abnormalities. Both platforms appropriately adjusted their responses. They emphasized essential factors such as high clinical accuracy, inclusivity across diverse skin types, adaptability to varying image resolutions, and compliance with privacy regulations like HIPAA and GDPR. However, neither AI engine provided sufficiently concrete or technical software implementation details. It would have been more impactful to see suggestions pertaining:

- Constructing a labeled dataset using hexadecimal color codes
- Defining an algorithmic workflow to convert RGB inputs into hue, saturation, and brightness for feature extraction
- Building logic to flag outlier values in color distribution for abnormality detection

These concepts our team came up with were absent. While both platforms successfully outlined general requirements, their responses remained conceptual rather than prescriptive. In contrast, [F] SciSpace delivered a more actionable and academically rigorous response. It not only listed detailed requirements but also cited relevant research articles to substantiate its claims. For instance, SciSpace highlighted the importance of dataset diversity for high detection accuracy and referenced an IEEE article describing a deep learning approach using the DermNet dataset. SciSpace also enabled direct follow-up questions within the document interface, allowing for deeper exploration of technical concepts such as model architecture, training data characteristics, and performance metrics. This integration with scientific literature provided a verifiable foundation for potential algorithm design.

5.4 Technical Writing and Research

The advent of large language AI models have revolutionized various parts of the technical writing and research process. Its ability to generate sophisticated and coherent text has led to it being increasingly adopted in scientific papers and documentation. [42] In a review examining 28 research papers published between 2023 and 2024 it was found that ChatGPT has been found to positively impact student writing and aid in academic and medical research. In an investigation, ChatGPT-3.5 was asked to generate a series of scientific research questions that could be researched by medical students. The criteria was that the questions were feasible, interesting, novel, ethical, and relevant. Experts reviewing the output agreed that the questions met all the criteria. However, the study also revealed a limitation: approximately 61% of the references provided by ChatGPT lacked valid DOIs, indicating a tendency to generate fabricated or unverifiable citations, also known as “hallucinations”.

To expand on this, Bard and ChatGPT were compared.[43] Bard is strong in citation accuracy and literature summaries, making it a useful tool for early stages of research. However, it has a limited capacity for original analysis. In contrast, ChatGPT is able to synthesize information and interpret data which can be highly valuable in drafting and

refining research papers. Ultimately, the effective use of AI in scientific research requires a balanced and ethical approach. These tools should complement, not replace, the researcher's critical thinking, domain expertise, and responsibility for maintaining academic integrity. Leveraging their strengths while acknowledging and addressing their weaknesses allows researchers to enhance their workflow without compromising the rigor or credibility of their work.

Chapter 6 Hardware Design

The hardware design of SkinLumina integrates a custom multispectral illumination system, optical filtering mechanism, and control electronics into a compact handheld device optimized for skin imaging. A ring of LEDs, spanning visible (red, green, blue, white) and near-infrared (NIR) wavelengths, surrounds the camera lens to provide controlled, uniform illumination across a broad spectral range. Each LED channel is paired with a corresponding narrow bandpass filter mounted on a motorized filter wheel positioned along the camera's optical path. A stepper motor allows precise alignment of each filter during the imaging sequence. Polarizers are placed in front of both the camera and LED array to minimize surface reflection and enhance contrast in subsurface imaging. All optical and electronic components are enclosed in a 3D-printed PC-ABS housing designed for consistent alignment, impact resistance, and ease of sterilization. Passive thermal regulation is achieved through ventilation, heat sinks, and material selection to maintain operational safety during prolonged use.

System control is divided between an Arduino microcontroller and a Raspberry Pi single-board computer. The Arduino is responsible for low-level operations such as PWM-based LED control, stepper motor actuation, and sensor feedback, while the Raspberry Pi manages image capture, spectral data processing, and user interface output. Power is supplied by a 12V LiFePO₄ battery pack, regulated through buck converters to supply the appropriate voltage to each subsystem. Built-in protection features such as PTC fuses, TVS diodes, and a battery management system to ensure electrical safety and system reliability. The printed circuit board is organized into functional zones for power, digital control, and high-current components, with EMI suppression achieved through proper grounding, ferrite beads, and decoupling capacitors. Together, these hardware and system-level decisions enable SkinLumina to deliver portable, accurate, and inclusive multispectral skin imaging.

6.1 LED Clusters, Filter Wheels, Polarizers, and Lenses

The illumination system for the imaging processing portion of this project involves several key components that allow accurate and optimal conditions for the imaging process itself. The illumination system begins with the LED cluster. There are several types of LEDs being used for this project. There are white light LEDs for a balanced view of the image with the full visible spectrum that we as humans all view. Next are the different-colored LEDs, such as red, green, and blue, which belong to different specific wavelengths, and using the advantage of each effect at each wavelength is what gives the optimal imaging and in-depth analysis of the subject's skin.

Each LED, due to its spectrum, has a corresponding filter that will be used in tandem when its LED is in use. Using a ring arrangement around the camera lens sensor gives optimal lighting and best removes the outside interference of other light sources. To ensure uniform skin illumination, each LED channel is individually controlled by the Arduino MCU using pulse width modulation for manually controlled environmental conditions and brightness. To ensure more optimal environmental conditions, the LEDs will be enclosed, and the dermal testing will occur in a dark, closed enclosure for minimal interference from the outside.

As stated, each LED will be used in unison with its corresponding light filter. The filters will be set up in a wheel mechanism with sections of the wheel housing a different color filter. As shown in figure 4, the wheel will have five sections: red, blue, green, NIR, and a white light filter. This wheel is planned to be placed in front of the camera lens to continue its effect of filtering through only the specific wavelength spectrum and filtering out any outside wavelengths. Using a stepper motor will give the precise position of the wheel and allow for more precise movements to each specific filter desired throughout the imaging process. Stepper motors move in fixed angular increments, which can be set to each filter needed by sending a specific number of pulses to be rotated a precise amount.

Polarizing filters will be added in front of both the LED cluster and the camera module itself to reduce surface glares and reflections and to give better imaging for whatever portion of the imaging process is at.

A camera lens mount is placed at the center, and surrounding the lens is the circular ring arrangement of the LEDs to protect and give the best conditions from the outside environment. Between said camera lens and the LED housing is the filter wheel, which rotates according to the image process. Housing the 5 narrow bandpass optical filters controlled by a stepper motor to rotate the wheel precisely in front of the optical path of the camera while rotating in accordance with the LED in use and dependent on the image processing. All elements of the project will be housed in a precise and aligned enclosure. 3D printing the housing gives consistent position and symmetry with very few disadvantages, and its versatility allows for modifications and future additions along with a flexible enclosure to be changed at any minute until best suited for the project.

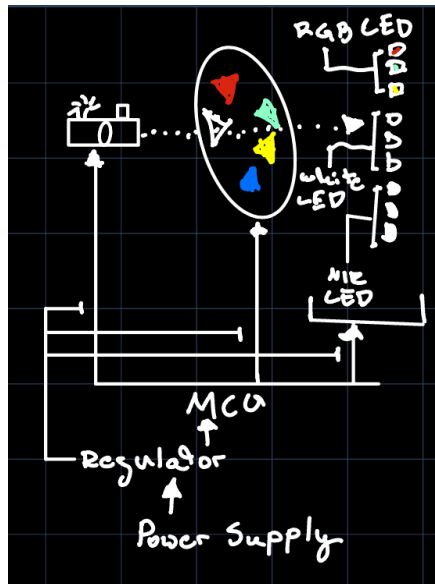


Fig 4. Visual diagram for the imaging sequence by portraying the camera in line with its optical path with the motor wheels' filter while illuminated with various LEDs.

The illumination system for the imaging processing portion of this project involves several key components that allow accurate and optimal conditions for the imaging process itself. The illumination system begins with the LED cluster. There are several types of LEDs being used for this project. There are white light LEDs for a balanced view of the image with the full visible spectrum that we as humans all view. Next are the different-colored LEDs, such as red, green, and blue, which belong to different specific wavelengths, and using the advantage of each effect at each wavelength is what gives the optimal imaging and in-depth analysis of the subject's skin. The red LED belongs to the 630 nm to 660 nm environmental conditions effect spectrum. Its spectrum when used for dermal imaging has deep tissue penetration properties because it penetrates farther into the skin than shorter wavelengths. Used to visibly see hidden blood vessels, capillaries, and vascular lesions. The green LED belongs to the 520 nm to 540 nm spectrum. Its spectrum, when used for dermal imaging, has mid-depth penetration and contrasts the blood of the skin because green light is absorbed by the body's hemoglobin, contrasting different blood areas. Blue LED belongs to the 450 nm to 470 nm spectrum used for level imaging since blue light penetrates only a small distance and is then scattered easily. Near-infrared LEDs belong to the 850 nm to 940 nm range and are used for deep subsurface imaging, as they penetrate the deepest out of all the LEDs, revealing the sub-dermal properties like deep vessels, skin layers, etc.

The image process begins with a standard white light illumination of the skin for analysis. As the LED is in use, the filter wheel is rotated to the white light spectrum filter, which is the broad spectrum visible to humans. As the camera captures and processes the image with the software in place, the wheel spins to the next color filter, and the next specific light spectrum begins. The red light from the LED illuminates the subject's skin, and the light is reflected off to be filtered through the red light filter, and the camera module captures the image to be processed with software, and the next filter color is rotated in the optical path. The green LED is called in use, and the image reflected from

the light is processed, and the image from the blue LED follows the same steps for image analysis. The final substage of this part is the NIR lights being turned on, and the final color filter is rotated in the optical path of the camera and processes the deeper features of the skin.

6.1.1 Optical System Architecture

Using short pulse width modulation pulses, it's easier to keep thermal measurements well below the hazardous level. Synchronizing the capturing subsystem within the imaging sequence system and its exposure whenever taking an image sample with the LED pulses is the method used to have efficient thermal regulation. Heatsinks and heat spreaders use raw materials, such as thin aluminum or copper plates, and their properties to divert heat away from sensitive components when they come into contact with them. Placing these near heat-generating systems like the PCB, LED system, and enclosure offers a cheap strategy to keep thermal regulation in check. Ventilation ports and slots embedded in the housing use the passive airflow to keep components well away from the level of thermal hazard. A more complex method uses a skin thermistor or infrared heat sensor to use software to connect with hardware for a system shutoff system.

For the 3D-printed main housing, a thermoplastic alloy of (PC) polycarbonate and (ABS) acrylonitrile-butadiene-styrene (PC-ABS). A bio-safe blend plastic that offers a lightweight, sturdy material composition and is compatible with alcohol and UV sterilization, which is important to medical care. Also, with its sturdy material composition, this offers physical impact resistance, which helps cover the faults of user error when in operating use. These reasons, in combination with the use of heat sinks and optimal heat, are used when combining the priorities of easy portability and thermal safety.

6.2 Microcontroller and Power Circuit Design

The heart of the project is the hybrid control architecture used in parallel, the Arduino and the Raspberry Pi. The Arduino microcontroller is used for low-level hardware, and the single-board computer Raspberry Pi for high-complexity image processing and user interface. The Arduino controls the real-time tasks like the LED sequencing using pulse width modulation, the stepper motor control for the filter wheel through standard GPIO, and reading the feedback response of its rotation for precise control. It operates on 5 volts and will communicate with the Raspberry Pi using a serial UART connection.

The Raspberry Pi will be in charge of the image captures and the camera interface as a whole and also in charge of the spectrum image analysis and the user interface through a display screen. After the Arduino finishes its scan cycle and as the whole image process concludes, the Pi will assemble the data, process the data from each mode during the imaging, and show the results to the operator.

The entire project is powered via a 12V LiFePO₄ battery pack. LiFePO₄ was chosen for its safety standards and stability. They have less tendency to thermal runaway and

explosions because of their chemical structure. In addition to this level of safety, there are PTC fuses to prevent overflow of power or voltage spikes; this works in unison with the TVS diodes to protect against transient voltage spikes. To manage and monitor the battery system, a BMS (battery management system) is selected to cover the 12V pack and to take care of it for cell balancing and charge control. This project also includes a shutdown peripheral mode whenever not in use to save power by entering a low-power state or completely shutting down the system. The battery pack power is fed into separate power rails covered in ferrite beads to minimize the electromagnetic interference. Along these rails are bulk capacitors at every regulator output to suppress “brownouts” and voltage/current spikes. A single star ground tie point splits into two paths at the 12V input protection point. One path is the grounding plane for the digital circuitry, such as the MCU, SBC, drivers, and communication. The other goes to the analog grounding plane, which covers the analog-to-digital portion and the grounding of the sensors. The sensors are a subgroup of inputs that cover the interconnecting sensory input that is feedback into the Arduino (communicated through I2C) to be used for feedback analysis, such as the filter wheel sensor, skin temperature sensor, current sensor, battery sensor, and the stop feature sensor.

Exiting the power pack and the grounding planes, the power flows into the two buck converters, which lower the voltage for the Arduino and Raspberry Pi, respectively. These buck converters are picked for their safety, such as internal overcurrent and thermal protection properties. One powers the Arduino and its peripherals at 5V and up to 1A, while the Raspberry Pi is powered at 3V up to 3A, while offering optimal power efficiency and low power loss.

6.2.1 Sensor Integration and PCB layout

The camera module is connected to the Raspberry Pi via a USB connection that is directly mounted. It's mounted directly behind the optical stack, aligned with the LED ring and the filter wheel. The imaging system is tightened with fasteners and a 3D-printed housing that holds the module securely. The camera signal and power paths are separated from the high current and EMI components like the motor or the driver and are connected through a USB port directly to the Raspberry Pi.

The filter wheel is controlled by a stepper motor that is in open-loop mode, which means that rotation of the filter wheel is based on a step count instead of sensor feedback, which saves hardware while putting more of a cost on the software. At startup the wheel is moved to a specific Arduino location to be marked as the 0 degree or a reference mark. Each rotation movement to a certain filter position is calculated by using the number of filters and its reference mark to ensure precise control while avoiding external parts for a simpler and more compact system.

The layout for the PCB will have extra space for mounting holes and brackets that align with the enclosure in a flush way. Using KiCad, the PCB can be organized into distinct zones that cover each distinct function for the project. Digital logic and control for the Arduino, the GPIO pins in use, and the I2C headers for the sensors, including all other peripherals. Another zone handles power regulation from the 12V input as it is being

stepped down using the buck converters. To produce the different voltages needed for the MCU and the SBC, respectively. Another section covers the high-noise or interference components like the LED clusters and the motor driver; the current lines for these are kept thick to lower resistance and any voltage drops while being kept separate from sensitive and low-noise components. Decoupling capacitors are placed at every key integrated circuit, while ferrite beads are used on the power rails that feed into the MCU and SBC. Using a 2-layer PCB design for the grounding plane helps provide shielding from EMI and stabilize proper return paths while stabilizing the logic signals. The current 2-layer design is expected to function and perform well given the level of complexity of the DermaLight project, but if it proves to be a challenge, then a 4-layer version with specific power and ground planes can be considered for the final.

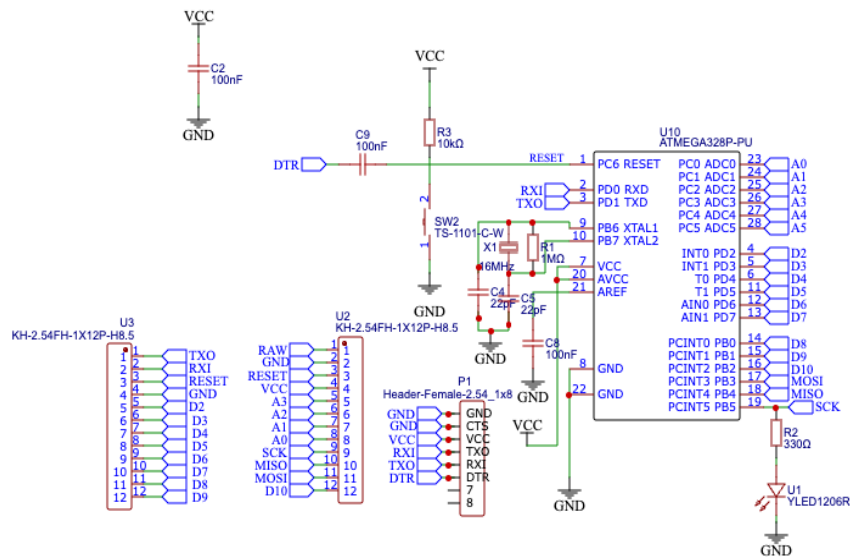


Fig 4.1 ATmega328 Board PCB Schematic

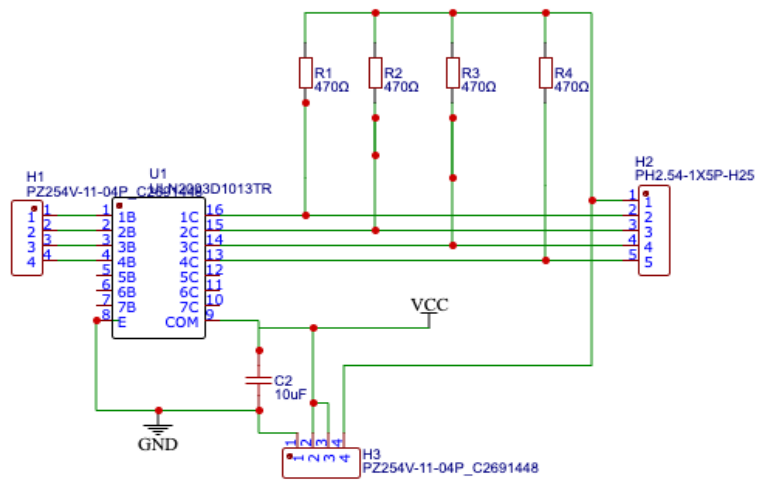


Fig 4.2 Stepper Motor Board PCB Schematic

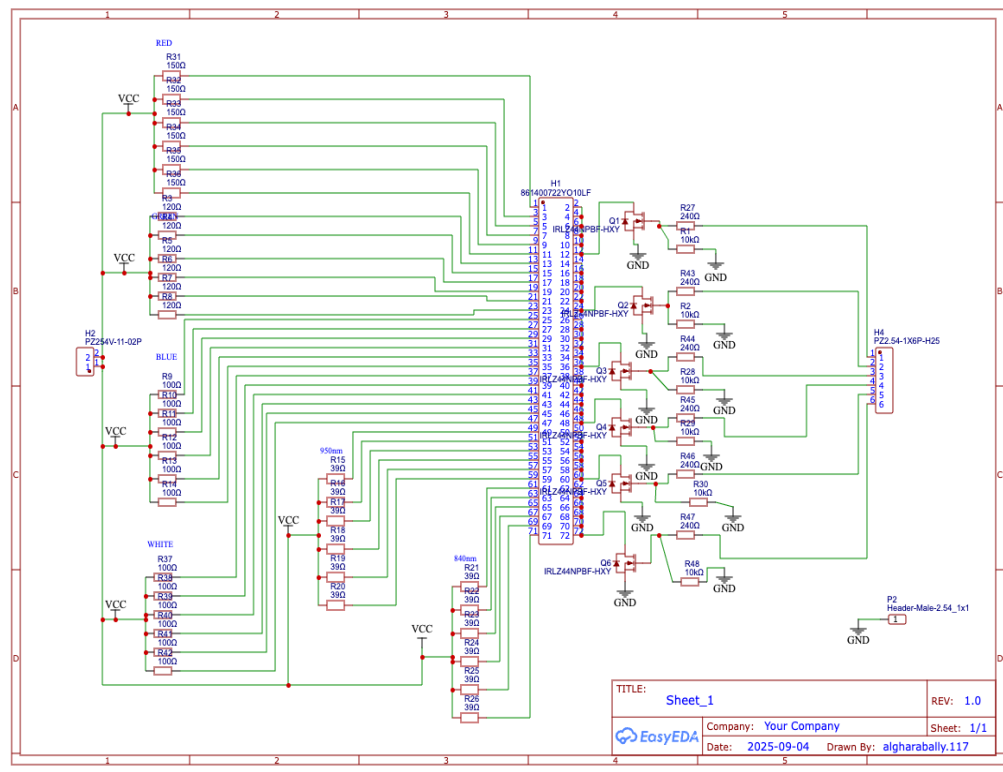


Fig 4.3 LED Driver Board PCB Schematic

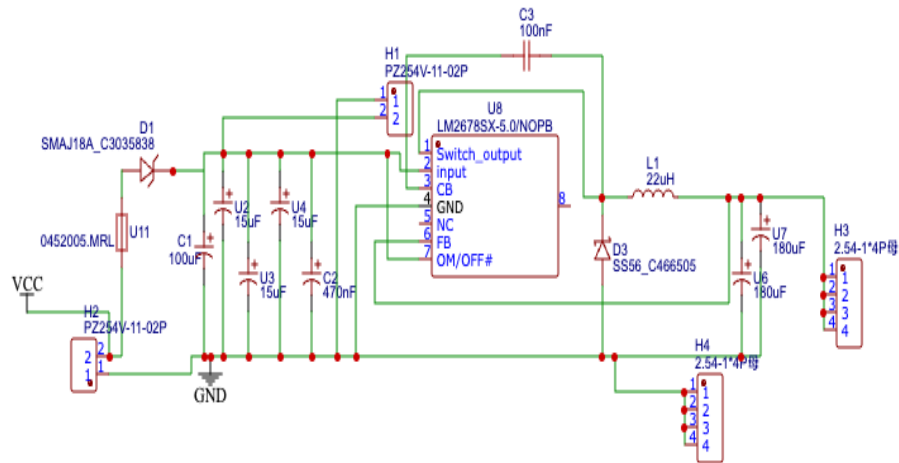


Fig 4.4 LM2678 5V Buck Converter PCB Schematic

Chapter 7 Software Design

This chapter covers the comprehensive software design for the SkinLumina device, highlighting a modular and scalable system that integrates Raspberry Pi and an Arduino for coordinated image capture and control. Key developments include leveraging the Raspberry Pi's 8MP IMX219 camera with libcamera for high-resolution image acquisition, optimized through manual tuning of exposure, gain, and white balance. A UART protocol enables synchronized communication between the Pi and MCU, while future work may integrate on-device CNNs for real-time diagnostic classification. Data transfer methods, including USB and Bluetooth via the HC-05 module, enable flexible image retrieval and device control. The LED/filter synchronization strategy employs non-blocking timing and state machines to ensure precise multispectral imaging aligned with filter positioning. Data processing incorporates skin tone calibration and two classification pathways: rule-based blob detection and machine learning models trained on multispectral features for lesion detection. Lastly, a user-friendly, cross-platform UI is proposed, built with React/Tailwind CSS or Flutter, features capture, analysis, history, and settings screens with LED controls.

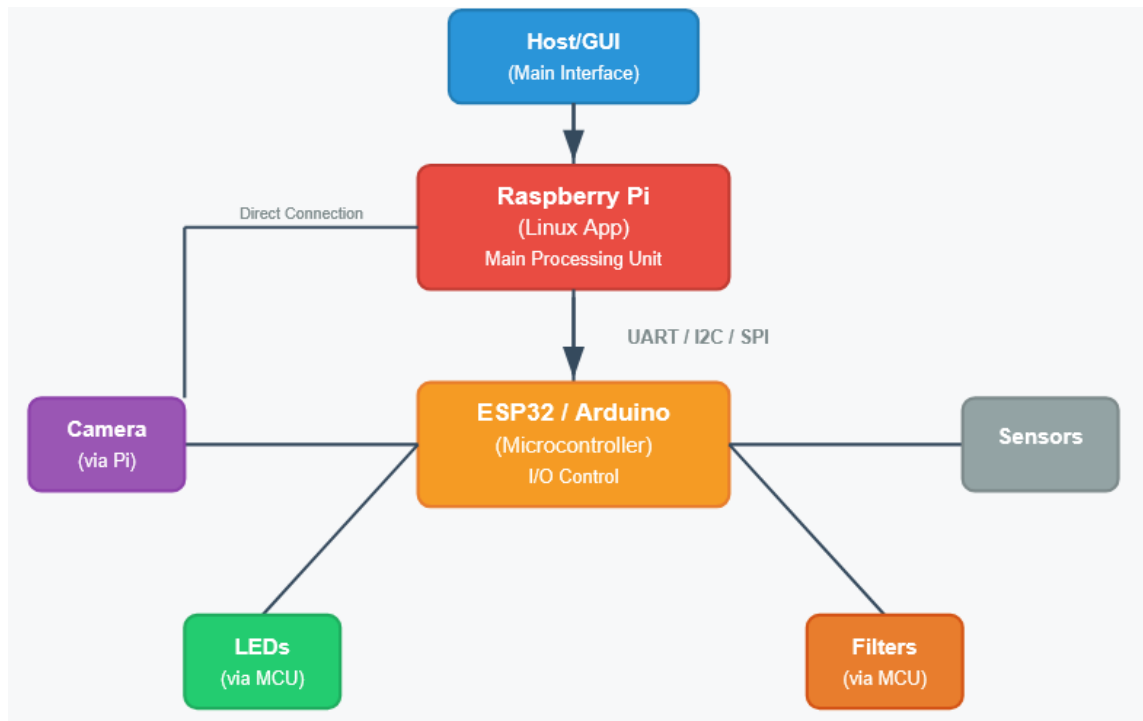


Fig 5. SkinLumina Device Workflow

Figure 5 outlines the device’s workflow, where a Raspberry Pi serves as the main processing unit, capturing high-resolution images using the IMX219 camera via libcamera. It adjusts imaging parameters and sends commands to the ESP32/Arduino microcontroller over UART/I2C/SPI. The microcontroller manages LEDs, filters, and sensors to coordinate illumination and spectral filtering. A host GUI interfaces with the Pi, enabling image capture control and data retrieval. This setup allows synchronized, multispectral imaging essential for accurate skin analysis.

7.1 Image Capture and Control

We will be combining a Raspberry Pi with an Arduino, this allows for a powerful and scalable design for SkinLumina. For image capture and control, the Raspberry Pi will be the image processing unit. For the connection of the Raspberry Pi to the 8MP IMX219 Camera Module, we will be using an open-source software library called libcamera to capture images, control camera parameters, and process image data prior to sending commands to the MCU.

In a 2019 thesis project, researchers used a Raspberry Pi 3 and Pi Camera Module to develop a real-time traffic cone detection system for robotics applications [36]. Although the task differed from SkinLumina’s biomedical goals, the study demonstrated that low-cost, real-time image processing is feasible using Raspberry Pi hardware. Their system achieved 30–35 FPS and successfully detected cones up to 2–3 meters away, using open-source tools such as OpenCV and edge detection algorithms.

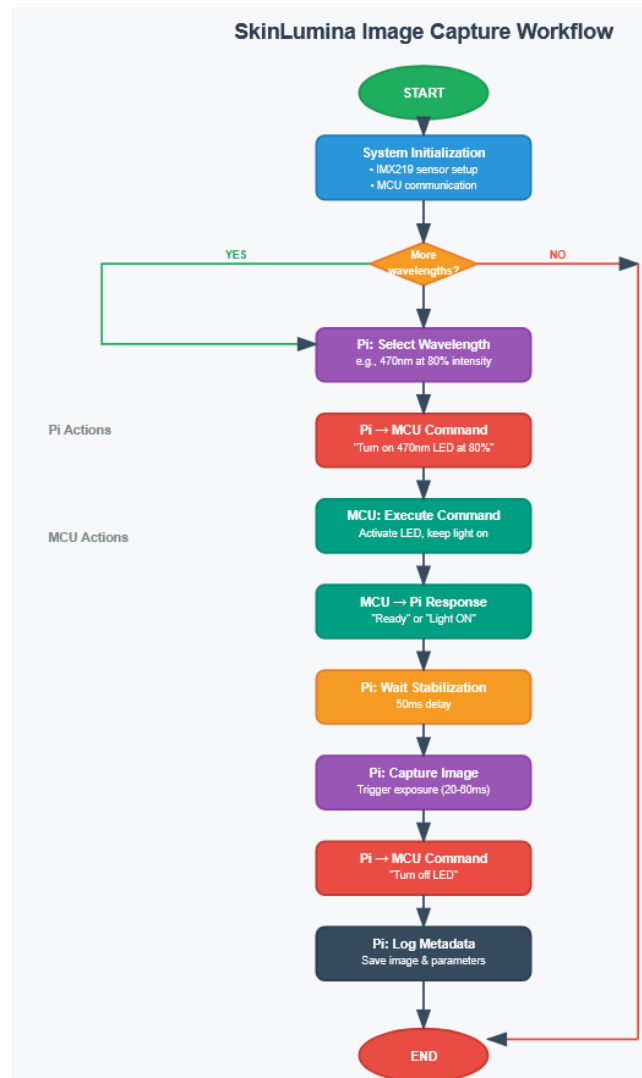


Fig 5.1 Sequential multispectral imaging process

Figure 5.1 outlines the sequential process used by the SkinLumina device to capture multispectral skin images. The process begins with system initialization. For each wavelength, the Raspberry Pi selects an LED setting and sends a command to the MCU to activate the LED. Once the MCU confirms the LED is on, the Pi waits briefly for stabilization before triggering image capture. After capturing the image, the Pi sends a command to turn off the LED and logs the metadata. The cycle repeats for each wavelength until all required images are captured. The workflow ensures precise LED control, timing, and metadata logging for consistent and high-quality image acquisition.

The image capture and control workflow for our project begins with camera initialization. The Raspberry Pi verifies that the 8MP IMX219 sensor is correctly connected and detected. This involves configuring the Pi's device tree overlays and ensuring I2C communication with the camera. The IMX219 works with the Raspberry Pi's unicam driver, which manages low-level sensor configuration and image streaming.

To enable seamless development and control, the Raspberry Pi is configured for headless operation. This involves enabling SSH and Wi-Fi connectivity prior to deployment by editing the `wpa_supplicant.conf` and `ssh` files on the Pi's boot partition. Once powered, the Pi can be accessed remotely via a terminal using its hostname (`raspberrypi.local`) or IP address. Remote access allows for live control of camera operations, image previewing, and log monitoring directly from a PC or mobile device.

Before each image is captured, the Raspberry Pi transmits a structured serial command to the MCU. Communication is handled via a UART interface, using a predefined command protocol. Capture resolution is configured to the sensor's native 3280×2464 pixels to ensure maximum detail for dermatological analysis. Key imaging parameters are then adjusted in software: exposure time is typically set between 20–60 milliseconds to control how long the sensor collects light; analog gain is kept as low as possible to minimize image noise in well-lit conditions; and white balance is manually configured to ensure consistent color representation across different sessions and wavelengths. Captured images can be saved in RAW format to preserve unprocessed sensor data for high-fidelity analysis, or in JPEG format when storage efficiency and real-time review are prioritized.

To automate the image capture process, a Python script running on the Raspberry Pi coordinates LED activation, camera triggering, and image storage. The script defines a capture sequence, iterating through various wavelengths (e.g., white, red, green, blue, NIR-850, NIR-940), and introduces brief delays to allow LED stabilization before each capture. The `os.system()` function or subprocess module is used to call `libcamera-still` with specific exposure, gain, and white balance parameters. Captured images are programmatically named with a timestamp and wavelength label, then saved to a designated directory on the Raspberry Pi for easy access and later transmission. Precise timing is essential to ensure repeatability and image quality. A short delay (~200 ms) is inserted after each LED activation to allow for optical stabilization before the image is taken. This is managed through non-blocking functions like `time.sleep()` in Python to avoid interrupting the flow of the script.

7.1.1 Adaptive Capture Routine

The SkinLumina device employs an embedded adaptive imaging algorithm running on the Raspberry Pi to ensure that every scan is automatically calibrated to the user's skin tone, local lighting conditions, and the optical characteristics of the device. This algorithm serves as the central control mechanism for coordinating the system's camera module, multispectral LED array, motorized filter wheel, and UART-based communication with the Arduino microcontroller. Its purpose is to harmonize all hardware subsystems so that each scan produces three synchronized outputs: a raw multispectral image, an annotated diagnostic image highlighting detected features, and a quantitative analysis plot containing numerical metrics such as blob counts, edge sharpness, and center-patch color values. By performing adaptive decision-making in real time, the software ensures that illumination, timing, and wavelength selection remain consistent across diverse skin tones and imaging sessions.

The imaging sequence begins with a baseline white-light illumination phase. At the start of each scan, the Raspberry Pi instructs the Arduino to set the white LED ring to a predefined low-intensity baseline level. This baseline setting provides a uniform, illumination-neutral starting point that allows the system to assess how light interacts with the user's skin without any spectral bias. A reference image is then captured using the Sony IMX219 camera module, and this raw frame is temporarily stored for analysis. This initial image is essential: it serves as a calibration anchor that allows the system to assess reflectivity, exposure levels, and variations in pigmentation before any wavelength-specific imaging occurs.

After capturing the baseline image, the algorithm samples a defined region of interest near the center of the frame to compute both the RGB and HEX color values of the skin. This center patch is intentionally positioned slightly below the geometric midpoint of the image, as this region typically corresponds to where the user places the area of interest and avoids vignetting or edge artifacts. The extracted color information provides an instantaneous measurement of skin tone and local reflectance characteristics, which the system then uses to adjust illumination parameters. Based on this sampled information, the algorithm executes its LED boost decision logic. If the red channel is disproportionately high relative to the others, the system compensates by boosting blue illumination; if green dominates, red is boosted; and if blue dominates, green is boosted. In cases where overall luminance is low—particularly relevant for darker skin tones—the white LED channel is elevated to improve exposure. This dynamic adjustment ensures that every scan maintains consistent contrast and visibility, regardless of the user's melanin concentration.

Once a decision is made, the Raspberry Pi sends a command to the Arduino over UART in the form "LED <color> <intensity>," setting the appropriate channel to its calculated brightness. The Pi then waits for an acknowledgment (ACK) before proceeding, ensuring deterministic hardware behavior and preventing race conditions between communication and illumination changes. With the updated LED settings in place, the Pi captures a second image under the optimized illumination. This boosted image typically provides the highest clarity, best contrast, and most accurate anomaly detection performance, as it is tailored specifically to the user's skin tone.

Following this, the algorithm proceeds to synchronize the filter wheel with the imaging process. The Pi instructs the Arduino to rotate the motorized filter wheel by one indexed position—typically one-fifth of a revolution—aligning the next spectral filter with the camera's optical path. The Pi again waits for an ACK to confirm that the wheel has reached the correct position. This sequence is repeated for each wavelength used in the multispectral scan, allowing the system to collect a complete stack of images across the visible and near-infrared spectrum.

For every captured frame, the Raspberry Pi immediately begins a multi-stage image processing workflow. Each image undergoes grayscale conversion, contrast-limited adaptive histogram equalization (CLAHE), Gaussian smoothing, and adaptive thresholding to isolate potential skin anomalies. Additional morphological operations remove artifacts and refine lesion boundaries. From these processed outputs, the system generates an annotated diagnostic image that overlays contours and numerical labels onto the original frame. Simultaneously, the Pi computes a variety of optical metrics—including blob count, blob size, edge profile characteristics, MTF50 sharpness, and center-patch RGB/HEX values—and synthesizes them into an analysis plot. This plot visually summarizes the diagnostic results for a given wavelength, providing clinicians or users with a structured understanding of the detected features.

After processing, the Raspberry Pi packages all outputs—raw image, annotated image, analysis plot, and a structured JSON metadata file containing LED settings, color readings, processing times, detected feature counts, and filter-wheel position. These files collectively represent a complete spectral snapshot of the scanned region. Finally, the Pi uploads all data to the backend server using a multipart POST request to the /media/upload endpoint. The server stores the images in Cloudinary and writes the metadata to MongoDB, enabling the SkinLumina web dashboard to retrieve these results in real time for display, comparison, or longitudinal tracking.

Through this integrated adaptive capture routine, SkinLumina intelligently calibrates illumination, synchronizes multispectral imaging events, and processes data on-device to ensure consistent, high-fidelity imaging performance across all skin tones. This algorithmic pipeline is fundamental to the device’s goal of delivering inclusive, reliable, and clinically meaningful dermatological imaging.

7.2 Bluetooth/USB Transmission

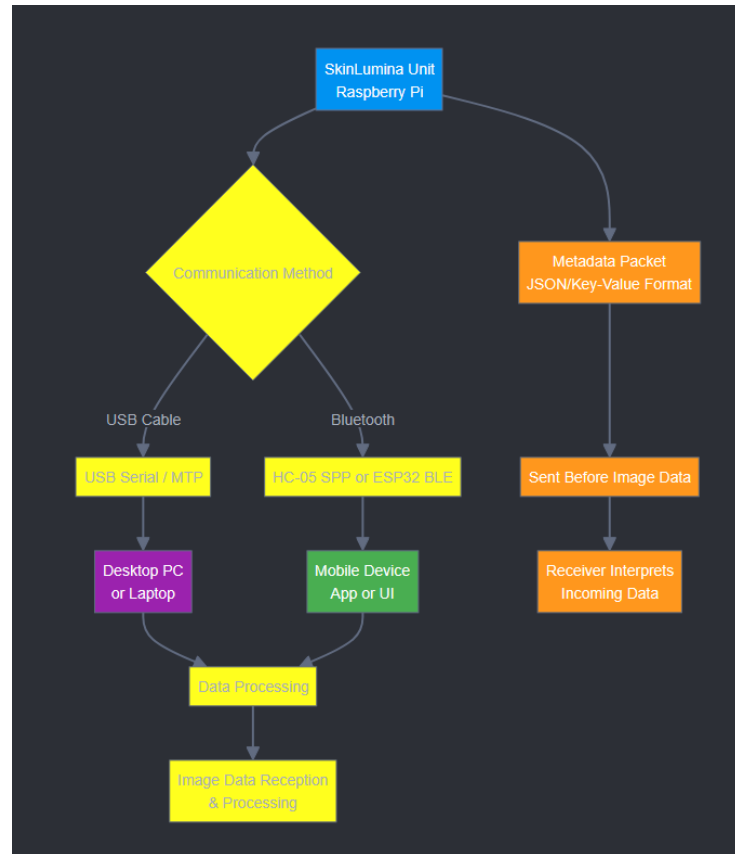


Fig 5.2 Raspberry Pi image and data transmission process.

Figure 5.2 shows how the Raspberry Pi unit transmits image data and metadata to an external device. Two communication methods are supported: USB cable and Bluetooth for mobile devices. Both paths lead to data processing, followed by image data reception and processing. Separately, a metadata packet is sent before the image data to help the receiver interpret incoming information correctly. This ensures that both the metadata and image data are properly aligned and understood during transfer and analysis.

The software design workflow for Bluetooth transmission in the SkinLumina project facilitates simple and reliable wireless communication between the MCU and the Raspberry Pi using the HC-05 Bluetooth module, focusing on sending commands and data. An Arduino uses C++ through the Arduino development environment, to manage hardware components like LEDs and handle Bluetooth communication. It begins by setting up the HC-05 module to communicate at a standard speed (9600 baud rate) and sends a message to indicate it's ready to operate. The Raspberry Pi, using the Python programming language with a Bluetooth library called pybluez, connects to the HC-05 by identifying its unique Bluetooth address and communication channel. When a scan is initiated, typically through a user interface on the Pi or a mobile app, the Pi sends a command to the Arduino to turn on a specific LED, such as a white LED, and the Arduino confirms the action by sending a message back indicating the LED is activated.

For a complete scan, the Pi sends a start-scan command, prompting the Arduino to cycle through different LEDs (e.g., white, near-infrared, and RGB) in a sequence, sending status updates to indicate the scan is in progress and then complete. The Pi can then request scan details, and the Arduino responds with metadata, including details like the image file name and LED settings used. If a preview image is needed, the Pi compresses the image to a smaller size, sends a message to start the image transfer, sends the image data in small parts, and signals when the transfer is finished, while the Arduino acknowledges each part and confirms the full image is received. Both devices handle errors by checking for error messages or managing connection issues, ensuring smooth communication.

Prior to Bluetooth communication being enabled, we will be working with USB transmission. One method would be plugging in a USB flash drive into the Raspberry Pi and copying the stored image files through a script. The other alternative is sending images directly from the Raspberry Pi to the desktop via USB. On the Pi, a python script will read through each image and transmit it over the serial connection. On the PC, a python script will listen and reconstruct the file.

7.2.1 UART Communication Protocol

The SkinLumina system operates on a dual-controller architecture in which the Raspberry Pi performs high-level decision-making, image analysis, and adaptive control, while the Arduino handles all real-time actuation of LEDs and motorized components. To coordinate these two roles, we implemented a UART-based communication protocol that offered the most stable and predictable method for exchanging commands during multispectral imaging. After evaluating alternatives such as I²C and SPI, UART proved to be the most reliable for continuous bidirectional messaging, particularly under the timing demands of synchronized LED adjustments and filter-wheel rotations. The protocol described below represents the final communication structure developed after extensive testing, refinement, and validation during system integration.

Communication between the Raspberry Pi and Arduino occurs through the Pi's /dev/serial0 interface operating at 9600 bps. Higher data rates were initially explored but led to inconsistent parsing on the Arduino whenever rapid PWM changes or stepper-motor movements occurred. The 9600-bps configuration provided a stable link that avoided packet loss and maintained consistent timing during the imaging cycle. Both devices operate using a standard 8-N-1 configuration, simplifying compatibility and ensuring predictable communication behavior.

To support clear and efficient command exchange, a lightweight text-based format was developed. Instructions such as “LED WHITE 20” or “LED RED 80” control the multispectral illumination intensities, while commands such as “STEP FIFTH” rotate the filter wheel to the next indexed position. This structure allows the Raspberry Pi to dynamically adjust hardware behavior based on the results of the adaptive capture algorithm. After receiving a command, the Arduino executes the corresponding action

and responds with a confirmation message indicating that the operation was successfully completed. This acknowledgment mechanism ensures strict synchronization: the Raspberry Pi does not issue a subsequent command until the previous one has been verified, preventing timing conflicts during image capture.

During development, the communication protocol underwent extensive testing to ensure robustness across the full multispectral acquisition cycle. Early iterations revealed occasional issues involving incomplete transmissions or malformed strings, which occurred most frequently during rapid sequences of LED changes and filter-wheel movements. To address this, the Arduino was programmed to return explicit error messages when encountering invalid commands or parameters. This closed-loop communication design allowed the Raspberry Pi to correct or resend instructions immediately, significantly improving reliability during continuous operation.

The team also characterized timing behavior to ensure that the communication system could support the precise sequencing required for synchronized imaging. Through a combination of software timestamps and oscilloscope validation, the round-trip latency—including command transmission, parsing, hardware actuation, and acknowledgment—was shown to remain within a few milliseconds. This predictable timing made it possible to coordinate illumination changes and filter-wheel indexing with camera exposure windows without relying on fixed delays. As a result, the imaging pipeline avoided drift, misalignment, or inconsistent illumination across wavelengths.

Ultimately, the UART protocol became a critical component of the SkinLumina architecture. The structured command format, deterministic acknowledgment system, rigorous timing characterization, and robust error handling together created a communication layer capable of supporting the demands of adaptive, multispectral imaging. This protocol ensures that the Raspberry Pi and Arduino function as a unified control system, enabling precise wavelength sequencing and consistent imaging performance across all operating conditions.

7.3 LED and Filter Synchronizations

The LEDs and filters in our project are central to its multispectral imaging system and are tightly integrated into both the optical and software design. We will first begin by defining our scan phases and specific group of LEDs that need to be triggered during each phase. LED toggling is managed through a combination of non-blocking timing functions, digital and analog output controls, and a simple state machine to sequence each scan phase.

During operation, each group of LEDs is assigned to a specific scan phase. The Arduino's `millis()` or `micros()` functions are used to track elapsed time without halting the main program loop, enabling non-blocking transitions between phases. A state machine

structure governs the scan sequence, ensuring that only the appropriate LED group is activated at any given time. Within each state, `digitalWrite()` is used to turn LEDs on or off, while `analogWrite()` provides optional PWM control for adjusting brightness to match calibration requirements or compensate for varying skin tones.

For more precise timing, timer libraries like `TimerOne` or `TimerThree` can be employed to generate hardware interrupts, ensuring consistent and repeatable LED switching intervals. This approach allows the system to trigger each LED group in a defined order, synchronize with camera capture events, and maintain accurate exposure across all wavelengths. The timeline (Figure 6) illustrates the synchronization between the LED illumination and filter wheel positioning during a full scan cycle of the SkinLumina device. The process begins with a baseline image using white LEDs to assess the user's skin tone. Following calibration, the system sequentially rotates the optical filter wheel to the correct position for each wavelength (e.g., RED, GREEN, BLUE, NIR-850, NIR-940) and activates the corresponding LED group. Each step includes a short stabilization delay to ensure accurate imaging under clean spectral conditions.

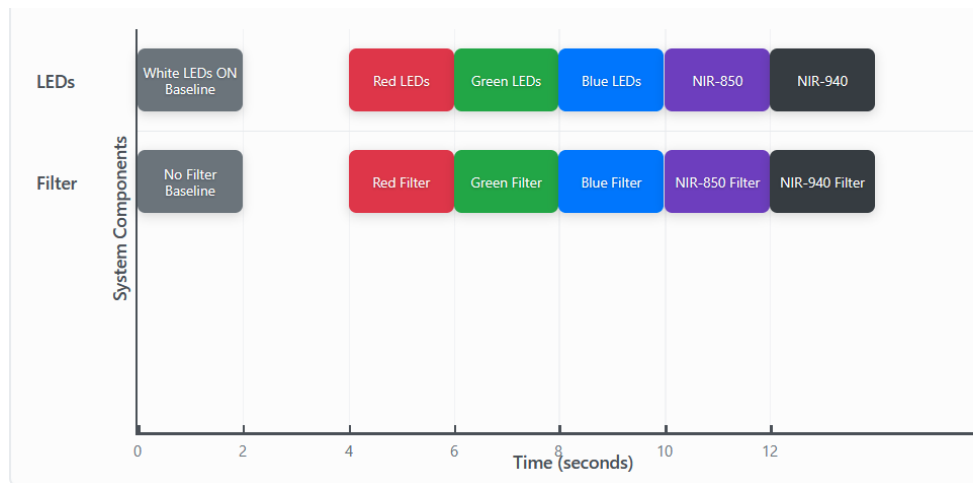


Fig 6. Synchronization Timeline

To implement LED control in the SkinLumina system, each group of LEDs is wired in parallel and connected to designated digital GPIO pins on the Arduino. A 300-ohm resistor is placed in series with the anode to limit current and prevent LED damage. The cathodes are connected to a common ground. This setup allows the Raspberry Pi to send commands to the Arduino to toggle specific LED clusters via serial communication. The Arduino code uses command parsing over UART to interpret instructions from the Raspberry Pi. When the Raspberry Pi sends a string like "red on" or "white off", the Arduino parses this input and toggles the corresponding GPIO pin using `digitalWrite()`. A non-blocking command handler built around `serialEvent()` ensures that incoming commands are processed asynchronously, without interfering with the main loop's timing logic. Table 4 provides a sequence of operations the Arduino workflow will follow.

Step	Device	Responsibility	Details
1	Raspberry Pi	Starts scan sequence	Sends "white on" to Arduino via Serial
2	Arduino	Receives "white on" via Serial.read()	Turns on white LED using digitalWrite(WHITE_GROUP_PIN, HIGH);
3	Raspberry Pi	Waits 200ms, then triggers camera (libcamera-still)	Captures white image
4	Raspberry Pi	Sends "white off" to Arduino	—
5	Arduino	Turns off white LED	digitalWrite(WHITE_GROUP_PIN, LOW);
6-11	Repeat	For red, green, blue, NIR850, NIR940	One LED at a time
12	Raspberry Pi	Saves image + logs metadata	File name, exposure, LED type, etc.
13	Both	System ready for next scan	Wait or loop

Table 4 Arduino Sequence of Operations

7.4 Data Processing

The data processing subsystem plays a critical role in the SkinLumina device, serving as the bridge between raw optical capture and clinically meaningful output. Its core function is to convert multispectral images acquired from the CMOS camera into structured information. The processing pipeline has been specifically designed to accommodate the unique variability of human skin tones while remaining efficient, lightweight, and compatible with embedded systems.

7.4.1 Tone Detection

The workflow begins with preprocessing, where each captured image is converted to grayscale, denoised using Gaussian or median filters, and contrast-enhanced to improve the visibility of relevant features. For skin tone detection, once the baseline white-light image is captured, the software will select a central patch of skin and from that patch it will collect the RGB values of all pixels and average it to a hexadecimal format. This hex code is then matched to a reference skin tone database, enabling the system to adjust LED intensity and exposure settings accordingly to compensate for melanin content and ensure balanced illumination in subsequent scans. The referenced skin tone database will be derived from the Fitzpatrick skin type scale (Figure 7), a dermatological classification system that divides human skin into six categories based on melanin content and response to UV exposure.

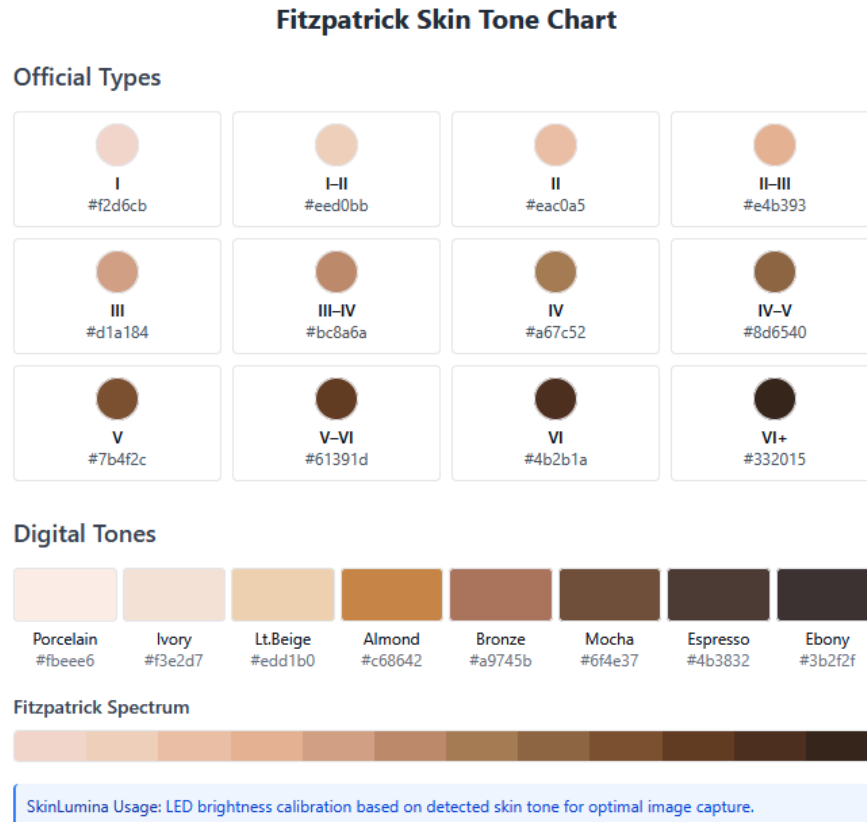


Fig 7. Fitzpatrick Skin Tone Classification Chart

The Fitzpatrick scale ranges from Type I (very fair, always burns) to Type VI (very dark, never burns), and each type can be approximated with a representative set of RGB or hex color values. By calculating the Euclidean distance in RGB space between the captured skin tone and each Fitzpatrick reference, the software can estimate the closest skin type. For example, a detected skin hex code of #4B3832 would likely map to Type V or VI due to its high melanin content. This classification then guides adjustments to LED intensity and camera exposure in follow-up scans, ensuring more consistent illumination and contrast across patients of different skin tones. Once tone-based exposure calibration is complete, the system proceeds to analyze the multispectral images for signs of skin abnormalities. This is achieved through classification algorithms described in the following section.

7.4.2 Data Classification

There are two possible methods for data classification. Blob detection can be created with conditional logic based on pixel intensity, shape, and position across wavelengths. For instance, if a dark spot appears in NIR-850/940 but is not visible in RGB, we can possibly conclude it is a subsurface lesion.

Logic Example:

if spot_NIR and not spot_RGB → flag as subsurface abnormality

Another example would be in scar detection, if a blob shows a strong contrast in red but fades in blue or green, it could be hyperpigmentation.

Logic Example:

if intensity_red > threshold and intensity_green < small → hyperpigmented region

Blob detection involves identifying connected regions in an image that share similar characteristics. The process typically begins with preprocessing, where the image is converted to grayscale and adjustments to contrast is made to enhance the visibility of potential blobs. To identify the blobs, algorithms can be used to detect regions that stand out. Thresholding can binarize images to separate potential blobs, like a dark spot on skin, from the background. Edge detection can identify boundaries of blobs using a method like Canny edge detection. Connected component analysis can also be used to group pixels into connected regions based on intensity or color similarity. A more sophisticated implementation of blob detection is provided by OpenCV's SimpleBlobDetector class that applies the following process [38].

The image is thresholded multiple times across a range of intensities. At each threshold, connected components are detected using findContours. The centers of these components are grouped based on proximity (using a configurable minDistBetweenBlobs), which helps identify consistent regions across thresholds.

The final set of blobs is refined using a series of filters:

By area: Keeps blobs whose size is between minArea and maxArea.

By circularity: Filters blobs based on how round they are

By convexity: Uses the ratio between the blob's area and the area of its convex hull.

By inertia ratio: Filters based on how elongated a blob is.

By color: Distinguishes blobs by whether they are lighter or darker than the surrounding background.

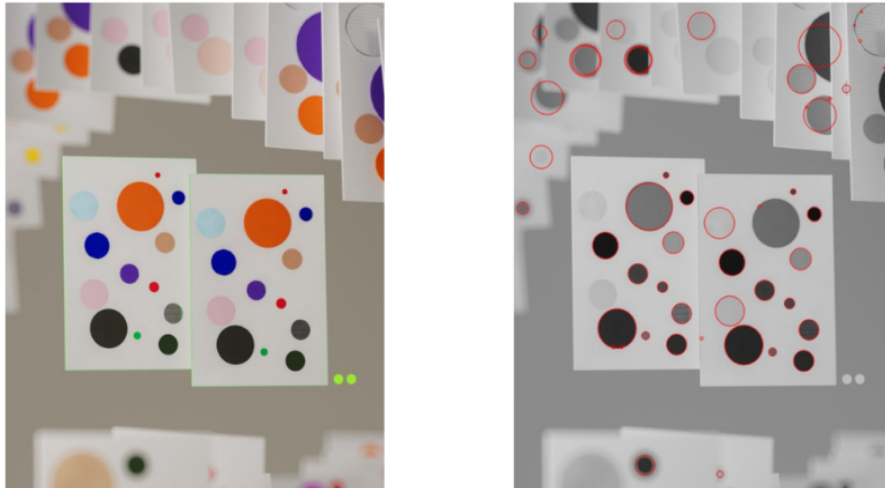


Fig 7.1 SimpleBlob Detector, Source: Adapted from [44]

Figure 7.1 illustrates blob detection from OpenCV. The colored image on the left shows the original input image, which consists of various colored and sized circular regions on a neutral background. These circles simulate the appearance of different blob-like structures similar in concept to lesions, moles, or pigmentation areas in skin imaging. The black and white image to the right illustrates the output of the blob detection algorithm applied to the same input image. Here, each detected blob is outlined with a red circle. The algorithm identifies blobs based on specific characteristics such as area, circularity, convexity, and color intensity. This is achieved using OpenCV’s “SimpleBlobDetector”.

Another method for data classification involves using machine learning algorithms to analyze features extracted from visible and near-infrared (NIR) skin images. Classical machine learning models such as logistic regression, support vector machines (SVMs), or random forests can be trained on manually extracted features to distinguish between patterns like scars, lesions, and normal skin. These features might include average pixel intensity, blob count, contrast differences across wavelengths, or shape descriptors from regions of interest. Once trained offline using labeled datasets, these models can be deployed on the Raspberry Pi to classify new image segments into diagnostic categories in real time.

For more advanced and automated classification, SkinLumina can incorporate a lightweight Convolutional Neural Network (CNN) trained on multispectral skin imagery. This CNN model can be developed using TensorFlow or PyTorch on a local machine. The training process begins with importing essential libraries such as `tensorflow.keras.models`, `tensorflow.keras.layers`, and `ImageDataGenerator`. Next, the dataset is organized into three labeled categories—normal, lesion, and scar—each stored in separate folders under the training and validation directories. Before feeding images into the CNN, they are preprocessed to ensure uniformity: all images are resized to the same dimensions, pixel values are normalized between 0 and 1, and class labels are inferred from the folder structure.

The CNN architecture is then defined as a sequential stack of layers, as illustrated in Figure 7.2. It begins with a Conv2D layer that identifies low-level features like edges and

textures, followed by a MaxPooling2D layer that reduces spatial dimensions while retaining the most salient features. A second convolutional layer, with more filters, extracts higher-level features, and another pooling layer further reduces dimensionality. The output is then flattened into a 1D vector, which feeds into a fully connected dense layer that learns complex feature combinations. To prevent overfitting, a Dropout layer disables 30% of neurons during training. Finally, the output layer uses a softmax activation function to return probabilities for the three classification categories: normal, lesion, and scar.

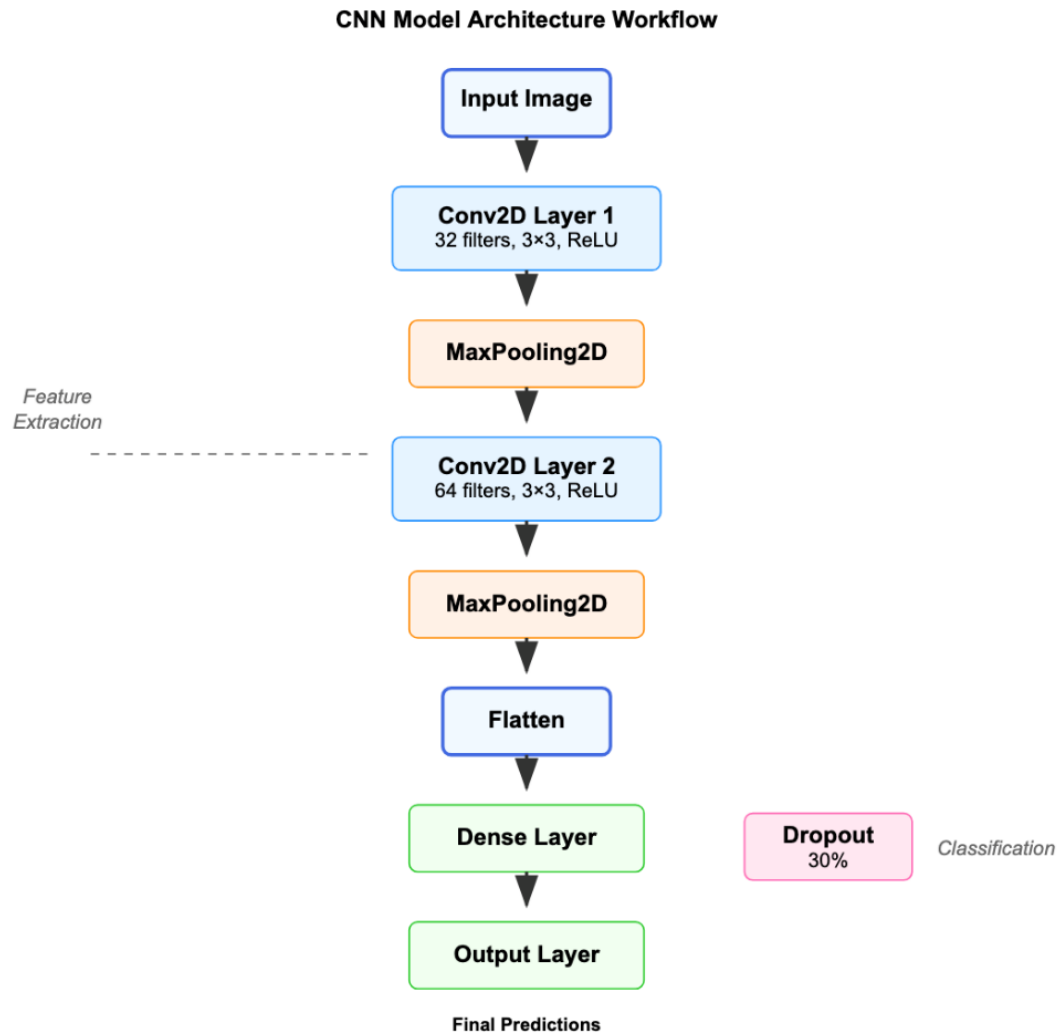


Fig 7.2 CNN Workflow

Once the CNN architecture is defined and trained on the labeled dataset, the next phase involves evaluating the model's performance. This includes analyzing metrics such as accuracy, precision, recall, and confusion matrices on the validation dataset to ensure the

model generalizes well to unseen images. If needed, hyperparameters such as learning rate, batch size, and the number of epochs can be adjusted to improve performance. Once a satisfactory accuracy level is achieved, the model is converted to TensorFlow Lite format (.tflite) for deployment on the Raspberry Pi. This conversion reduces the model's size and optimizes it for edge inference. On the Raspberry Pi, the trained TFLite model can be integrated into the existing image capture workflow, where each newly captured multispectral image is passed through the model to generate a real-time classification. The output can then be displayed on the frontend interface, providing immediate diagnostic feedback to the user.

When a new image is captured by the Raspberry Pi, it is either processed immediately on the device using the deployed CNN model or sent to the Flask server via a POST request. The backend handles model inference and returns the classification results along with confidence scores or diagnostic annotations. These results are then fetched by the React frontend using asynchronous requests. The user interface dynamically updates to display the image alongside the classification output in an intuitive display.

7.4.3 Software Architecture Diagram for Adaptive Capture Pipeline

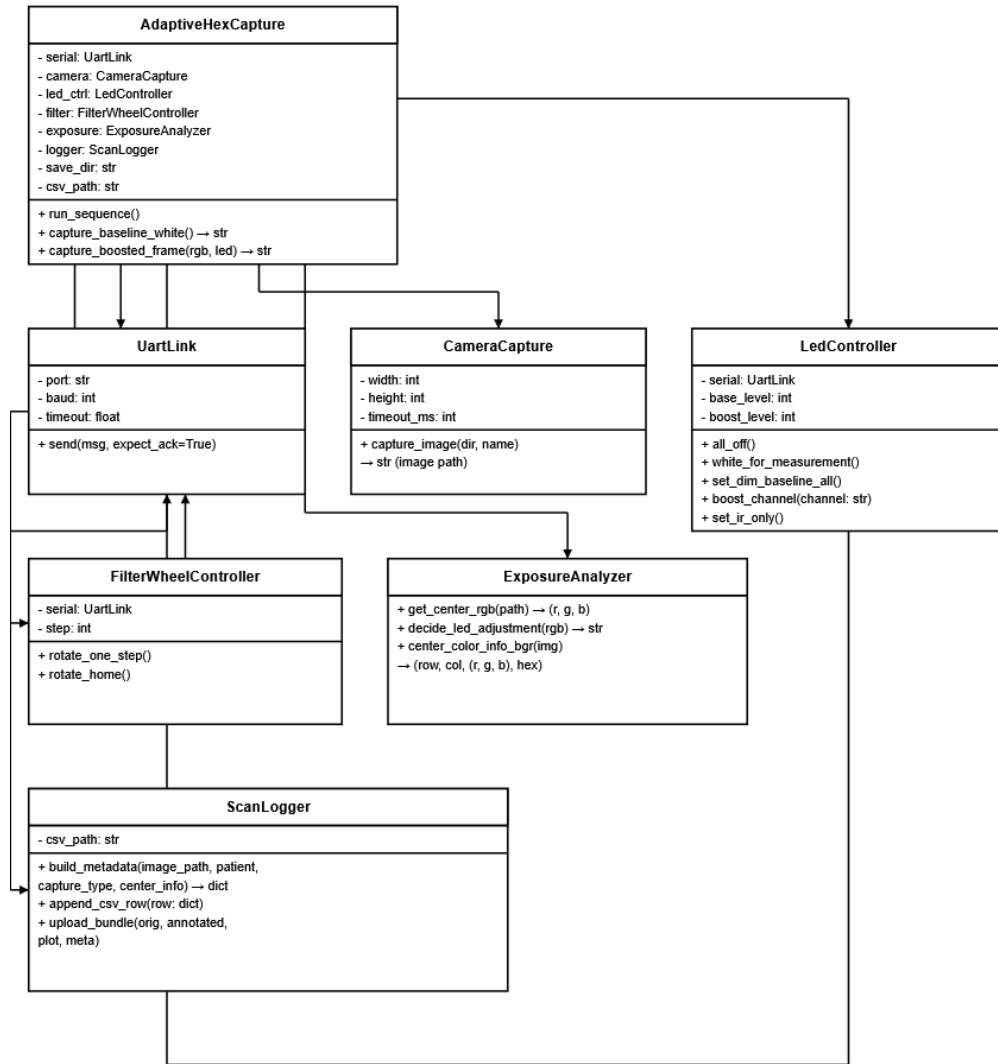


Figure 7.4. Unified software architecture of the Raspberry Pi adaptive capture pipeline, showing class responsibilities and interaction flows among control, communication, imaging, and logging modules.

Figure 7.4 illustrates the software architecture implemented on the Raspberry Pi to control the full adaptive imaging workflow. The system is organized into modular, object-oriented components that separate responsibilities for communication, illumination control, camera capture, exposure analysis, filter-wheel actuation, and data logging. This design allowed the team to iteratively test and refine individual subsystems while maintaining a coherent high-level capture pipeline.

At the highest level, the AdaptiveHexCapture class coordinates the entire multispectral imaging sequence. It manages UART communication, camera operation, LED illumination, filter-wheel rotation, exposure analysis, and data logging. This controller

performs the baseline capture, extracts the center-patch RGB values, determines the appropriate LED boost for the user's skin tone, captures the boosted frame, and then advances through the remaining filter positions. The class enforces a deterministic sequence so that camera exposure, LED updates, and motor commands occur without timing conflicts. The UartLink class implements the communication layer between the Raspberry Pi and Arduino. All commands, such as LED adjustments or filter-wheel steps, are transmitted through this interface and must be acknowledged before the system proceeds. This handshake protocol prevents race conditions, ensuring that each physical action fully completes before the next capture stage begins.

The CameraCapture class manages all interaction with the `rpicam-still` tool. It defines consistent capture parameters, including resolution, timeout, and file handling, so that all baseline, boosted, and multispectral frames are acquired under identical imaging conditions. This consistency is necessary for valid quantitative comparison across wavelengths. Illumination control is handled by the `LedController` class. It sets dim baseline intensities, applies spectral boosts, switches between visible and near-infrared channels, and verifies all changes through UART acknowledgments. This class implements the adaptive skin-tone logic: fair skin, which reflects green and blue strongly, receives boosted blue/green illumination to avoid overexposure, while darker skin, which absorbs more red light, receives a red-channel boost to maintain sufficient reflectance and contrast.

The `FilterWheelController` class regulates the stepper-driven filter wheel. It issues rotation commands, waits for acknowledgments, and ensures that each optical filter is correctly positioned before image capture. Accurate alignment is essential for labeling and interpreting multispectral frames. The `ExposureAnalyzer` class processes the baseline image to extract RGB values from a defined off-center sampling region. It uses this measurement to determine which LED channel should be boosted for balanced illumination across different skin tones, directly driving the adaptive behavior of the capture routine. Together, these components form a streamlined, modular pipeline that links spectral decision-making with low-level hardware control, enabling stable, reproducible, and adaptive multispectral imaging.

7.4.4 Data Processing and Classification Full Pipeline

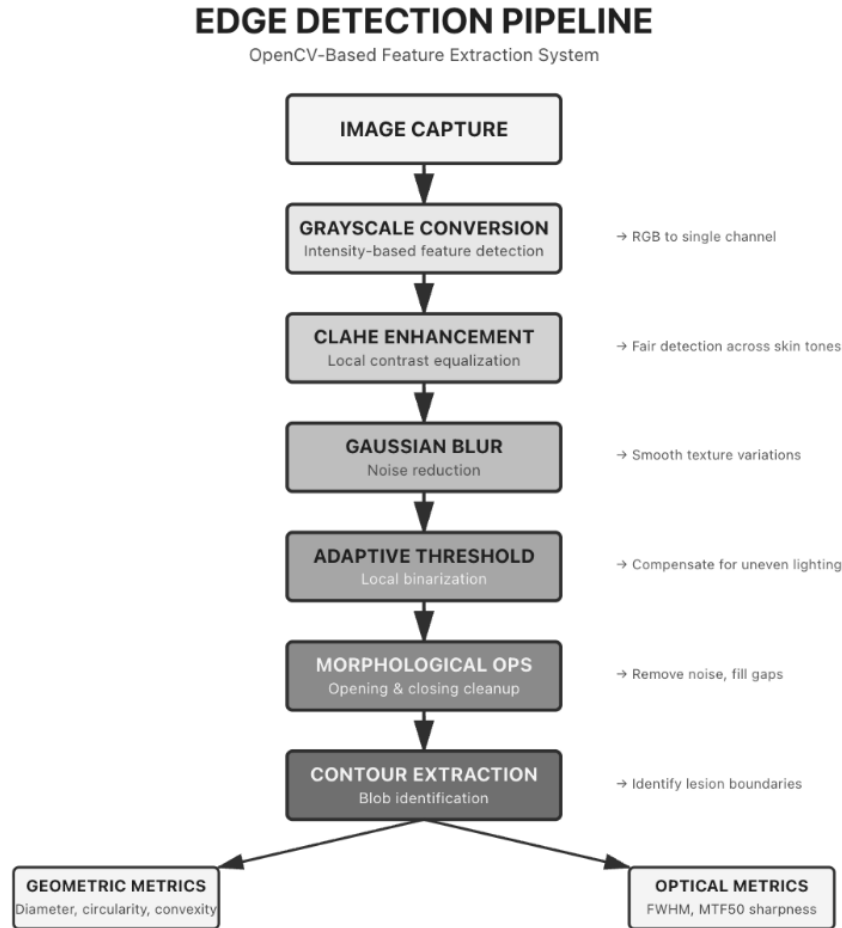


Figure 7.4.4 Edge Detection Pipeline

The final stage of SkinLumina’s software pipeline performs a complete transformation of the captured multispectral images into quantitative descriptors that characterize the surface and subsurface features present in each frame. This stage is executed automatically on the Raspberry Pi immediately after the adaptive capture routine and is responsible for producing the annotated outputs and the metadata JSON. The processing flow is implemented entirely in the integrated script, where each step—grayscale conversion, enhancement, thresholding, blob extraction, morphological refinement, and quantitative classification—is reflected directly in the methods and functions called during analysis.

Each image enters the processing pipeline through the `analyze_image()` function, where it is first converted to grayscale to isolate the intensity structure that most strongly encodes pores, pigmentation boundaries, and lesion-like features. The grayscale frame is then

passed to the `BalancedBlobDetector` class, which implements a combination of CLAHE-enhanced adaptive thresholding and OpenCV's relaxed blob detector. These two detection methods operate in parallel to increase robustness: the CLAHE-adaptive path excels at discovering faint, low-contrast features, particularly on darker skin tones where reflectance is limited, while the relaxed detector identifies more circular, well-defined structures that may appear under boosted or infrared illumination. The system then merges the resulting detections and removes duplicates based on spatial proximity to create a single, balanced set of candidate anomalies for each image.

Once blobs are detected, the classification stage begins within the `BlobAnalyzer` class. Here, the system computes spatial, geometric, and intensity-based descriptors for every feature. The code extracts the centroid, pixel area, circularity, convexity, and an ellipse fit that provides additional shape parameters. Each diameter measurement is automatically converted into micrometers using the calibrated pixel pitch values supplied as command-line arguments (`--px-x-um` and `--px-y-um`).

The metadata file itself serves as the structured record of each scan. It includes timestamped information such as the center-pixel RGB and HEX values, which document the illumination conditions and skin-tone compensation applied during capture. It also contains feature-level classifications, blob counts, timing data, and summary metrics for each image type (baseline, boosted, and infrared). These metadata fields are uploaded alongside the annotated images to the backend through the multipart upload routine implemented in `upload_to_server()`, enabling the React dashboard to retrieve and display real-time diagnostic information.

Collectively, this data-processing and classification pipeline converts raw sensor data into interpretable quantitative measures that support visual inspection, longitudinal tracking, and multispectral comparison. By tightly integrating enhancement, detection, geometric interpretation, and statistical summarization within a single automated script, SkinLumina ensures that each captured image produces a consistent set of clinically relevant descriptors, independent of skin tone, lighting variability, or wavelength band.

7.5 User interface

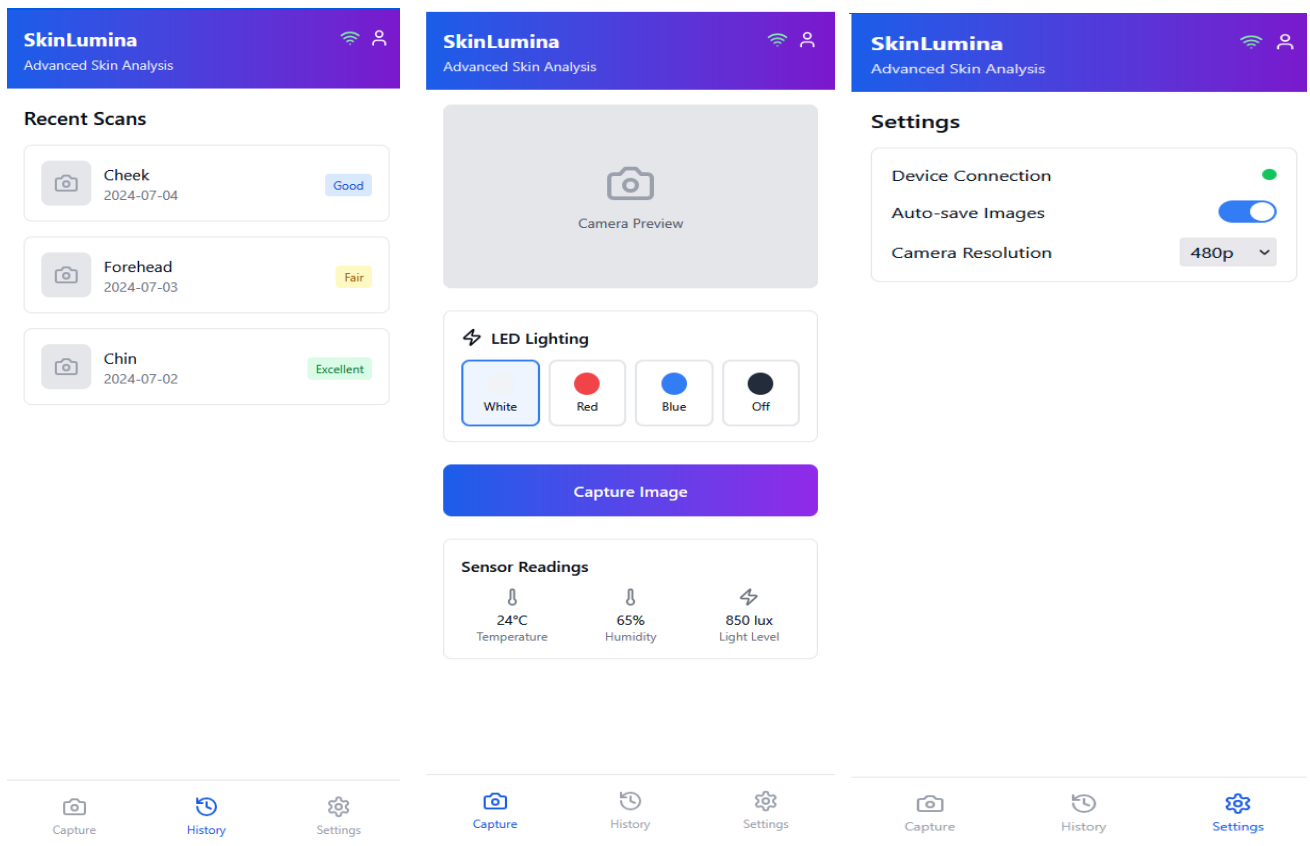


Fig 7.3 Sample User Interface

The sample user interface (Figure 7.3) for SkinLumina demonstrates a clean, modern design that is well-suited for web and mobile deployment. The layout includes core elements such as device connection status, an auto-save image toggle, and a camera resolution selector.

To ensure the website remains scalable and responsive across platforms, adopting a cross-platform UI framework is the goal. Several viable options exist, each with its own advantages depending on the project's priorities. React with Tailwind CSS is particularly effective for web-first applications and allows for later transition to mobile using tools like React Native or Capacitor. It offers a high degree of customization, modern styling utilities, and a large developer ecosystem. Flutter is another strong option, especially for teams that want a single codebase for both web and mobile. Ionic, which works with Angular, React, or Vue, is tailored for apps that start on the web and need to scale to native environments. It works seamlessly with Capacitor for packaging web apps into

mobile platforms. Lastly, React Native remains a solid choice for mobile-first development, although its web support is still maturing.

To fully support SkinLumina's hardware-integrated features and image analysis capabilities, the UI should be organized into several functional screens. The capture screen should include a live camera preview, LED control buttons for different light modes, a capture button, and optionally a timer. The Analysis screen will display the captured image, include overlay filters or annotations if applicable, and show key metrics such as blemish scores or pigmentation levels, with options to save, retake, or proceed. A history screen is necessary to allow users to review past scans, organized in a scrollable gallery or list view, with options to delete or share entries. The settings screen should be expanded to include user preferences and possibly a theme selector in future versions. Additionally, a connectivity panel could support device pairing via Bluetooth or Wi-Fi, and display battery or signal status. An user profile section can provide login functionality and track user-specific data over time.

7.5.2 UI Image Fetching Workflow

Beyond design, implementing the UI also involves defining the communication pathway between the Raspberry Pi, where image capture occurs, and the frontend application. Flask serves as the lightweight backend layer that hosts captured images, responds to device control requests, and manages data exchange. When an image is captured on the Pi, it is sent to the Flask server through a POST request to an /upload endpoint. This endpoint receives the image file and saves it with a timestamped filename to a designated folder.

The Flask server also exposes two additional routes: /images to list all uploaded images, and /images/<filename> to retrieve individual image files for display. On the front end, React uses Axios to send a GET request to the /images endpoint and dynamically renders the returned filenames as image elements. These are then displayed in a responsive grid layout using Tailwind CSS. The images themselves are sourced directly from the Flask server via URL.

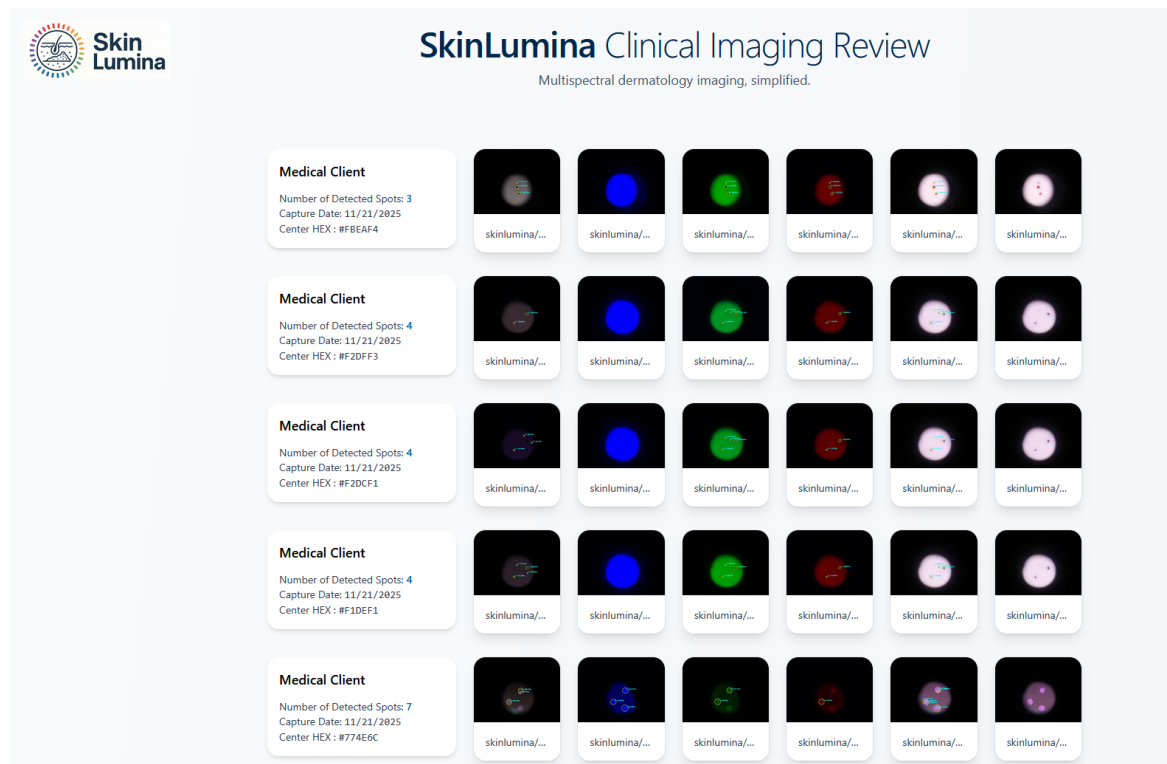
This decoupled architecture where Flask handles backend image management and React handles presentation ensures modular development, platform scalability, and real-time responsiveness. It enables users to control the SkinLumina device, view live captures, and analyze skin features directly through a modern and intuitive web interface.

7.5.3 Final User Interface

The final SkinLumina user interface provides a streamlined and clinically oriented view of all multispectral imaging data captured by the device. The design emphasizes clarity, rapid data interpretation, and consistency across captures. The interface presents a grid of uploaded captures—each containing a baseline image, boosted-illumination images, and multispectral captures under each visible and NIR filter. The layout enables clinicians or researchers to compare wavelength responses side by side. Using a responsive React

frontend, the display automatically resizes thumbnails and maintains a clean and minimal design across desktop resolutions, ensuring that all images, metadata, and annotations remain legible.

The interface organizes scans by patient, date, and detected-anomaly count. For each imaging session, the system displays the processed center HEX reading extracted by the Raspberry Pi, which allows the UI to communicate the illumination environment and skin-tone compensation used during capture. This organization allows users to quickly evaluate the quality of each scan before opening detailed inspection windows.



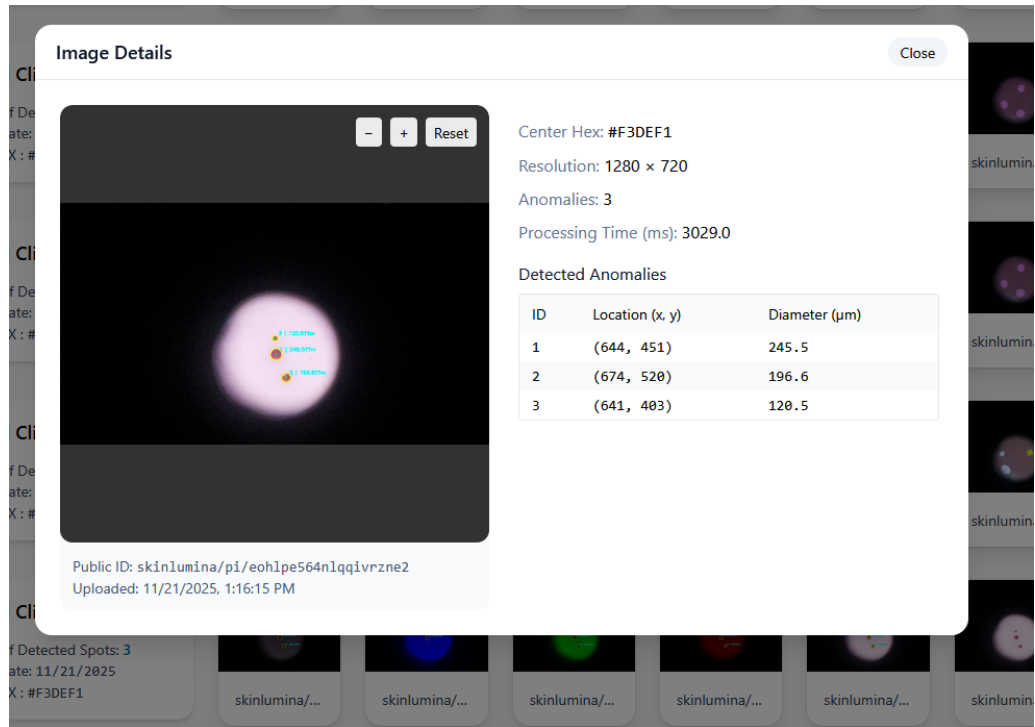
7.5.3 SkinLumina Website

Figure 7.5.3 shows the SkinLumina website. The website was developed using a full MERN stack architecture, with MongoDB Atlas serving as the database, Express and Node.js providing the backend API, and a React/Tailwind frontend deployed through Render. Image assets and variants (original, annotated, and plot images) are stored in Cloudinary, and the metadata generated by the Raspberry Pi script, such as the center HEX readings, blob counts, feature diameters, processing time, and filter-wheel position, is stored in MongoDB and retrieved by the frontend through a REST API.

The React client displays all uploaded captures in a card-based layout, where each card summarizes key metadata such as number of detected spots, capture date, and center HEX value. The images shown in the grid represent multispectral captures under white, red, green, blue, 850 nm, and 940 nm illumination. Each card links to a detailed modal

view, allowing users to further inspect the annotated output and the quantitative information extracted during processing.

As seen in the UI screenshot, the top of the interface includes the project title *SkinLumina Clinical Imaging Review* and a navigation layout aligned with clinical software design principles. The front-end logic dynamically maps Cloudinary public IDs to image URLs and renders updated metadata in real time as new captures are uploaded from the Raspberry Pi.

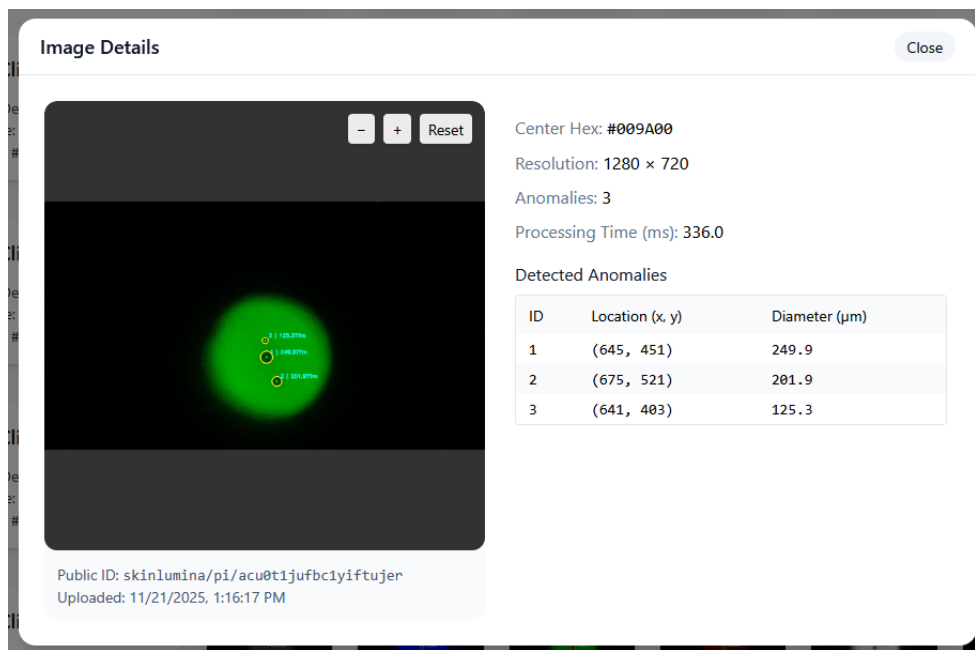


7.5.4 Image Details for Annotated Baseline Scan with Adjusted LEDs

Selecting an image opens a detailed modal that displays the annotated frame alongside all extracted metadata. Figure 7.5.4 corresponds to a baseline scan after the adaptive LED routine has been applied. The left side of the modal displays the full annotated image, where feature centroids and measured diameters are overlaid directly on the skin phantom. The right-side panel presents a structured metadata summary including the center HEX value (#F3DEF1 in the displayed sample), the camera resolution (1280 × 720), the number of detected anomalies (three), and the total processing time (approximately 3029 ms).

The anomaly table provides exact coordinates and micrometer-scale diameters for each detected feature—245.5 μm, 196.6 μm, and 120.5 μm—which correspond to the contours extracted during the blob analysis stage. This modal demonstrates the complete end-to-end functionality of the system: the Pi executes adaptive LED adjustment and capture, the

algorithm performs blob detection and geometric classification, the annotated output is uploaded to the cloud, and the frontend renders it in an interpretable format suitable for clinicians or researchers.



7.5.5 Image Details for Annotated Scan with Adjusted LEDs Under Green Filter

Figure 7.5.5 corresponds to a capture taken beneath the green filter after the filter wheel rotated during the multispectral sequence. The annotated image clearly shows the effect of green illumination on the underlying features. In this case, the center HEX value shifts to a green-dominant #009A00, reflecting the spectral behavior of illuminated tissue under the specified wavelength. The detection pipeline again identifies three anomalies, with measured diameters of 249.9 μm, 201.9 μm, and 125.3 μm.

The modal interface remains consistent across wavelengths, enabling clinicians to compare how different LEDs and filters affect feature visibility and contrast. Because the system stores all measurements in micrometers and displays them uniformly across all scans, the platform supports multispectral analysis without requiring any manual calibration from the user.

7.6 Security Considerations

SkinLumina captures high-resolution images of human skin that may contain personally identifiable or medically sensitive information, data security is a critical design consideration. Our software stack implements a multi-layered approach to protect captured images during storage, transmission, and access.

On the Raspberry Pi, all image files are saved to a protected directory with strict file permission settings to prevent unauthorized access. The default pi user owns this directory, and permissions are set to `chmod 700`, allowing only the designated user to read, write, or execute. This follows the principle of least privilege, minimizing the risk of local file leakage through SSH or other services. In addition, the Raspberry Pi operating system is routinely updated, and firewall rules are enforced via `ufw` to restrict incoming connections to only known hosts. Optional steps such as disabling the default pi user, enforcing SSH key-based login, and using secure deletion tools can further enhance device-level security.

While the current implementation operates within a local network, future versions of SkinLumina that incorporate cloud connectivity or web-based access must transition to secure HTTPS endpoints. This can be achieved through a reverse proxy such as Nginx, paired with a TLS certificate from Let's Encrypt. By enforcing HTTPS-only communication, the system prevents the interception of sensitive image files and metadata in transit. To further secure HTTP communication, the Flask backend can be extended with Flask-Talisman [40] to apply HTTP security headers such as HSTS, X-Content-Type-Options, and X-Frame-Options.

Even in local deployments, it is essential to ensure that only authorized applications or users can trigger image capture, upload, or classification routines. We will implement token-based authentication for the Flask API, where each client must include a valid bearer token in the request header. These tokens are securely stored in environment variables and rotated periodically. For expanded user management, Flask extensions such as Flask-Login or Flask-Security can be integrated to enforce session-based or role-based access control (RBAC), distinguishing between user roles such as administrator, clinician, or guest. This guards against misuse and ensures that only verified users can access diagnostic data or modify device settings. Sensitive configuration data such as API keys and secret tokens are never hard-coded in the source code. Instead, they are loaded from a secured `.env` file and accessed via environment variables. Flask's debug mode is disabled in production to prevent accidental exposure of stack traces and internal variables. Cross-site request forgery protection is enforced using Flask-WTF when receiving POST requests through forms.

Together, these measures form a secure foundation for handling sensitive dermatological data. As the system evolves toward potential clinical or telemedicine applications, these safeguards will ensure user trust, maintain data confidentiality, and uphold compliance with emerging healthcare data protection standards.

7.7 Future Works

Future development of the SkinLumina system could focus on optimizing and fully integrating the machine learning techniques discussed earlier, particularly convolutional neural networks CNNs, directly on the Raspberry Pi platform. While Section 7.4.2 outlines the use of CNNs for lesion classification, future iterations may shift toward deploying these models on-device for real-time, standalone diagnostic capability. As demonstrated by Akalya et al. (2025) [41], models such as VGG16 can be successfully run on Raspberry Pi hardware for skin condition classification, achieving impressive accuracy despite limited computational resources.

To support this on-device integration, additional preprocessing steps such as normalization, augmentation, and resizing may be necessary to maintain consistent model performance. Further refinement may involve adopting lightweight CNN architectures—such as MobileNet or SqueezeNet—specifically designed for embedded environments. This would not only improve inference speed and reduce reliance on external servers, but also enhance user privacy, lower latency, and make the system more practical for deployment in remote or resource-constrained settings.

7.7.1 Personalized Skin Care Monitoring and Tracking

An impactful direction for future development in the SkinLumina platform is the implementation of personalized skin monitoring, a feature that allows long-term users to track changes in skin condition over time. This enhancement transforms the system from a single-scan diagnostic tool into a longitudinal health monitoring platform. By enabling users to compare baseline and follow-up scans, the system supports early detection of progressive conditions, evaluation of treatment effectiveness, and documentation of natural skin changes.

The tracking process begins with the creation of a baseline scan, during which the system captures the user's initial skin condition and stores it alongside relevant metadata—such as imaging parameters, detected regions of interest, and skin tone classification—in a secure, user-specific profile. Subsequent scans are automatically analyzed against this baseline using a combination of visual similarity checks, classification shifts, and quantitative metrics that track changes in size, shape, color, or texture. The system flags significant deviations from the baseline and summarizes them as alerts or annotations within the scan history. This not only helps reduce false positives but also ensures that users are only notified when meaningful changes occur, enabling a focused and clinically relevant progression analysis.

To support this functionality, the user interface could also include a dedicated "Progress" screen that visualizes scan history in a scrollable timeline, with each session displayed alongside its date, status tag (e.g., New Lesion), and thumbnail preview (illustrated in Figure 7.4). Users can compare any scan against the baseline using an interactive side-by-side viewer that offers a split slider, an image overlay with adjustable transparency, or a color-coded difference heatmap (illustrated in Figure 7.4.1). Additional features include the ability to annotate specific regions, add personalized notes (e.g., Post-Treatment), and export reports in PDF format for personal records or clinical consultation.

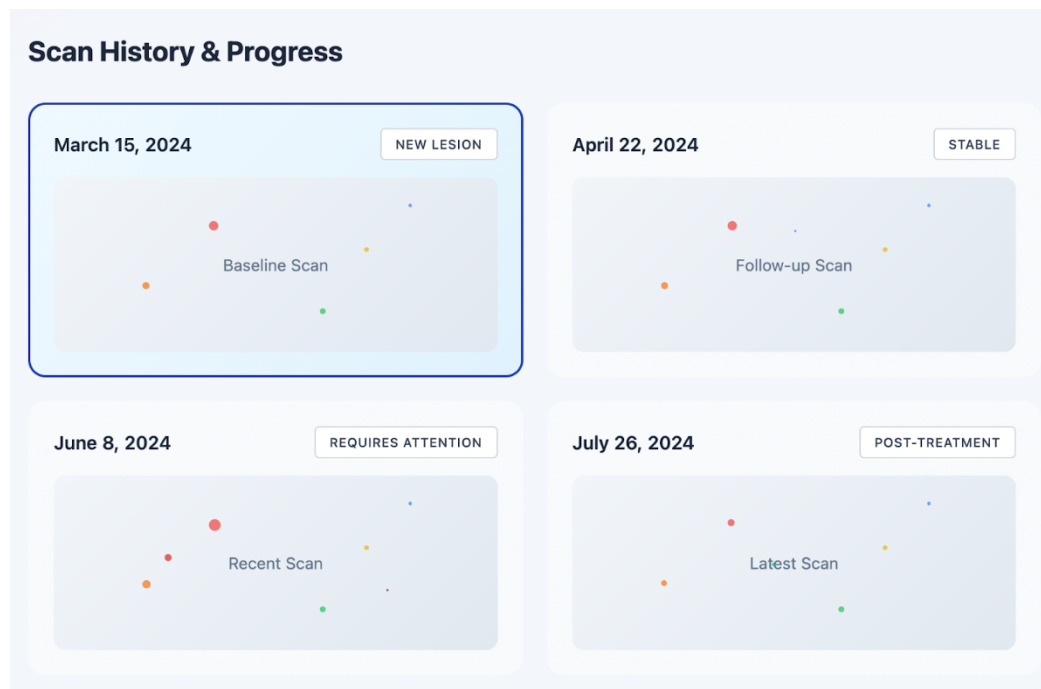


Fig 7.4 Scan History Screen

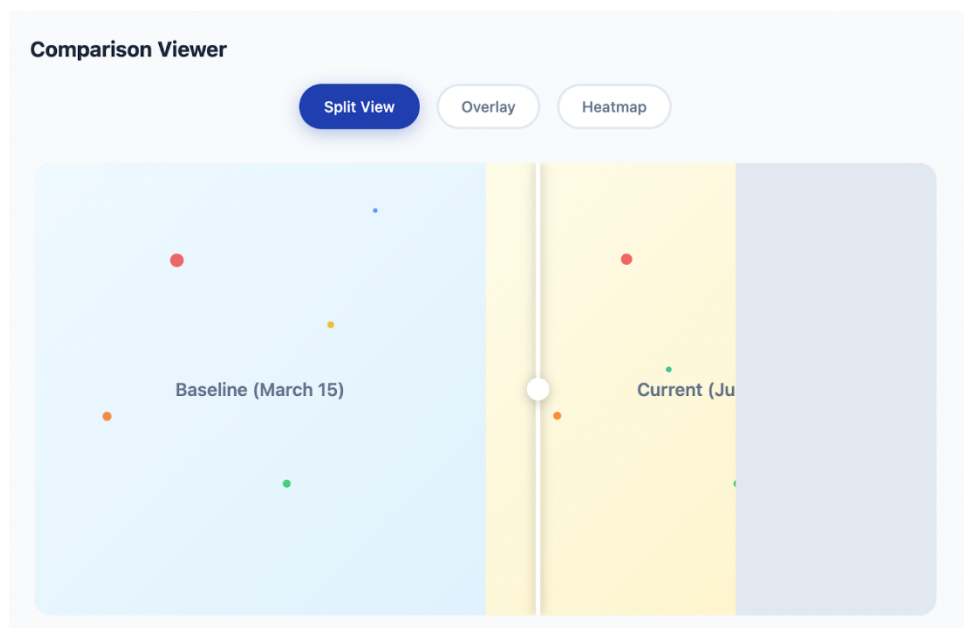


Fig 7.4.1 Side by Side Viewer

Chapter 8 System Fabrication/Prototype Construction

The fabrication and construction of the SkinLumina prototype is the culmination of the system's optical, electrical, and mechanical integration. The goal of this phase was to produce a stable, portable, and spectrally accurate skin imaging system. Each component was assembled with consideration for compactness, safety, and alignment accuracy. This chapter describes the steps taken in prototype construction, including the fabrication of the printed circuit board, design and 3D printing of the housing, integration of optical elements, wiring of control electronics, and final system assembly. The prototype was built to be compact, portable, and thermally stable during extended imaging cycles. Because the device uses high-power LEDs and is fully enclosed, thermal buildup was a significant concern. The system was constructed using low-cost materials such as PC-ABS thermoplastic and standard electronic components, which required thoughtful thermal design to prevent overheating or deformation. This chapter details the full prototype fabrication process, with an emphasis on thermal control measures, optical alignment, and integration of the 3D-printed mechanical components with the custom PCB.

8.1 PCB Design

The printed circuit board (PCB) was designed to support modular operation and organized functionality. The layout is divided into three main zones. One section is dedicated to the Arduino microcontroller, motor driver, and PWM circuits that control the LED array and stepper motor. The circuit design is based off of schematics tested and verified prior to ordering a custom PCB. This digital zone is shielded from EMI using a ground plane and ferrite beads. The second zone includes the power regulation circuits. Two buck converters step down the 12V input from the battery pack into 5V and 3.3V rails. These voltages supply the Arduino and Raspberry Pi, respectively. Bulk capacitors and PTC fuses are placed near power inputs to prevent surges and regulate voltage under variable load. The final zone handles analog components including I2C sensors for temperature, current, and filter wheel feedback. Analog and digital grounds are separated and tied at a single star point to reduce cross-interference.

The PCB uses a two-layer design with wide traces for high current paths, particularly for the LED clusters. Each LED channel is driven independently using PWM signals from the Arduino. Decoupling capacitors are placed at each integrated circuit. Ground pours are placed strategically to reduce noise. High-current components are separated from sensitive digital lines. USB and GPIO headers are routed directly to the Raspberry Pi, which mounts separately but interfaces through connectors placed along the PCB perimeter. The PCB is compact and mounts flush with the internal base of the enclosure using brass standoffs and M2 fasteners.

Throughout testing the PCB was noted to have a heat output. Actions were then taken to minimize thermal overheating or deformation to the system components. The PCB was laid out to prevent thermal coupling between high-current and sensitive digital zones. The power regulation and LED driver circuits are isolated from the camera interface and communication lines. Thick copper traces were used in the power sections to reduce resistance and heating under load. Ferrite beads and bulk capacitors were placed at voltage regulator outputs to suppress transient spikes and brownout conditions. PTC fuses protect against current surges, while the battery management system shuts down the device under overtemperature or overvoltage scenarios.

8.2 Housing of SkinLumina

The mechanical housing of SkinLumina was modeled in SolidWorks and printed using fused deposition modeling. The housing is designed to ideally fit in one hand while maintaining precise alignment between the LED ring, filter wheel, and camera sensor. The enclosure is printed in PC-ABS thermoplastic. This material provides strength, flexibility, and thermal stability. It also supports alcohol and UV sterilization for future clinical use. The main housing consists of two interlocking sections. The lower section holds the electronics and power system. The upper section supports the optical assembly.

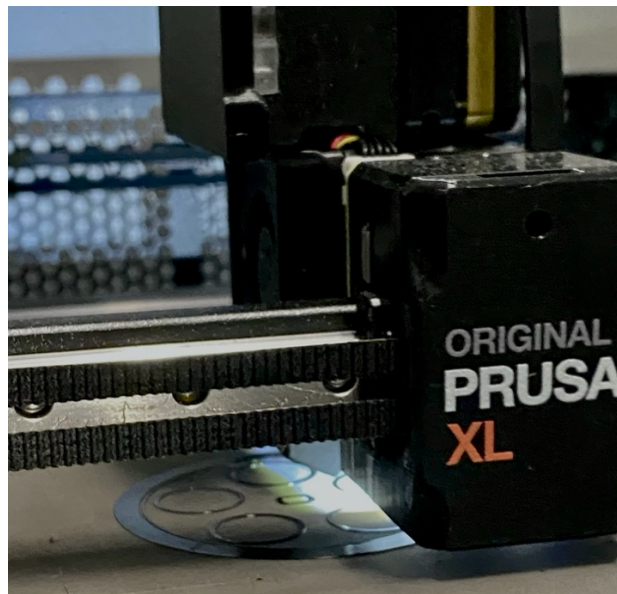


Fig 8. Original Prusa XL Semi-assemble Single-toolhead 3-D printer

An optical filter wheel will be printed in accordance to the optical filters chosen in the project specifications chart. A housing lens tube will also be constructed by 3-D printing to secure and adjust the optical lens design. A printing device pictured in figure 8 shows the Original Prusa XL Semi-assemble Single-toolhead printer. An example of a printer that can collaborate with AutoCAD-AutoDESK or other similar softwares to design and print housing components. This specific device has a build area of 360 mm x 360 mm x 360 mm with a layer height of 0.1 mm to 0.3 mm. These constraints so not interfere with

our device pieces due to the goal of having a light-weight and hand-held system. The priority is for the filters and lenses to be as compact as possible. Calculating focal lengths and testing on component parts will ensure our system fits and is secured in the objective and tube lens design.

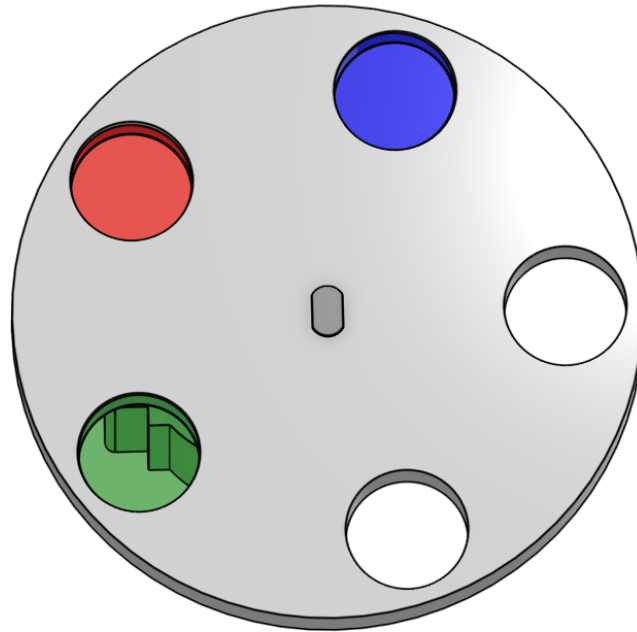


Fig 8.1 Optical Filter Wheel 3-D printer prototype 1

A prototype housing component for the optical filters is shown in figure 8.1, where OnShape was used to draw, add measurements, design, and print the optical filter wheel. This optical filter wheel took into consideration the measurements of the individual optical filters and the connecting tip on the rotating motor wheel. Ensuring a thickness that works with the system, the thickness of the filter wheel was chosen to be 0.5mm thick. The lens stack and cover for the system to block out stray light are also to be printed in a similar fashion.

8.2.1 LED Configurations

Circular mounting points are used to align the LED ring with the filter wheel. A circular filter wheel, printed separately in black PLA, is embedded within the optical path. It contains five radial cutouts for optical filters. These include red, green, blue, NIR, and white light filters. The wheel is rotated by a stepper motor with a direct shaft coupling. A feedback sensor detects the zero-position at system startup. The stepper motor is controlled by the Arduino. It advances the filter wheel to the next position during each illumination step.

The LED ring is mounted in front of the camera module and spaced using an optical isolation shield. This ensures that each LED spectrum is delivered uniformly across the imaging area. Polarizers are placed in front of both the LEDs and camera lens to reduce surface glare. These components are secured in modular slots within the housing. The camera is positioned at the center of the system, aligned with the optical axis. The entire optical path is enclosed to prevent ambient light interference. This design will allow space for the optical filter wheel to fit and rotate through the main housing tube with minimum friction. Securing the rotating motor wheel properly will be vital in achieving this design.

8.3 Battery and Raspberry Pi Design

The enclosure is to be assembled with countersunk screws and allows access to the power switch, charging port, and USB interface for the Raspberry Pi. Internal wiring is routed through printed cable guides. Ventilation slots are embedded near the PCB and battery compartment. Passive thermal management is achieved through a combination of strategies. Aluminum heat spreaders are mounted behind the LED clusters to draw heat away from high-power components. Heat-conductive pads are used between the PCB and the base enclosure to distribute localized heat buildup. Vents integrated into the housing allow for natural convection to assist with airflow. The material choice of PC-ABS also contributes by resisting thermal deformation and maintaining structural integrity. These methods ensure that the device remains within safe temperature limits during continuous use.

Final system integration was validated by ensuring alignment between the camera sensor and each optical filter. The stepper motor was tested to rotate the wheel accurately to each of the five filter positions. LED brightness and thermal safety were verified using the PWM controller. The Arduino was programmed to cycle through the LEDs in synchronization with the filter wheel and trigger the camera via the Raspberry Pi. Software was used to confirm successful image capture under each spectral condition. Battery life was evaluated under full system load. The housing was subjected to minor drop and vibration testing to validate mechanical durability.

8.3.1 Cable and Wire Management

The wires management within the SkinLumina system was carefully planned to ensure mechanical stability, electromagnetic compatibility, and ease of maintenance. Each functional subsystem, the LED array, camera module, filter wheel motor, sensors, power supply, and user interface, is routed through dedicated paths within the 3D-printed housing. The enclosure includes built-in cable guides and clips that secure wiring against internal surfaces, keeping cables clear of optical paths and moving components. Signal wires are routed on opposite sides of the housing from high-current lines to minimize electromagnetic interference. Power lines for the LED clusters and motors use thicker-gauge wire and are twisted to reduce inductive noise. All internal connections terminate in locking connectors to support modular assembly and reduce the risk of disconnection during operation or transport.

The internal wire harness uses heat-resistant insulation and incorporates strain-relief features where cables exit the PCB or interface with moving parts. JST connectors are used for low-power sensor and control lines, while terminal blocks and barrel jacks support higher-current power delivery. Cable lengths are kept as short as possible to reduce voltage drops, and excess slack is coiled and anchored to mounting posts to prevent shifting. The filter wheel motor cable is routed through a central opening and protected by a flexible sheath to allow movement while preventing abrasion. USB and camera data lines are shielded and physically separated from noisy subsystems like motor drivers and switching regulators. This layout ensures reliable operation, protects sensitive signals, and allows tool-free access to all major components during troubleshooting or upgrades.

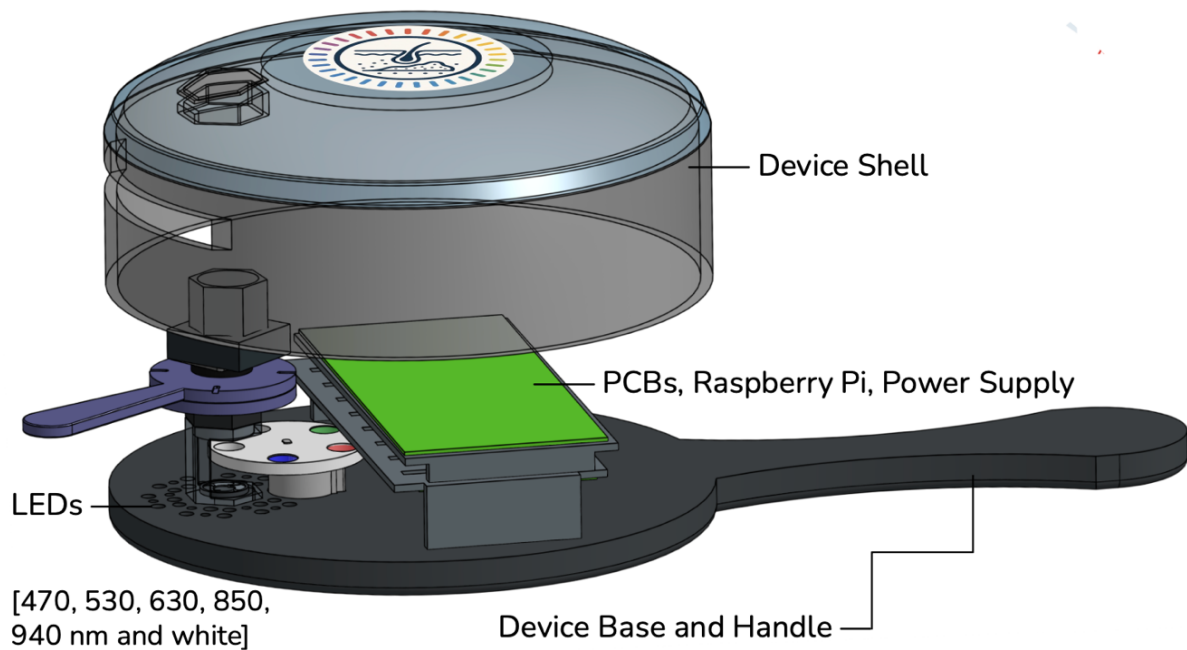


Fig 8.2 CAD Housing Unit with Shelving System for PCBs and Wiring

Wiring is organized to help with troubleshooting and prevent electrical issues. Power and signal paths are kept separate and clearly routed. This layout shown in figure 8.2 makes it simple to find and fix problems or update parts as needed. The system can support future changes in hardware without needing a full redesign, making it reliable and adaptable for long-term use. The prototype successfully for SkinLumina combines multispectral illumination, precise optical filtering, modular electronics, and handheld usability. Each fabrication step supported the project's clinical and engineering goals. The result is a compact and functional imaging platform ready for further software development, testing, and validation.

Chapter 9 System Testing and Evaluation

This chapter outlines the comprehensive testing, validation, and integration of the SkinLumina imaging system. The primary objective of this stage was to verify that each subsystem: optical, electrical, mechanical, and computational operates in coordination to produce consistent, safe, and high-quality multispectral images across a range of skin tones. Testing was performed to ensure that every design choice, from LED selection to power regulation, met its functional purpose and contributed to the system's overall imaging performance. Special attention was given to verifying optical alignment, electrical stability, thermal regulation, and wavelength isolation, all of which are essential for reliable biomedical imaging. The use of synthetic skin phantoms provided a controlled means of replicating real tissue optical properties, allowing for accurate and repeatable evaluation without human subject testing.

Beyond verifying subsystem functionality, this chapter also focuses on the system's integration and readiness for clinical use. Performance benchmarks such as spatial resolution, spectral fidelity, switching latency, and adaptive illumination accuracy were established to measure operational success. Data analysis from hardware and software testing confirmed that SkinLumina meets these targets, validating its adaptive calibration process and multispectral depth-imaging capabilities. Together, these efforts demonstrate the feasibility of SkinLumina as a fully functioning prototype capable of translating optical engineering principles into practical, inclusive dermatological diagnostics. The testing described in this chapter lays the groundwork for future human studies, clinical validation, and continued system refinement.

9.1 Hardware and Software Testing

This section presents detailed testing and validation of SkinLumina's hardware and software subsystems. Each test was designed to ensure functional reliability, synchronization, and optical safety while confirming that the system performs as a cohesive, adaptive imaging platform. The following subsections describe the major testing categories, results, and their significance to the system's overall functionality.

Power Regulation and Buck Converter Testing

The electrical subsystem testing began with verifying the efficiency and safety of the LM2678 buck converter, which regulates power delivery from the 12 volt LiFePO₄ battery to a stable 5 volt output. Stable voltage regulation is essential for maintaining consistent LED brightness and camera operation.

The PCB layout for the converter illustrated optimized trace routing for minimal electrical noise and heat dissipation. Efficiency was evaluated using a DC electronic load to simulate output current draws at 0.5, 1.0, 1.5, and 2.0 amperes. Input and output voltages and currents were recorded at each step, and power was calculated using $P = V \times I$. Conversion efficiency was then derived as $\eta = P_{out} / P_{in}$.

Load (A)	V_{in} (V)	I_{in} (A)	P_{in} (W)	V_{out} (V)	I_{out} (A)	P_{out} (W)	Efficiency (%)
0.5	12.00	0.27	3.240	4.80	0.50	2.400	74.07
1.0	12.00	0.52	6.240	4.60	1.00	4.600	73.72
1.5	12.00	0.82	9.840	4.50	1.50	6.750	68.60
2.0	12.00	1.12	13.440	4.30	2.00	8.600	63.99

Table 5 Buck Converter Test Parameters

The measured input and output parameters for the buck converter test performed was used to calculate the conversion efficiency shown in table 5. The results table 6 show the converter achieved about 74 percent efficiency under light loads and about sixty four percent at full load, maintaining steady voltage output from 4.8 to 4.3 volts. No oscillations or overheating were observed. This confirmed safe, reliable operation and adequate electrical performance to power the LEDs, CMOS sensor, and control units.

Buck Converter Efficiency vs. Output Current

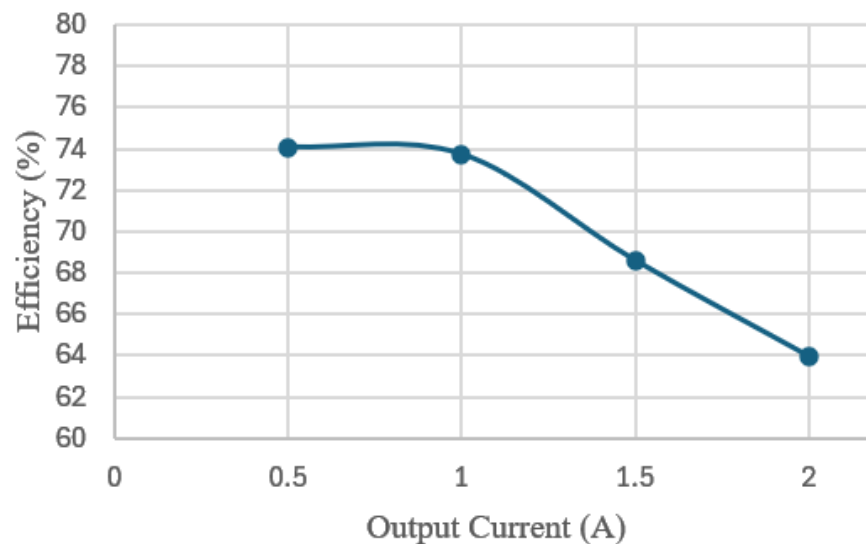


Table 6 Buck Converter Efficiency vs Output Current

The converter's stable performance across multiple load levels validates the electrical design's ability to provide continuous power for the optical and control subsystems. Reliable power delivery supports consistent LED illumination and image capture, which are essential for maintaining accuracy in multispectral imaging.

Software Workflow and Synchronization Testing

Software validation focused on the coordination of the capture, analyze, and display sequence. The Raspberry Pi controlled image acquisition, LED sequencing, and real time feedback processing, while the Arduino handled timing and motor control. The communication process is diagrammed in Figure 9.1, which shows how LED modulation and filter wheel rotation are synchronized through serial handshakes.

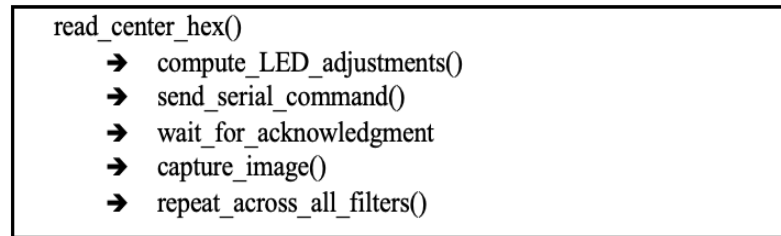


Fig 9.1 Serial Communication and Image Capture Sequence

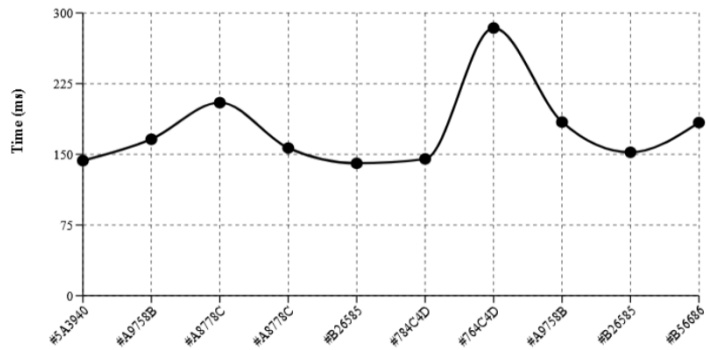
During operation, the Raspberry Pi initialized camera parameters, transmitted LED intensity data, and triggered image captures. The Arduino received commands, adjusted PWM signals for the LEDs, rotated the filter wheel, and returned a ready acknowledgment to the Pi before each new image capture. Testing confirmed no data losses or delays across cycles, ensuring stable synchronization between optical and electronic operations.

Hexadecimal Color Detection Testing

Hexadecimal (HEX) color detection serves as the foundation for SkinLumina's adaptive illumination feature. This test evaluated how accurately the system could extract skin reflectance data from captured images to guide real time LED brightness adjustments.

Using OpenCV and NumPy, the software extracted the R-G-B values of the center pixel and its surrounding neighborhood, averaged the results to minimize noise, and converted them into a six digit hexadecimal color code. This color code quantified the dominant reflectance of the imaged area. The detection performance is shown in table 7, which displays detection times and repeatability across ten trials.

Detection Time vs. HEX Code Detection



Hex Code Detection

Table 7 HEX Color Detection Performance

Detection times ranged between 140 and 280 milliseconds, with 95 percent consistency under controlled lighting. These results validated that the adaptive feedback mechanism can make near real time adjustments to illumination, ensuring accurate imaging across different skin tones.

9.2 Performance Evaluation

The performance evaluation phase focused on assessing how efficiently and accurately the SkinLumina system operates as an integrated imaging platform. This stage measured key performance metrics such as spatial resolution, spectral fidelity, LED switching speed, and thermal regulation to verify that the system meets biomedical imaging standards for stability, precision, and safety. Each test was designed to evaluate how well the optical, electrical, and computational subsystems interact under realistic imaging conditions, ensuring reliable synchronization and consistent results across repeated scans. By quantifying imaging sharpness, wavelength accuracy, and temperature stability, the evaluation confirmed that SkinLumina can perform rapid, multispectral scans under five seconds while maintaining clear image contrast and safe operating conditions suitable for extended diagnostic use.

Spatial Resolution Testing

Spatial resolution determines how well fine skin details can be captured and resolved. Testing was performed using a custom Python tool developed for SkinLumina that calculated three resolution metrics: Full Width at Half Maximum (FWHM), edge width, and Modulation Transfer Function at fifty percent contrast (MTF50). Results are plotted in table 8, showing an inverse relationship between FWHM and MTF50. As image blur increases, FWHM broadens and spatial frequency response decreases, confirming proper focus calibration.

FWHM vs. MTF50 Spatial Frequency

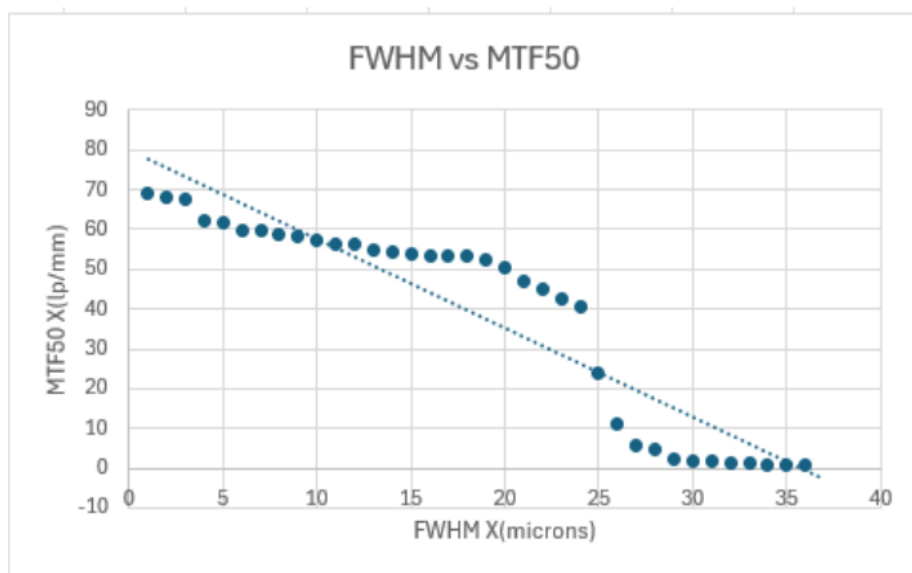


Table 8 The chart illustrates the inverse relationship between the full width at half maximum (FWHM) of the point spread function and the MTF50 spatial frequency.

Radial spatial resolution results in table 9 show that the MTF50 values remained consistent across the imaging field, demonstrating minimal field curvature and confirming precise optical alignment.

Radial Spatial Resolution

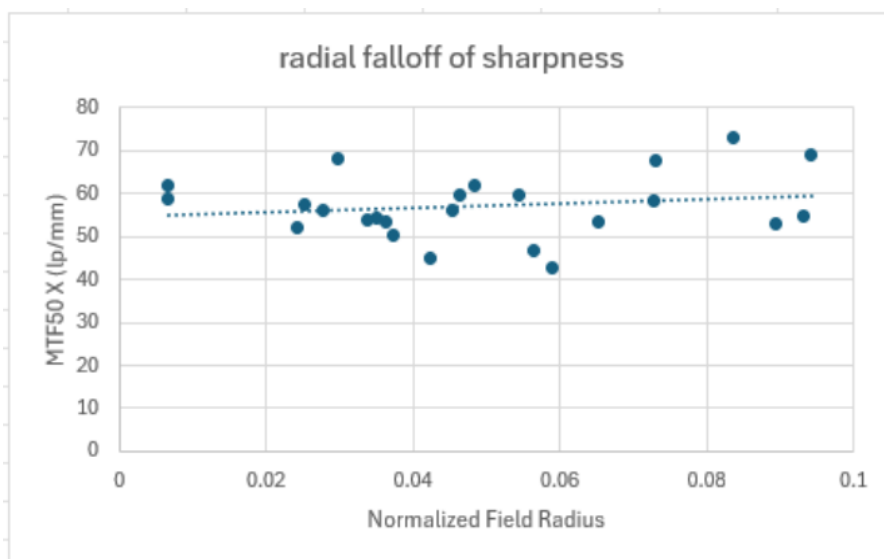


Table 9 This illustrates the radial falloff of image sharpness, showing how spatial resolution varies with distance from the image center.

Thermal Management and Power Stability

Thermal control was tested under extended operation. The LiFePO₄ battery maintained a stable twelve point eight volt output, and ventilation holes designed in the 3D-printed housing near the Raspberry Pi and power components ensured adequate airflow. System temperatures remained within 3 degrees Celsius of ambient, confirming that the thermal design effectively prevents overheating during prolonged imaging sessions.

9.3 Optoelectronic Feasibility Study and Testing

The success of the SkinLumina system depends on verifying the performance of its core optoelectronic components, which include the multispectral LED array, achromatic lens system, and CMOS imaging sensor. Each element was tested for alignment, wavelength fidelity, and image quality to ensure the system could safely and reliably capture multispectral data. The optical and electronic subsystems were designed to maximize clarity, minimize distortion, and provide consistent imaging across visible and near-infrared wavelengths. Together, they form the foundation for accurate, inclusive imaging of different skin tones.

The optical design uses two achromatic doublet lenses with focal lengths of 50 and 75 millimeters to reduce chromatic aberration and balance magnification with field of view. Bench testing confirmed precise focus and alignment on the camera sensor, producing sharp, distortion-free images. The camera was verified to respond linearly to intensity changes across the full color spectrum. A circular aperture between the lenses helped reduce spherical aberration, and polarization testing confirmed that cross-polarization effectively reduced glare while enhancing subsurface visibility. These adjustments collectively improved image contrast and depth accuracy.

The LED array and optical geometry were refined to achieve even illumination and accurate spectral control. LEDs were angled at thirty degrees toward the imaging field to prevent hot spots and combined with Lambertian reflectors for uniform lighting. Comparisons between hyperspectral and multispectral imaging confirmed that SkinLumina's discrete multispectral design provided faster capture times, under five seconds per scan, while maintaining sufficient spectral resolution for biomedical use. These optoelectronic tests verified that the system performs safely, consistently, and effectively for inclusive dermatological imaging.

LED Illumination Profile Testing

Each LED in the multispectral array was tested for emission accuracy using an Ocean Optics HR2000CG UV NIR spectrometer. Visible LEDs (470, 525, and 630 nanometers) operated at 20 mA, while near infrared LEDs (850 and 940 nanometers) were tested at 100 mA. The measured emission profiles are shown in Figure 9.

Measured Spectral Emission LED Profiles

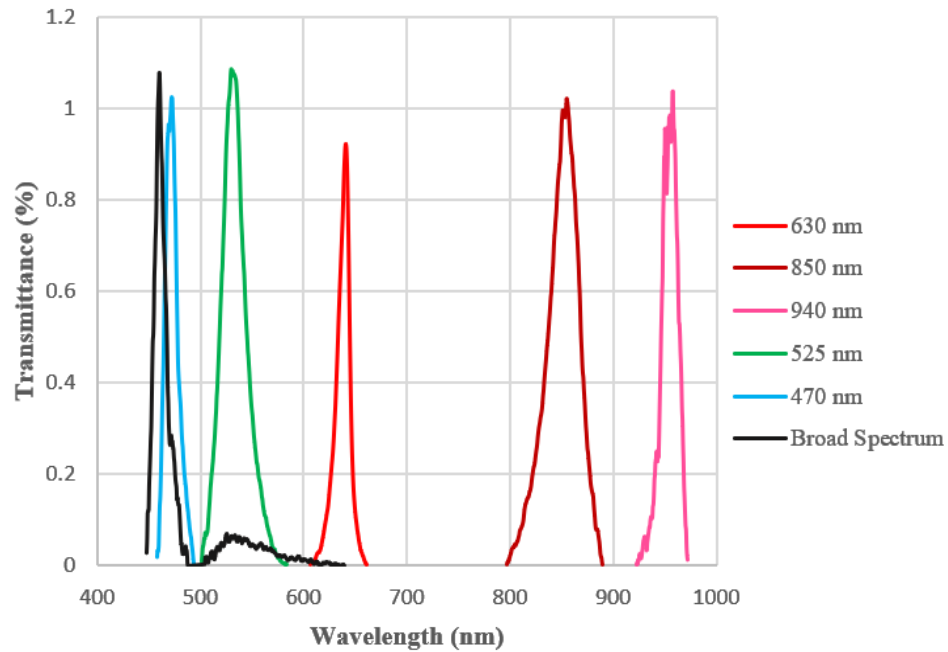


Table 10 The measured data used to generate the converter efficiency profile as a function of output current.

The visible LEDs displayed distinct narrow peaks separated by over 100 nanometers, and the white LED emitted broadly from 430 to 650 nm with a strong 450 nm peak. The near infrared LEDs produced peaks at 850 and 940 nm, confirming alignment with the therapeutic optical window (600 to 1300 nm) critical for deeper tissue imaging.

LED Output Calibration

Each LED in the SkinLumina system was tested to verify optical power, wavelength accuracy, and safety. Using a power meter, the optical output was confirmed to remain below 10 milliwatts per square centimeter, ensuring safe operation while maintaining strong image quality. Printed color targets and synthetic skin phantoms were used to confirm that each filter properly aligned with its corresponding LED, isolating the correct wavelength and blocking unwanted light.

The testing confirmed that shorter visible wavelengths penetrated only surface layers, while near-infrared LEDs reached deeper into the tissue model, validating our wavelength selection for layered skin imaging. Since near-infrared light is not visible to the eye, we used detection cards and the CMOS camera to verify emission and balance brightness between visible and infrared channels. Pulse width modulation adjustments were applied to ensure uniform illumination and consistent exposure across all wavelengths.

Penetration Depth and Skin Phantom Testing

Penetration depth was calculated using measured absorption and scattering coefficients of fabricated skin phantoms composed of Smooth On Dragon Skin silicone, titanium dioxide for scattering, and India ink for absorption.

The absorption behavior of the artificial skin phantom was modeled using India ink as a broadband absorber dispersed in the silicone material. The relationship between the absorption coefficient and ink concentration follows the expression

$$\mu_a(\lambda) = \epsilon_{a,ink}(\lambda) \times C_{ink} \quad (1)$$

The absorption coefficient $\mu_a(\lambda)$ represents light absorption at wavelength λ , where $\epsilon_{a,ink}(\lambda)$ is the specific absorption of India ink. C_{ink} is the fractional concentration of ink in the mixture. The dermis used 100 g of silicone with 0.46 g of ink, and the epidermis used 20 g of silicone with 0.092 g of ink. Since C_{ink} remained constant, its effect was negligible in the wavelength-dependent analysis.

Absorption Coefficient Approximations

λ (nm)	$\epsilon_{a,ink}(\lambda)$ (mm ⁻¹ per %)	C_{ink}	μ_a (mm ⁻¹)
470	25	0.0046	0.115
530	18	0.0046	0.083
630	10	0.0046	0.046
850	2.5	0.0046	0.012
940	2.0	0.0046	0.009

Table 11 The Calculated Absorption Coefficient Based off of India Ink

Values of $\epsilon_{a,ink}(\lambda)$ in table 11 were approximated from published measurements of the India ink absorption spectra reported by Di Ninni et al. (2010) and Madsen et al. (1992).[45, 46] These sources provide spectral dependence of India ink's absorption, which decreases progressively from the visible to near-infrared range. Applying these approximations allowed estimation of $\mu_a(\lambda)$ for each illumination wavelength used in SkinLumina. The resulting trend confirms that absorption decreases by roughly a factor of five from 470 nm to the NIR wavelengths, consistent with the expected optical response of biological skin layers.

The scattering behavior of the artificial skin phantom, $\mu_s'(\lambda)$, was modeled using titanium dioxide (TiO₂) as the main scattering agent dispersed in the silicone mixture. The reduced scattering coefficient was approximated using the combined relationship

$$\mu_s'(\lambda) = \mu_s(\lambda)(1 - g) = A(1 - g)\left(\frac{\lambda}{\lambda_0}\right)^{-b} \quad (2)$$

As seen in equation (2), A is a proportionality constant determined by the TiO_2 concentration. The anisotropy factor, g , is determined to be approximately 0.8–0.9, representing forward-directed scattering within the silicon samples. The reference wavelength, λ_0 , was set to 500 nm. The coefficient, b , in (4) represents the wavelength-dependent scattering slope. This typically ranges from 0.7 to 1.2 for TiO_2 . [47]

In this phantom, TiO_2 was added at a fixed concentration of approximately about 1 gram of TiO_2 powder per 100 grams of total silicone base. Using this approximation, the reduced scattering coefficients (μ_s') were estimated at each LED wavelength. The results follow the expected inverse wavelength dependence where scattering is strongest in the blue LED region and decreases steadily toward the near-infrared, allowing for deeper light penetration at longer wavelengths.

The penetration depth equation:

$$\delta = \frac{1}{\sqrt{3\mu_a(\mu_a + \mu_s')}} \quad (3)$$

This was used to determine light propagation depth. Equation (3) combines the effects of absorption μ_a and reduced scattering μ_s' to describe how light travels through the material at different wavelengths. Results showed that visible wavelengths penetrate about one to two millimeters, while near infrared wavelengths reach several millimeters deeper.

Greater absorption or scattering results in a smaller penetration depth, keeping light closer to the surface, while smaller values allow light to reach deeper layers. Applying this relationship to each LED and NIR wavelength shows that shorter visible wavelengths penetrate less deeply within the phantom, whereas longer near-infrared wavelengths reach farther. The results in table 12 confirm the expected optical behavior of the SkinLumina phantom and demonstrate the device's ability to separate surface and subsurface features using multispectral illumination.

Estimated Phantom Penetration Depths

λ (nm)	μ_a (mm ⁻¹)	μ_s' (mm ⁻¹)	δ (mm)
470	0.115	2.5	1.05
530	0.083	2.0	1.39
630	0.046	1.5	2.17
850	0.012	1.0	5.26
940	0.009	0.9	6.37

Table 12 The Estimated Phantom Penetration Depths

Layered phantom imaging confirmed that shorter wavelengths captured surface pigmentation and longer wavelengths visualized deeper tissue regions. The penetration depth calculations modeled how visible and near-infrared light moves through skin-like materials. Shorter wavelengths were absorbed and scattered near the surface, while longer wavelengths penetrated several millimeters deeper. These results confirm that the silicone mixtures accurately mimic light transport in biological tissue and guided the design of the three-layer skin phantom and LED wavelength selection.

Polarization and Filter Wheel Isolation Testing

Cross polarization testing demonstrated that glare from the skin surface was significantly reduced when using linear polarizers on both the LED array and the camera sensor. This allowed clearer imaging of subsurface structures. Filter wheel tests confirmed precise wavelength isolation for each LED channel, preventing spectral overlap and ensuring accurate multispectral imaging. Another part of filter wheel testing was the timing with the camera shutter and ensuring they were on the same rotation change when each image is captured.

9.4 Overall System Integration

System integration combined all optical, electrical, and software components into a functional, portable imaging device. The 3D printed housing, designed in Onshape, aligned the optical system while holding the power and control electronics. The LEDs were mounted at thirty degree angles towards the skin sample being imaged for optimal illumination, and the polarizer handle allowed manual adjustment of polarization orientation. Airflow vents near the Raspberry Pi and battery improved cooling performance and allowed the cables to be accessed from outside of the system.

The PCBs were mounted beneath the optical platform, with the LED driver board on top and the Raspberry Pi and battery positioned behind for compact organization. This configuration allowed modular assembly and efficient wiring for testing. System synchronization between the Pi and Arduino ensured coordinated operation during the full multispectral imaging cycle, which was completed in less than five seconds. Once the system was fully integrated, we were able to truly test the device's accuracy as a whole compared to just individual components testing.

Camera and Lens Pairing

To meet diagnostic imaging standards, the SkinLumina system required a camera and lens setup capable of high resolution, low distortion, and strong signal-to-noise performance. The goal was to minimize chromatic aberration across both visible and near-infrared wavelengths while maintaining sharp focus for fine skin features such as pigmentation and texture.

The design process began with theoretical calculations for magnification, field of view, and spatial resolution based on the CMOS sensor's pixel size. Using these parameters, we estimated a spatial resolution of about 3–4 micrometers per pixel. Achromatic doublet lenses with focal lengths of 50 mm and 75 mm were selected to balance magnification, optical clarity, and compact design. Optical simulations in Zemax verified beam paths, spot size, and chromatic performance before finalizing lens choices. This can be seen in figure 9.2.

Zemax Lens Ray Path Diagram

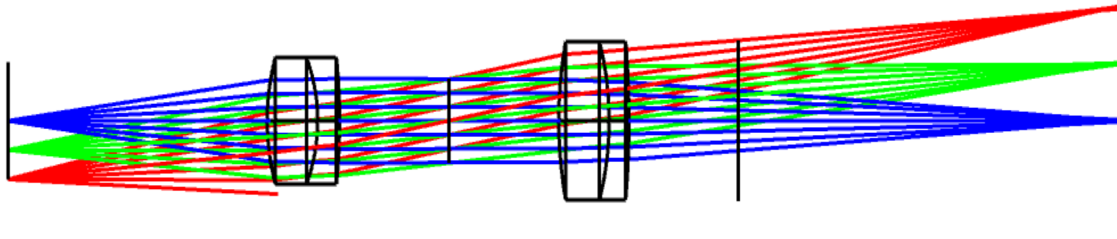


Fig 9.2 Ray-trace diagram of the SkinLumina optical system modeled in Zemax.

During physical testing, we used provisional lenses to capture calibration target images, refining the spacing between lenses until optimal focus was achieved across all wavelengths. The camera's RGB and hexadecimal pixel values were analyzed under each LED illumination to confirm accurate color response and minimal spectral overlap. Combining simulation and experimental validation ensured the final lens and camera pairing achieved precise alignment, high-resolution performance, and spectral accuracy for clinical-grade multispectral imaging.

9.5 Project Testing and Integration Conclusion

Comprehensive testing of the SkinLumina system confirmed that it functions as a stable, adaptive multispectral imaging platform designed to enhance inclusivity in dermatological analysis. Through the integration of visible and near-infrared illumination, polarization control, and real-time spectral calibration, SkinLumina delivers clear imaging of both surface and subsurface skin features across a wide range of skin tones. Hardware testing demonstrated strong electrical performance, safe voltage regulation, and efficient thermal management, while software testing validated synchronization, accurate HEX-based adaptive illumination, and fast processing response.

Optoelectronic validation further verified LED spectral alignment, consistent wavelength penetration through phantom skin layers, and effective polarization in reducing surface glare. These results confirm the system's electrical reliability, optical precision, and software adaptability, establishing SkinLumina as a dependable prototype for inclusive and high-fidelity dermatological imaging. Continued testing beyond Senior Design will focus on IRB-approved human trials, user interface refinement, and expanded clinical validation to confirm system performance across diverse skin tones and medical environments.

9.6 After Senior Design Plan

Following the successful development and testing of the SkinLumina prototype, the next stage of work focuses on expanding its capabilities, improving its clinical usability, and integrating intelligent data analysis to enhance diagnostic accuracy. The team has already achieved one of its primary stretch goals by creating a companion web-based software platform for real-time data visualization. This interface connects directly to the SkinLumina system, allowing images to be viewed as they are captured, processed, and analyzed. Users can switch between spectral channels, observe reflectance variations, and export data for further study. Building on this foundation, the goal is to evolve the current platform into a secure dermatologist-facing portal where clinicians can log in to view patient imaging records, compare scans across time, and interpret multispectral data directly through an intuitive dashboard.

Future expansion will center on integrating artificial intelligence into this platform to assist in image interpretation and diagnostic support. Machine-learning algorithms trained on diverse datasets of multispectral skin images could automatically detect and classify lesions, scars, and pigmentation irregularities. These models would analyze both spectral and spatial features, producing color-coded diagnostic overlays and probabilistic assessments to guide dermatologists in early detection and treatment planning. By combining real-time imaging with AI-based analytics, SkinLumina can move beyond image capture toward meaningful clinical insight generation.

Further improvements to the device itself will focus on modularity and adaptability. The optical assembly will be refined to allow quick replacement of lenses, apertures, and filters, supporting various imaging depths and research needs. Continued software development will ensure seamless integration between the hardware and the online platform, making data transfer, visualization, and interpretation both fast and reliable. Through these efforts, SkinLumina will transition from a functional prototype into a clinician-ready, AI-enhanced imaging system capable of providing equitable, accurate, and accessible dermatological assessment across all skin tones.

Chapter 10 – Administrative Content

This chapter outlines the administrative aspects of the SkinLumina project, including budgeting, material sourcing, team responsibilities, and project scheduling. This section provides a transparent overview of how resources are allocated, the estimated costs for components and prototyping, and how work is distributed among team members. Additionally, it outlines key milestones and timelines for both Senior Design 1 and 2, offering a structured roadmap to guide development and ensure the project stays on track.

10.1 Budget

For our Budget we are trying to keep costs low to show that you can make an affordable but impactful imaging system, thus we are trying to keep our total costs below \$500. For our budget we are splitting up the allotment of funds into 3 main categories: Optical, Electrical, and Housing. Obviously, this budget is subject to change as we add/remove parts or decide if we need to make upgrades to meet our engineering specifications. As far as the financing for this project goes, we are currently self-funded. The current spending plan is listed in table 5, but we aim to keep under budget. We are currently seeking/in talks with a few possible sponsors, so we will update this section regarding funding if changes become apparent.

Budget Retroactive May 29th	
Category	Estimated Cost
Optical	\$200
Electrical/Software	\$100
Prototyping/Housing	\$75
Total Estimated Cost	\$375

Table 5. SkinLumina Budget

10.2 Bill Of Materials

Below in table 5.1 is the cost for each expected part in use, along with its quantity amount. Everything ended up to an estimated cost of under 300\$.

Component	Name	Qty	Unit Cost (USD)	Total Cost
<u>Optical</u>				
Multispectral LEDs (470 nm, 530 nm, 630 nm, 850 nm and 940 nm)	LED-SPECTRA-KIT1 (Digi-Key)	4 sets	\$2.00	\$8.00
White LEDs for initial baseline skin scan	QBL8IW15C-CW110 (DigiKey)	4	\$2.50	\$10
Optical bandpass filters (narrowband)	FB470-10, FB530-10, FB630-10, FB850-10 (Thorlabs)	3	\$180	\$540
Collimating lenses or diffusers	LLC0200-UB (LEDIL)	2	\$5.00	\$10.00

Optical window (clear acrylic or polycarbonate)	ACR-CLEAR-25x2 (McMaster-Carr)	1	\$5.00	\$5.00
Linear polarizers for LEDs (to reduce specular reflection)	LPVIS100-MP2 (Thorlabs)	4	\$2.00	\$8.00
Linear polarizer for CMOS camera sensor	LPVISE100-A (Thorlabs)	1	\$5.00	\$5.00
Mini filter wheel (motorized or manual)	FW1A (Thorlabs)	1	\$20.00	\$20.00
CMOS camera module (e.g., OV2640 / IMX219)	OV2640-FPC (Arducam)	1	\$10.00	\$10.00
Camera lens mount + spacer	M12-MOUNT-KIT (Arducam)	1	\$5.00	\$5.00
Subtotal (Optics)				**\$613**
<u>Electronics & PCB</u>				
Microcontroller (STM32 / ESP32 / Pi Pico)	ESP32-DEVKITC-32D or ARDUINO	1	\$10.00	\$10.00
Custom PCB fabrication + prototyping	JLCPCB-2LAYER	2	\$40.00	\$80
LED driver ICs / MOSFETs	IRL540N (Infineon)	8	\$1.50	\$12
Stepper motor + driver (for filter wheel)	28BYJ-48 + ULN2003 (Keyestudio)	1	\$8.00	\$8.00
Voltage regulators (3.3V, 5V)	AMS1117-3.3/5.0	2	\$1.50	\$3.00
Passive components (resistors, caps, headers)	RC-PASS-KIT1 (SparkFun)	1 set	\$10.00	\$10.00
Bluetooth module (e.g., HC-05 or ESP32 onboard)	HC-05 (ZS-040)	1	\$5.00	\$5.00
Subtotal (Electronics)				**\$128.00**
<u>Power System</u>				

3.7V Li-ion battery (2500 mAh)	18650-LG2500 (Samsung)	1	\$12.00	\$12.00
TP4056 charging module	TP4056-MICROUSB	1	\$2.00	\$2.00
Boost converter (3.7V to 5V)	MT3608 Module (DROK)	1	\$3.00	\$3.00
Power switch + connector hardware	Mini Slide Switch + JST-PH (Adafruit)	1	\$2.00	\$2.00
Subtotal (Power)				**\$19.00*
<u>Enclosure & Build</u>				
3D printed or laser-cut housing	Custom Fabrication	2	\$25.00	\$50.00
Screws, adhesives, internal mounts	Maker Kit (assorted)	1 set	\$5.00	\$5.00
Thermal insulation / foam padding	Foam Sheet 3mm (McMaster-Carr)	1 set	\$3.00	\$3.00
Subtotal (Build)				**\$58.00*
<u>User Feedback & Testing</u>				
Piezo buzzer	PS1240P02BT (TDK)	1	\$1.50	\$1.50
Test calibration targets (color cards, fake moles)	ColorChecker Passport Photo 2	1 set	\$5.00	\$5.00
Micro-USB or USB-C cable	USB-C-1M (Anker)	1	\$3.00	\$3.00
Subtotal (Testing & Feedback)				**\$9.50**
Grand Total Estimated Cost:				**\$827.5*

Table 5.1 Bill of Materials

10.3 Work Distribution

The table 5.2 outlines the distribution of responsibilities among the SkinLumina project team. Each member was assigned a primary role based on their academic background and technical strengths, ensuring a balanced and collaborative workflow. Optical tasks such as imaging, LED configuration, and filter integration were led by optical engineering

students, while the electrical engineer managed power systems, PCB layout, and motor control. The computer engineer focused on software development, including image capture, processing logic, and interface design. Shared responsibilities, such as hardware integration and system testing, were coordinated jointly to ensure smooth project execution across all subsystems.

Distribution of Work		
Task	Responsibility (Primary)	Responsibility (Secondary)
Visible Imaging System	Tatiana C.	Ryan R.
NIR Imaging System	Ryan R.	Tatiana C.
LEDs and Filters	Tatiana C.	Ryan R.
Camera + Optical Stack	Ryan R.	Tatiana C
Power System	Abdullah A.	Tiffany T.
PCB Layout	Abdullah A.	Ryan R.
Other Necessary Circuits (motor, LED, etc.)	Abdullah A.	Tiffany T.
Software Development	Tiffany T.	Abdullah A.
Camera Interfacing and Control Logic	Tiffany T.	Abdullah A.
Image Capture + Data Processing	Tiffany T.	Abdullah A.

Table 5.2 Distribution of Work

10.4 Project Milestones

The table 5.3 outlines our group's project milestones for both Senior Design 1 and 2. It contains both the start date as well as the projected end date for the major tasks we are undertaking during this project.

Project Milestones SD 1 and SD 2			
Task	Description	Start Date	End Date
Initial Research	Analyze dermatology imaging needs, review existing systems	5/19/2025	7/7/2025
System Design Draft	Hardware architecture, optical layout, electrical schematics	5/26/2025	6/6/2025
Component Procurement	Order LEDs, lenses, filters, MCU, camera, power modules	5/30/2025	6/26/2025
Prototype Development	Assemble initial working prototype (LEDs, filters, camera, MCU)	6/6/2025	7/26/2025
Firmware Development	Program MCU to control LEDs, motor, and camera trigger	7/2/2025	8/30/2025

Project Milestones SD 1 and SD 2			
Optical Testing	Evaluate lighting and filter combinations on test subjects	7/7/2025	10/30/2025
Final Integration & Testing	Combine all hardware and software into final device and run full scan sequences	10/30/2025	D-DAY roughly middle of November.

Table 5.3 Project Milestones

Chapter 11 Conclusion

The SkinLumina project represents a significant advancement in the development of portable skin imaging systems. It is grounded in interdisciplinary expertise spanning optics, electronics, biomedical engineering, and software development. The system is designed to offer a reliable, efficient, and inclusive solution to a critical health equity gap. Current diagnostic imaging systems often lack the ability to perform consistently across diverse skin tones. SkinLumina addresses this limitation through a customizable multispectral imaging platform that is compact, energy efficient, and adaptable to various clinical settings.

From conceptualization to prototype development, this project has followed a rigorous and iterative process of design, evaluation, and refinement. Every component and software decision has been guided by extensive benchmarking and feasibility testing. The team has remained committed to the principles of safety, performance, and clinical readiness, as evidenced by adherence to relevant electrical safety standards, Institutional Review Board protocol submission, and alignment with international engineering and biomedical guidelines. Ongoing testing and validation reflect a continued focus on delivering a robust imaging platform capable of meeting real-world clinical demands.

SkinLumina also reflects a thoughtful approach to the ethical and social dimensions of medical technology. By embedding inclusivity into the core functionality, the project challenges longstanding biases in commercial dermatological tools. The modular architecture of the device allows for imaging across a broad spectrum of skin tones and establishes a scalable framework for future enhancements, including advanced machine learning algorithms and cloud-based clinical workflows. This design philosophy ensures the platform remains adaptable and forward compatible with emerging technologies.

As the project transitions into Senior Design Two, the primary focus will remain on validating optoelectronic performance and ensuring full integration of all subsystems. However, the scope will expand to include the fabrication of a fully enclosed mechanical housing, further development of the graphical user interface and imaging software, and the exploration of additional system features identified in earlier planning phases. With continued refinement, comprehensive validation, and appropriate support, the SkinLumina system has the potential to serve as a clinically meaningful diagnostic tool that contributes to closing the equity gap in dermatological imaging and care.

Appendices

Appendix A – Copyright Permissions

This appendix provides documentation of copyright permissions requested for any third-party images, figures, diagrams, or content used in the SkinLumina project report or presentation materials. It ensures compliance with intellectual property regulations and proper attribution of all externally sourced content.

We have received your message and a Canfield representative will be contacting you shortly.

Questions? [Email us](#) or call 800.815.4330.

Regards,
The Canfield Scientific Team

Your message:
Dear Canfield Scientific,

I hope this message finds you well.

My engineering team at the College of Optics and Photonics (CREOL), University of Central Florida, is currently developing an undergraduate-level imaging device for skin analysis. As part of our research and design process, we have been studying existing solutions in the field, and your product stood out as one of the most relevant and advanced in this space.

Given the limited number of specialized solutions available and the alignment of your technology with our project goals, we would greatly appreciate the opportunity to reference your product and website in our final project report. This would be strictly for academic purposes and help provide industry context to our work.

Please let us know if you would be open to this, or if there are any guidelines or preferred citations we should follow.

Thank you for your time and consideration. I look forward to your response.

Best regards,
Tatiana Cutrone
Photonics and Optics Engineer, Team Lead / Undergraduate Researcher
College of Optics and Photonics (CREOL)
University of Central Florida
ta858667@ucf.edu
570-472-7017

Above is an email requesting access to use images of Canfield Scientific's existing products.

Appendix B – LLMs and other AI Chat Log/Resources

A -]https://chatgpt.com/s/t_6865dbe27b108191a68311c23b9db1ff

B - https://chatgpt.com/s/t_68674a6279208191bd0601116d210893

C - <https://claude.ai/share/16100773-95db-4f40-8a1f-2c00779108d5>

D - https://chatgpt.com/s/t_685dca8e52e88191aee197dda65c251e

E - https://grok.com/share/c2hhcmQtMg%3D%3D_875d3df7-4c4c-404e-be44-7f55d50d16dd

F - [The AI for Academic Research | SciSpace](#)

Appendix C – References

1. *Visia: The Gold Standard in Facial Skin Analysis*. 2025; Available from: <https://www.canfieldsci.com/imaging-systems/visia-complexion-analysis/>.
2. *Veos: Refined, Powerful and Pocket Sized*. . 2025; Available from: https://www.canfieldsci.com/imaging-systems/veos/?language_code=en.
3. Jothishankar, B. and S.L. Stein, *Impact of skin color and ethnicity*. Clinics in Dermatology, 2019. **37**(5): p. 418-429.
4. Sorbellini, E., M. Rucco, and F. Rinaldi, *Photodynamic and photobiological effects of light-emitting diode (LED) therapy in dermatological disease: an update*. Lasers Med Sci, 2018. **33**(7): p. 1431-1439.
5. Celli, J.P., et al., *Imaging and Photodynamic Therapy: Mechanisms, Monitoring, and Optimization*. Chemical Reviews, 2010. **110**(5): p. 2795-2838.
6. Kirill Kulikov, T.K., *Laser Interaction with Heterogenous Biological Tissue*. 2018.
7. Visscher, M.O., et al., *Chapter 38 - From Image to Information: Image Processing in Dermatology and Cutaneous Biology*, in *Imaging in Dermatology*, M.R. Hamblin, P. Avci, and G.K. Gupta, Editors. 2016, Academic Press: Boston. p. 519-535.
8. Vasefi, F., N. MacKinnon, and D.L. Farkas, *Chapter 16 - Hyperspectral and Multispectral Imaging in Dermatology*, in *Imaging in Dermatology*, M.R. Hamblin, P. Avci, and G.K. Gupta, Editors. 2016, Academic Press: Boston. p. 187-201.
9. Oniga, M., et al., *Towards an integrated imaging for melanoma diagnosis: A review of multispectral, hyperspectral, and thermal technologies with preliminary system development*. Comput Biol Med, 2025. **185**: p. 109570.
10. Jagadeesha, N., A. Trisal, and V.N. Tiwar. *Skin Tone Assessment Using Hyperspectral Reconstruction from RGB Image*. in *2023 15th International Conference on COMmunication Systems & NETworkS (COMSNETS)*. 2023.
11. Martinsons, C., *Handbook of Advanced Lighting Technology (Photobiological Safety)*. 2016.
12. *Detect Skin Cancer with AI-Driven Precision*. 2025; Available from: <https://www.dermasensor.com/>.
13. Fossum, E.R., *CMOS image sensors: electronic camera-on-a-chip*. IEEE Transactions on Electron Devices, 1997. **44**(10): p. 1689-1698.
14. Theuwissen, A.J.P., *Solid-state Imaging with charge coupled devices*. 2011: Springer.
15. Rinner, B. and M.C. Wolf, *An Introduction to Distributed Smart Cameras*. Proceedings of the IEEE, 2008. **96**: p. 1565-1575.
16. Yaroslavsky, A.N., et al., *Optical properties of selected native and coagulated human brain tissues in vitro in the visible and near infrared spectral range*. Phys Med Biol, 2002. **47**(12): p. 2059-73.

17. Pogue, B.W. and M.S. Patterson, *Review of tissue simulating phantoms for optical spectroscopy, imaging and dosimetry*. J Biomed Opt, 2006. **11**(4): p. 041102.
18. Park, B., et al., *Multispectral LED-based imaging system for non-invasive skin diagnostics*. 2017.
19. Thorlabs. *Optical Filters and Filter Wheel Guide*. 2024.
20. Gao, L. and R.T. Smith, *Optical hyperspectral imaging in microscopy and spectroscopy – a review of data acquisition*. Journal of Biophotonics, 2015. **8**(6): p. 441-456.
21. Qi, X., et al., *Liquid Crystal Tunable Filters For Hyperspectral Imaging: Principles and Applications*. 2013.
22. Anderson, R.R. and J.A. Parrish, *The Optics of Human Skin*. Journal of Investigative Dermatology, 1981. **77**(1): p. 13-19.
23. Jacques, S.L., J.C. Ramella-Roman, and K. Lee, *Imaging skin pathology with polarized light*. J Biomed Opt, 2002. **7**(3): p. 329-40.
24. Lademann J., e.a., *Optical Properties of Human Skin in vivo*. Journal of Biomedical Optics, 2006.
25. Mack, K. *Proving Lambert's Law: Understanding cosine Reflections*. 2025; Available from: <https://lawshun.com/article/how-can-i-prove-or-demonstrate-lamberts-cosine-law>.
26. Waldwick, B., et al., *Performance improvements in back panel display lighting using near-Lambertian diffuse high-reflectance materials*. Optical Engineering + Applications. Vol. 6696. 2007: SPIE.
27. Ilişanu, M.A., F. Moldoveanu, and A. Moldoveanu, *Multispectral Imaging for Skin Diseases Assessment-State of the Art and Perspectives*. Sensors (Basel), 2023. **23**(8).
28. Rey-Barroso, L., et al., *Visible and Extended Near-Infrared Multispectral Imaging for Skin Cancer Diagnosis*. Sensors (Basel), 2018. **18**(5).
29. Benvenuto-Andrade, C., et al., *Differences between polarized light dermoscopy and immersion contact dermoscopy for the evaluation of skin lesions*. Arch Dermatol, 2007. **143**(3): p. 329-38.
30. MidOpt. *Optical Bandpass Filters - product catalog*. 2023; Available from: <https://midopt.com>.
31. Hernández-Bule, M.L., et al., *Unlocking the Power of Light on the Skin: A Comprehensive Review on Photobiomodulation*. Int J Mol Sci, 2024. **25**(8).
32. Lister, T., P.A. Wright, and P.H. Chappell, *Optical properties of human skin*. J Biomed Opt, 2012. **17**(9): p. 90901-1.
33. Barun, V.V., et al., *Absorption spectra and light penetration depth of normal and pathologically altered human skin*. Journal of Applied Spectroscopy, 2007. **74**(3): p. 430-439.
34. Lee, J., et al., *Design and Implementation of Embedded-Based Vein Image Processing System with Enhanced Denoising Capabilities*. Sensors (Basel), 2022. **22**(21).

35. Horton, L., et al., *The effects of infrared radiation on the human skin*. Photodermatology, Photoimmunology & Photomedicine, 2023. **39**(6): p. 549-555.
36. Optics, E. *Achromatic Doublet Lenses for Broadband Imaging*. 2024; Available from: www.edmundoptics.com.
37. Thorlabs. *Achromatic Doublet Lens Specifications and Design Tools*. 2024; Available from: www.thorlabs.com.
38. Palmer, G.M., et al., *Quantitative diffuse reflectance and fluorescence spectroscopy: tool to monitor tumor physiology in vivo*. J Biomed Opt, 2009. **14**(2): p. 024010.
39. Born, M., & Wolf, E., *Principles of Optics*. 1999: Cambridge University Press.
40. Bi, J., et al., *Large AI Models and Their Applications: Classification, Limitations, and Potential Solutions*. Software: Practice and Experience, 2025. **55**(6): p. 1003-1017.
41. Parisineni, S.R.A. and M. Pal, *Enhancing trust and interpretability of complex machine learning models using local interpretable model agnostic shap explanations*. International Journal of Data Science and Analytics, 2024. **18**(4): p. 457-466.
42. *Journal of Technical Writing and Communication*. 2024. **54**(4).
43. Dobhada, S. and L. Rajpurohit, *Bard versus ChatGPT: An adjunct to scientific writing*. Oral Oncology Reports, 2024. **9**: p. 100182.
44. Moukthika, M., *Blob Detection Usin Simple CV*. 2025.
45. Di Ninni, P., F. Martelli, and G. Zaccanti, *The use of India ink in tissue-simulating phantoms*. Opt Express, 2010. **18**(26): p. 26854-65.
46. Portesi, C., et al., *MgB2 magnetometer with a directly coupled pick-up loop*. Superconductor Science and Technology, 2006. **19**(5): p. S303.
47. Jacques, S.L. and B.W. Pogue, *Tutorial on diffuse light transport*. J Biomed Opt, 2008. **13**(4): p. 041302.